Characterizing global gene expression and antiviral response in *Frankliniella occidentalis* infected with *Tomato spotted wilt virus*

by

Derek Joseph Schneweis

B.S., Kansas State University, 2011

AN ABSTRACT OF A DISSERTATION

submitted in partial fulfillment of the requirements for the degree

DOCTOR OF PHILOSOPHY

Department of Plant Pathology
College of Agriculture

KANSAS STATE UNIVERSITY
Manhattan, Kansas

2017

Abstract

Frankliniella occidentalis, the western flower thrips, transmits the plant-pathogenic virus, *Tomato spotted wilt virus* (TSWV), through a circulative-propagative transmission strategy. The virus infects and replicates in the insect, traversing membrane barriers as it moves from the midgut to the salivary glands for subsequent inoculation of a plant host. Based on well-characterized virus-vector systems, many molecular interactions occur as the virus completes an infection cycle in the vector, and knowledge of transcriptome-wide response of thrips to TSWV has been limited. My research goals were to gain insight into i) the molecular responses that occur in thrips vectors of orthotospoviruses, ii) the role of antiviral defense in viruliferous thrips, and iii) plant transgenic-based strategies for studying thrips gene function and crop-pest control. To this end, my specific research objectives were to: 1) generate, assemble, and annotate a RNA-Seq-derived transcriptome for *F. occidentalis* using the thrips genome, and to quantify global gene expression in response to TSWV activity in larval, pre-pupal, and adult developmental stages, 2) conduct a time-course experiment to determine the effect(s) of challenging TSWV-exposed and non-exposed thrips with dsRNAs of *F. occidentalis* Dcr-2 or AGO2 by hemocoel injection, and 3) construct transgenic plants expressing a thrips-gene specific dsRNA hairpin to target a vital gene. My research has catalogued insect response to TSWV activity in thrips during development and provides candidate sequences for functional analysis of genes involved in insect development and defense. Successful silencing of the antiviral RNAi pathway in thrips revealed increased mortality and decreased offspring production in both virus-exposed and non-exposed insects. Arabidopsis plants were developed to express dsRNA of vacuolar ATP synthase (V-ATPase) and preliminary feeding bioassays to explore the effect of these transgenics on thrips fitness indicate a need for further description of thrips dsRNA uptake. In total, my research

contributes new basic knowledge underpinning the complex and dynamic relationship between thrips vectors and the plant viruses they transmit.

Characterizing global gene expression and antiviral response in *Frankliniella occidentalis* infected with *Tomato spotted wilt virus*

by

Derek Joseph Schneweis

B.S., Kansas State University, 2011

A DISSERTATION

submitted in partial fulfillment of the requirements for the degree

DOCTOR OF PHILOSOPHY

Department of Plant Pathology
College of Agriculture

KANSAS STATE UNIVERSITY
Manhattan, Kansas

2017

Approved by:

Major Professor
Dr. Dorith Rotenberg

Copyright

Abstract

Frankliniella occidentalis, the western flower thrips, transmits the plant-pathogenic virus, *Tomato spotted wilt virus* (TSWV), through a circulative-propagative transmission strategy. The virus infects and replicates in the insect, traversing membrane barriers as it moves from the midgut to the salivary glands for subsequent inoculation of a plant host. Based on well-characterized virus-vector systems, many molecular interactions occur as the virus completes an infection cycle in the vector, and knowledge of transcriptome-wide response of thrips to TSWV has been limited. My research goals were to gain insight into i) the molecular responses that occur in thrips vectors of orthotospoviruses, ii) the role of antiviral defense in viruliferous thrips, and iii) plant transgenic-based strategies for studying thrips gene function and crop-pest control. To this end, my specific research objectives were to: 1) generate, assemble, and annotate a RNA-Seq-derived transcriptome for *F. occidentalis* using the thrips genome, and to quantify global gene expression in response to TSWV activity in larval, pre-pupal, and adult developmental stages, 2) conduct a time-course experiment to determine the effect(s) of challenging TSWV-exposed and non-exposed thrips with dsRNAs of *F. occidentalis* Dcr-2 or AGO2 by hemocoel injection, and 3) construct transgenic plants expressing a thrips-gene specific dsRNA hairpin to target a vital gene. My research has catalogued insect response to TSWV activity in thrips during development and provides candidate sequences for functional analysis of genes involved in insect development and defense. Successful silencing of the antiviral RNAi pathway in thrips revealed increased mortality and decreased offspring production in both virus-exposed and non-exposed insects. Arabidopsis plants were developed to express dsRNA of vacuolar ATP synthase (V-ATPase) and preliminary feeding bioassays to explore the effect of these transgenics on thrips fitness indicate a need for further description of thrips dsRNA uptake. In total, my research

contributes new basic knowledge underpinning the complex and dynamic relationship between thrips vectors and the plant viruses they transmit.

Table of Contents

List of Figures

List of Tables

Acknowledgements

First, I would like to thank Dr. Dorith Rotenberg. Dorith is deeply invested in the success of her students, and she has played the major role of mentor during my development as a scientist. Her continued passion and drive for scientific research is infectious, and this energy facilitates continuous progress. I would also like to thank Dr. Anna Whitfield for her never-ending support and care. Anna was always there to offer me a smile and she continually pushed me to be better. Anna and Dorith both are fantastic scientists that I strive to impress, and I will continue to focus on developing the skills they have passed on to me as a budding scientist.

I thank my committee members Dr. Doina Caragea, Dr. Yoonseong Park, and Dr. Rollie Clem for the compassion they showed me. They continually challenged me as a creative scientist, and I greatly appreciate their investment in the development of my dissertation.

I have had the opportunity to engage in many collaborative projects during my time at Kansas State University. I would like to thank Dr. Ismael Badillo-Vargas for his continued friendship and support during my dissertation work. I also greatly appreciate the work done by both Joshua Ames and Dr. Jonathan Oliver in regards to constructing and selecting transgenic plants. I also need to thank the Applied Bioinformatics group for their help with development of my computational tools. I specifically thank Dr. Susan Brown and Jennifer Shelton for always providing much needed advice.

The work I discuss throughout this thesis would not exist without the help of Jim Spurlock and Terri Branden. Their continued monitoring of both our growth chambers and the greenhouses was instrumental in all of my plant science work. They helped me on issues ranging from broken growth chamber parts to building new greenhouse benches out of rusty nails and old wood.

Finally, I thank my other, Sarah Brooks, for always keeping me in the light. When challenges leapt from the shadows, she stood by my side, always holding my hand. Additionally, I would not be here without my family. I thank my mom, Kayla Schneweis, for fostering the scientist in me and for continually asking me to question my surroundings. I thank my dad, William Schneweis, for supporting me and for always believing in me and my ability to create. I also thank my siblings, Brandi and Nick Schneweis, for always being my stability and balance.

Dedication

"*One looks back with appreciation to the brilliant teachers, but with gratitude to those who touched our human feelings. The curriculum is so much necessary raw material, but warmth is the vital element for the growing plant…"* – Carl Jung

I would like to dedicate this dissertation to all of the teachers in my life, both inside the classroom and out. I have received the gift of education from many wonderful mentors, and all that defines me as an educated man arises from what I have learned by teachers who, far from merely teaching, have guided, supported, challenged, believed in, and questioned me along the way. I thank you all and continue to build upon the passions you have instilled in me.

Chapter 1 - Introduction and Literature Review

Introduction

The plant disease caused by *Tomato spotted wilt virus* (TSWV) has characteristic symptoms of yellow ring-spots, mottling, necrotic leaf spots, and general yellowing on the infected plant leafs. This symptomology was first described in 1915 when Brittlebank documented it as a tomato disease (Brittlebank, 1919). Twelve years later, Pittman determined that thrips acted as the vectors and agent of disease for transmission of TSWV. Samuel and others identified that the disease was established through plant infection by a virus (Pittman, 1927, Samuel et al., 1930). Early in the description of the virus-vector system, scientist described how adult thrips in two species (i.e. *F. schultzei* and *T. tabaci*) were transmitters as long as the virus was acquired during the larval stage (Linford, 1932, Samuel et al., 1930). The early description of this important interaction was the groundwork for further exploration of the thrips-TSWV vector system. While the original classification of TSWV into a virus grouping was difficult, many suggested that TSWV might resemble myxoviruses (Milne, 1970). Later in 1984 Milne and Francki identified that TSWV should be the first member of a plant-infecting virus group in the family Bunyaviridae (Milne and Francki, 1984). It was not until seven years later that a group of plant infecting viruses was classified as *Tospovirus* in the family *Bunyaviridae* (Francki et al., 1991). The *Bunyaviridae* family was more recently changed by the International Committee on Taxonomy of Viruses (ICTV) to the order *Bunyavirales* and is now described by three families of animal-infecting viruses (*i.e. Hantaviridae, Nairoviridae,* and *Phasmaviridae*), two newly described arthropod-specific virus families (*i.e. Feraviridae* and *Jonviridae*), and a three plant-infecting families (*i.e. Tospoviridae*, *Fimoviridae*: previously un-assigned

Emaravirus, *Phenuiviridae*: previously un-assigned *Tenuivirus*). Tospoviridae currently consists of 28 approved or described species (Gonzalez-Scarano and Nathanson, 1996, Oliver and Whitfield, 2016).

The virion structure for *Bunyavirales* is spherical and surrounded by glycoprotein spikes (Elliott, 1990), with a membrane that encapsulates three separate RNA molecules, protected by the N protein, that comprise the viral genome (L, M, and S) and a few copies of the RNA-dependent-RNA-Polymerase (RDRP) protein (Elliott, 1990). This order of viruses is one of the largest orders of animal viruses. Excluding the Hantaviruses, arthropod vectors transmit all other virus groups: mosquitoes, ticks, midges, sandflies, and thrips (Beaty and Bishop, 1988). The *Tospoviridae* family is comprised only of plant infecting viruses, and insects in the order *Thysanoptera* are the sole transmitters.

Frankliniella occidentalis, the Western flower thrips, is described as a super vector for TSWV-vector interaction biology and they are the predominate transmitters of the TSWV. Thrips (*i.e. F. occidentalis*) feed on fruits, vegetables and ornamental crops and cause major crop losses through direct feeding damage and transmission of viruses. They have high locomotory activity, high fecundity, a short generation time, preference for concealed spaces, a wide range of host plants, and they puncture epidermal and mesophyll plant cells (Morse and Hoddle, 2006). Thrips are able to acquire virus as young larva and transmit as adults, yet there is very little known about the molecular interactions between the insect and the virus. A thorough investigation and description of thrips vector competency (the inherent ability of a vector to harbor, replicate, and transmit a virus) at the molecular level is necessary for establishing a scientific understanding of the dynamic and complex molecular interaction between TSWV and

F. occidentalis, and it will enable the development of novel biological strategies for controlling the plant virus and its insect vector.

To that end, the overarching goal of my research was to advance the understanding of the molecular interaction of thrips and TSWV interactions and develop tools for both functional analysis of thrips genes and for biotech-based approaches to managing thrips populations. The objectives of my dissertation chapters are as follows: Objective 1 – provide a description of global transcriptome-level interaction response of *F. occidentalis* during Tomato spotted wilt virus infection, Objective 2 – silence the RNAi pathway genes Dicer 2 (DCR-2), and Argonaute 2 (AGO-2) during TSWV infection and measure changes in TSWV, and Objective 3 – develop and test transgenic *Arabidoposis thaliana* expressing dsRNA hairpins to target *F. occidentalis* V-ATPase-B transcripts for RNAi-based silencing during feeding.

Virus Genus: *Orthotospovirus*

The genus *Orthotospovirus* contains many plant infecting viruses that cause diseases of important ecological and agricultural plant species. Members of *Orthotospovirus* are plant-infecting viruses in the order *Bunyavirales*. *Orthotospovirus* was originally monophyletic with only *Tomato spotted wilt orthotospovirus* (TSWV) as a species. In 1990, a second *Orthotospovirus* was discovered, *Impatiens necrotic spot orthotospovirus* (Law and Moyer, 1990), that was followed by many more identifications providing the current number of 28 described species within the genus (Oliver and Whitfield, 2016). *Orthotospoviruses* such as TSWV have a large plant host range infecting more than 900 species within over 90 monocotyledonous and dicotyledonous plant families. This is similar to *Impatiens necrotic spot*

orthotospovirus (INSV) with at least 300 plant species in 85 different monocotyledonous and dicotyledonous families (Pappu et al., 2009, Persley et al., 2006).

Orthotospovirus populations are genetically diverse, due in part to their tripartite viral genome and capacity for genome re-assortment and genome-segment-specific adaptation. For example, the intergenic region (IGR) of the S RNA is correlated with competitiveness of this genome segment within reassortant isolates providing a coding strategy that serves as a regulatory function that influences the occurrence of the segment in the viral populations. Selection within genomic segments provides evidence of parental phenotypes that can be mapped to specific genome segments as well as the generation of novel phenotypes (Qiu et al., 1998, Qiu and Moyer, 1999). Mechanical transfers of TSWV have been shown to produce defective mutants (i.e. loss of ability to produce glycoproteins, truncated L RNA) providing insight into the real-time evolution occurring with *Orthotospoviruses* (Rensende et al., 1991). Variability and selection pressures across the tripartite genome provide capacity for cassette switching of multiple genes within the virus genome, and genomic variability with these types of selection traits provides the virus with the capacity to break host resistance, reinforcing the need for novel ways to manage this virus disease.

Strong early resistance to *Orthotospoviruses* is important because they cause systemic infection within the plant host, with early infection causing the most damage. Black et al. identified gene accessions of the bonnet pepper (*i.e. Capsicum chinense*) that were resistant to TSWV, and then later identified the resistance as the *Tsw* gene for a single dominant gene (Black et al., 1996, Black et al., 1991). The resistance established by the *Tsw* gene is challenging to maintain because of previously described mechanisms of evolution for *Orthotospoviruses*. For example, a TSWV strain was identified with the ability to break the resistance even before it was

determined that the Tsw gene conferred TSWV resistance (Boiteux and Nagata, 1993). Later in 2003, pepper varieties in the Almería region of Spain, also with the Tsw resistance gene, were infected with a resistance breaking isolate of TSWV (Margaria et al., 2004). Another resistance gene identified from *Lycopersicon peruvianum* was introgressed into the fresh market tomato cultivar Stevens (*Sw5*) (Stevens et al., 1991). *Sw5* was shown to provide resistance to TSWV and to two other tomato-infecting *Orthotospoviruses*: *Groundnut ringspot orthotospovirus* (GRSV) and *Tomato chlorotic spot orthotospovirus* (TCSV) (Boiteux and Giordano, 1993). This coiled coil, nucleotide binding, leucine-rich repeat resistance gene was identified as broken in 2004 when leaf samples were collected from resistant tomatoes in Italy and TSWV was detected in all of the field samples tested (Ciuffo et al., 2005, Spassova et al., 2001). The determinants of the ability for TSWV to overcome the R gene were mapped through reassortant genotypes, and the ability was derived from the M RNA segment (Hoffmann et al., 2001). Host resistance was also established through transgenic resistance using the N gene in tobacco (Gielen et al., 1991) and the NSm gene (Prins et al., 1997). The resistance using the N gene was also later broken through reassortant genotypes (Hoffmann et al., 2001). The variability of the viral genome derived from reassortant RNA segment switching provides a challenging target for durable plant resistance and new ideas for control are necessary for dampening the loss produced by *Orthotospoviruses*.

Virus Species: *Tomato spotted wilt orthotospovirus*

Tomato spotted wilt virus orthotospovirus (TSWV) has caused an estimated $1.4 billion in losses in the U.S. alone over ten years (Riley et al., 2011). It is considered one of the most economically important plant pathogenic viruses, and the virus can produce losses of up to 100% (Rosello et al., 1996). TSWV is a globally distributed virus and it is prevalent in areas in which it can be vectored by thrips (Tentchev et al., 2011). The devastation caused by TSWV is partially

due to its wide host range of food, fiber, and ornamental crops. The diversity of TSWV haplotypes is large with a total of 224 isolates sequenced from southern Europe. A large percentage (83%) displayed clustering into three clades representing Spain, France, or the USA. The rest of the grouping (17%) represents natural reassortants.

The genus *Orthotospovirus* are enveloped, spherical, and approximately 85-120nm in diameter (Black et al., 1963, Vankamme et al., 1966). The virion contains an RNA-dependent-RNA-polymerase (RDRP), which is necessary for replication in the host cell, and three pseudo-circular nucleocapsids comprised of the Small (S) RNA (2.9 kb for TSWV), the Medium (M) RNA (4.8 kb for TSWV), and the Large (L) RNA (8.9 kb for TSWV)(Oliver and Whitfield, 2016). The tripartite genome is ecapsidated with the nucleocapsid (N) protein (DeHann et al., 1989) (Figure 1.1). The L RNA codes for the RDRP in the negative sense orientation and contains complementary 3' and 5' ends of 62 nucleotides at the 5' end and 66 nucleotides at the 3' end with an open reading from of 2,875 amino acids (DeHaan et al., 1991). The L protein produced is much larger than the animal-infecting viruses of the same order, and it is present and unprocessed in the virus particle (vanPoelwijk et al., 1993).

The M RNA encodes the nonstructural viral movement protein (NSm) in the positive-sense orientation. This protein was identified to associate with cell walls and cytoplasmic membranes in aggregates with nucleocapsid in close proximity to the plasmodesmata (Kormelink et al., 1994, Storms et al., 1998). Tubule structures comprised of NSm are documented within both a plant system (protoplasts) and an insect cell system (Storms et al., 1995), and NSm has been shown to support long-distance movement and cell-to-cell movement with the c-terminus being required for function (Lewandowski and Adkins, 2005). Further description has determined that the amino acid group $EEEEE^{284-288}$ is essential for long-distance

movement and the amino acid group D^{154} is essential for tubule formation and cell-to-cell movement (Li et al., 2009). The negative-sense encoding of the M RNA produces the G_n and G_c proteins as a polyprotein (Beaty and Bishop, 1988). The viral glycoprotein precursor is cleaved into the two glycoproteins (G_n and G_c) and transported from the endoplasmic reticulum (ER) to the Golgi complex where they are retained and accumulate (Adkins et al., 1996, Kikkert et al., 1999, Kikkert et al., 2001).

The S RNA encodes the N protein in negative sense and the viral nonstructural silencing suppressor (NSs) in the positive-sense orientation (Oliver and Whitfield, 2016). The N protein binds cooperatively to single stranded RNA and is deficient at binding double-stranded TSWV RNA (Richmond et al., 1998). NSs has been shown to post-transcriptionally silence GFP transgenes (Bucher et al., 2003, Takeda et al., 2002a), function as a silencing suppressor in the tick system (Garcia et al., 2006), and act to enhance baculovirus replication when used within a recombinant (Oliveira et al., 2011). It is currently thought that NSs binds small double-stranded RNA molecules and potentially long dsRNA molecules to suppress both Dicer-mediated cleavage and RISC directed silencing of the viral genome (Schnettler et al., 2010a). It is not clear how the NSs protein functions in the thrips vector.

The first nine nucleotides occurring at the 3’ end of all of the genomic RNAs are inverted in complementarity to the 5’ ends allowing for base-paring and the generation of the pseudo-circular structure for the RNA molecules (DeHann et al., 1989, Kellmann et al., 2001). TSWV uses a cap-snatching mechanism with potentially a single base complementarity. The cleaved leader lengths range from 13 to 18 nucleotides and occur preferentially at an A residue (Duijsings et al., 2001). The virion must enter the host cell and un-coat to allow for replication. The RDRP initiates the replication cycle to produce positive sense RNA for synthesis of protein

through the use of host ribosomes. The orthotospovirus genome and molecular structure provides the ability for both plant infection and insect infection.

Thrips Vector Species: *Frankliniella occidentalis*

Frankliniella occidentalis is currently known as one of the most efficient thrips vectors of *Orthotospoviruses* with the ability to transmit seven of the currently tentative 28 species (Oliver and Whitfield, 2016). It is proficient at transmitting four *Orthotospoviruses* specifically: *Tomato spotted wilt orthotospovirus* (TSWV), *Tomato chlorotic spot orthotospovirus* (TCSV), *Groundnut ringspot orthotospovirus* (GRSV), and *Impatiens necrotic spot orthotospovirus* (INSV) (Wijkamp et al., 1995). It is able to transmit TSWV petunia leaf disks more efficiently than any other thrips species at the adult stage of three or four days after emergence (Inoue et al., 2002). It is a member of the insect order Thysanoptera (family Thripidae) and classified taxonomically in the hemipteroid assemblage. The western flower thrips are haplodiploid producing haploid males from unfertilized eggs and diploid females from fertilized eggs (arrhenotoky) (Moritz, 1997), while the males are smaller than the females. Western flower thrips metamorphosis is intermediate between holo- and hemi-metabolism, and it is often referred to as re-metabolism due to the dissolution and reconstruction of several imaginifugal structures during pupation (Moritz, 1995, Takahashi, 1921). Remodeling occurs in the alimentary canal, mouthparts, musculature, and small changes occur in other organ systems (Heming, 1973). Thrips have a high reproductive capacity and can develop from egg to adult within 14 days of 23°C at 16h:8h light:day (Moritz et al., 2004). Females have been shown to damage plant tissue by oviposition of the female *F. occidentalis* inhabiting flowers and fruit

(Navas et al., 1991). After the female places the eggs within the plant tissue, the insects will develop and emerge to feed.

Thrips develop through a first (L1) and second (L2) instar larval stages in which they are continuously feeding (Lewis 1973). They then molt into a quiescent pre-pupal (P1) and pupal (P2) stage during which feeding does not occur and the thrips can fall to the soil for pupation (Lewis, 1973). During this stage the pupa appear to have aversion to direct contact with other thrips. The P2 stage then ecloses as winged males and females with the capacity to fly (Lewis, 1973). Hatching of the thrips egg takes 2-4 days with the first L1 stage being about half of the length of the second (Gaum et al., 1994, Reitz, 2008). At lab conditions, the adult lifespan is much longer when compared to the immature development time with development taking approximately 12 days depending on the temperature, while the adults can live for 26 days (Reitz, 2008) (Figure 1.2).

Thrips are polyphagous feeding on vegetable, fruit, and ornamental crops, which can result in distortion, discoloration, stunting, and silvering of plant parts (Hansen et al., 2003). The adults and larva prefer concealed spaces, such as flowers and curled leafs, portraying a thigmotactic behavior (Hansen et al., 2003, Reitz, 2009). This behavior is easily identified when observing thrips within a controlled environment in which they huddle together in groups. Targeting thrips with insecticides is challenging because of their thigmotatatic behavior and ability to develop resistance quickly (Bielza, 2008, Cifuentes et al., 2012, Lopez-Soler et al., 2008). Thrips feed in a piercing-sucking manner by piercing leaf cells with the mandible (Hunter and Ullman, 1989), and they feed on a variety of cell types within pollen, flower structures, and vegetative portions of plants. During feeding, the insect punctures the leaf epidermis and withdraws cytoplasm from mesophyll cells (Whitfield et al., 2005b). The paraglossal sensilla

appear to have the dual function of chemosensory and mechanosensory traits allowing the thrips to perceive the plant tissue during feeding (Hunter and Ullman, 1992). Thrips have been documented probing the leaf tissue using non-ingestion probes, lasting about one second, in which movement of the salivary pump muscles occur with the generation of saliva droplets at the tip of the mouthcone. Short- and long-ingestion probes also occur in which the insect is withdrawing cell contents and engaging cibarial muscles throughout the ingestions. The long-ingestion probes involve intricate process of engaging motion in the thrips head, mouthcone, and muscles. It is likely that these varying probing approaches are important for western flower thrips transmission of TSWV (Stafford et al., 2011).

Tomato spotted wilt orthotospovirus-Frankliniella occidentalis interaction

The insect-virus interaction is described as persistent-propagative in which the virus infects and replicates in the insect vector. The western flower thrips vector system, as a whole, is prolific within the natural habitat. In a single study of 302 native plant species, a total of 113 species representing 35 plant families were susceptible to TSWV, with eighty six percent of the plants acting as ovipository hosts for western flower thrips (Stobbs et al., 1992). This efficiency and broad host range makes the western flower thrips-TSWV vector system one of the most important for scientific inquiry.

TSWV is able to infect and replicate within the thrips vector. Transmission electron microscopy and serological tools describe the ingestion of TSWV particles by both adult and larval western flower thrips. After ingestion of TSWV, adults display TSWV particles accumulating within the cytoplasm of the midgut epithelial cells (Ullman et al., 1992b), with immunocytochemical evidence that nonstructural proteins are present (i.e. NSs) and both N and

NSs are increasing within the insect-host cell (Ullman et al., 1993, Wijkamp et al., 1993). Successful infection is early during development with the majority of thrips becoming viruliferous in the second larval stage (Wijkamp and Peters, 1993). Virus acquisition appears to occur at all feeding stages, but it must occur at the young larval stages (L1 and L2) as a prerequisite for transmission as adults (Ullman et al., 1992b, van de Wetering et al., 1996) (Figure 1.2).

TSWV infects and replicates in several types of thrips tissues from the midgut epithelium, visceral muscle cells, to the salivary glands. It binds and enters the epithelium of the anterior midgut with midgut one supporting a robust TSWV infection in the larval stage (Montero-Astúa et al., 2016, Nagata et al., 1999). Midgut two and three are rarely to moderately infected, indicating that these gut regions are less competent for the support of virus infection (Montero-Astúa et al., 2016). Virus infection subsequently spreads to the circular and longitudinal midgut muscle tissues in the late larval stage (Nagata et al., 1999). It then replicates and disseminates within the visceral muscle cells until reaching the principal salivary glands of the insect (Montero-Astúa et al., 2016, Ullman et al., 1993, Ullman et al., 1995, Wijkamp et al., 1993). It is likely that the virus moves through the tubular salivary glands and the efferent duct that leads from the salivary reservoir to the primary salivary glands (Montero-Astúa et al., 2016). TSWV can be successfully acquired or inoculated in periods of five minutes during the larval stages, but transmission reaches an optimum after an Acquisition Access Period (AAP) of 21.3h and an Inoculation Access Period (IAP) of 42.7h (Wijkamp et al., 1996b). During the adult stage, the infection occurs in the visceral muscle tissues covering the midgut and foregut, but appears to be abolished in the midgut epithelium (Montero-Astúa et al., 2016, Nagata et al., 1999). The virus infection of the principal salivary glands appears to be greater in the adults when compared

to the other tissue symptoms (Montero-Astúa et al., 2016), and the successful infection of the salivary glands appears to be dependent on a dose-response with relation to virus titer and transmission (Montero-Astua et al., 2014, Montero-Astúa et al., 2016, Rotenberg et al., 2009a). A viruliferous thrips is more likely to transmit at multiple events if it harbors high titer of TSWV (Rotenberg et al., 2009a).

Viral glycoproteins of TSWV (G_n and G_c) decorating the virion play critical roles in virus binding and acquisition in the thrips midgut epithelium. The G_n glycoprotein embedded in the viral membrane acts to bind to the thrips midgut (Figure 1.1). A soluble form of G_n (i.e. Gn-S) can bind in a similar fashion and inhibit the amounts of virus in the thrips gut (Montero-Astua et al., 2014, Whitfield et al., 2004). Glycoproteins interact with thrips proteins, but the receptor for midgut epithelial cell entry is currently unknown (Bandla et al., 1998, Kikkert et al., 1998). The G_c protein is cleaved at acidic pH indicating a potential function as a fusion protein with an acidic endosome similar to other Bunyaviruses (Cifuentes et al., 2012, Whitfield et al., 2005a). The virus enters the host cell and begins replication, and TSWV-N, the membrane glycoproteins (G_n and G_c), and NSs appear to be compartmentalized within viroplasms (Ullman et al., 1995). This infection cycle occurs at each cell type as the virus moves to the salivary glands. The virus particles are present in the salivary vesicles indicating that the Golgi apparatus is important for transport to the salivary ducts (Wijkamp et al., 1993).

Feeding behavior is different between the males and females. Higher scar production and lower orthotospovirus transmission has been observed for female thrips. Males tend to transmit at higher rates when compared to females, while transmission efficiency continually drops as the insects age (van de Wetering et al., 1998). It is clear that virus infection status of the thrips induces behavioral shifts noticeable in feeding habits. Male thrips infected with TSWV tend to

feed more than uninfected males, with feeding behavior frequencies increasing up to threefold, providing a greater opportunity for an inoculation event to occur. Males also make three times more non-ingestion probes (probes in which they salivate and leave cells undamaged) compared to non-infected males further increasing the odds of cell survival after virus inoculation (Stafford et al., 2011). Preference tests have indicated that more thrips can be found on infected pepper plants than non-infected pepper plants. It appears that more offspring are also produced on infected plants and L1s hatched earlier from eggs while pupating faster on TSWV-infected plants (Maris et al., 2004). There are currently no reports of a pathogenic effect of TSWV on the thrips vector.

With persistent infection of the vector host, it is apparent that some host response might occur during TSWV infection. A partial transcriptome was originally sequenced, using Sanger sequencing technologies, to identify *F. occidentalis* transcript sequences, initiating the -omics era for western flower thrips (Rotenberg and Whitfield, 2010). A total of 894 contigs and 11,806 singletons were identified with 31% having significant similarity to protein sequences. An initial batch of 74 sequences was identified as insect innate immunity transcripts, providing the annotation platform for further transcriptomics studies (Rotenberg and Whitfield, 2010). A transcriptome was further built with the addition of 454 Roche sequencing to construct a resource for identification of thrips specific transcripts. The hybrid transcriptome provided insight into exploration of the thrips proteome. A total of 5.3% of the protein spots identified were differentially regulated during virus infection. This is a relatively low number of responsive genes, which could be indicative of a level of vector competency where the host is not greatly perturbed (Badillo-Vargas et al., 2012). This is the first research to provide candidate responsive proteins to virus infection within *F. occidentalis* challenged with TSWV, and from this research

RNAi was established through injection with dsRNA targeting the V-ATPase-B transcript (Badillo-Vargas et al., 2015). Further transcriptome description exists for the salivary glands of *F. occidentalis*. Many genes were identified for detoxification and inhibition of plant defense responses and extra-oral digestion of plant structural tissues (Stafford-Banks et al., 2014). Current transcriptome resources, proteome resources, and genome resources for the western flower thrips provide the groundwork for a new –omics era of scientific inquiry for the thrips vector (Rotenberg et al., 2015).

Insect Transcriptome Responses to Plant Viruses

Transcriptome analysis through the use of RNA-seq has become a powerful approach for developing an understanding of ecological and molecular interactions associated with plant-virus-vector biological systems. Examples of vector transcriptome-wide published studies exist for plant viruses that are transmitted by various modes, *i. e.*, non-circulative/stylet-borne, non-circulative/ semi-persistent, circulative/non-propagative, and circulative/propagative (Table 1.1). Encompassing these transmission modes are vectors enriched in the order Hemiptera (aphids, leaf hoppers and planthoppers), including soybean aphid (*Aphis glycines*)(Cassone et al., 2014a), black-faced leafhopper (*Graminella nigrifrons*)(Cassone et al., 2014b, Chen et al., 2012b, Zhang et al., 2010), pea aphid (*Acyrthosiphon pism*) (Brault et al., 2010), whitefly (*Bemisia tabaci*) (Luan et al., 2011), white-backed planthopper (Sogatella furcifera) (Xu et al., 2012). Exploration of the insect response during interaction with a plant virus is of major interest for unraveling foundational concepts of vector competence and for the development and deployment of novel strategies for controlling vector-borne diseases.

Detailed exploration and cataloguing of global expression patterns during plant virus transmission provides insight (hypotheses) into how the virus perturbs the insect vector system. One common set of biological processes revealed by transcriptome-wide analysis of plant virus-insect vector systems is collectively associated with insect innate immunity (Table 1.1). Differentially expressed transcripts within immune gene categories can be identified as common across different insect vectors with contrasting transmission strategies. Autophagy is dynamically differentially expressed within aphid, whitefly, and planthopper. During autophagy, double-membrane vesicles engulf protein aggregates and non-functioning organelles and transport them to lysosomes for degradation (Brackney, 2017). Insect infecting viruses (*e.g.* *Vesicular stomatitis virus* VSV) are known to induce autophagy in *Drosophila* cells and adult *Drosophila* (Shelly et al., 2009), and autophagy was also significantly induced in the gut between two and four days post-infection during *Tomato yellow curl leaf virus* (TYLCV) infection in whitefly (Wang et al., 2016a). Identification of autophagy as responsive to arbovirus infections in natural virus-vector interactions is currently limited (Brackney, 2017), but further exploration will elucidate its role in insect innate immune response.

Scavenger receptors have many different functions ranging from lipid transport, transport of cargo within the cell, and pathogen clearing (Canton et al., 2013). These along with CLIP-domain serine protease and TOLL pathway transcripts appear to change in virus infected aphid and leafhopper. CLIP-domain serine proteases are present in hemolymph of insects and they function in innate immune responses when they activate prophenoloxidase (proPO) or the Toll-ligand Spätzle (Kanost and Jiang, 2015). The proteolytic activation of Spätzle by CLIP-domain serine protease forms an active Toll ligand leading to synthesis of antimicrobial peptides along with activation of prophenoloxidase for melanization response (Kanost and Jiang, 2015). Further

description is needed for describing this response during virus infection, but it is known that the phenoloxidase (PO) cascade is active in mosquito cells lines against Semliki forest virus (SFV) (Rodriguez-Andres et al., 2012). Other common categories of differentially expressed transcripts also reside within more general categories such as: cellular respiration, proteolysis, transcription, transport, protein and lipid metabolism, and ubiquitin-proteasome pathways (Table 1.1). Common responses spanning different virus-vectors and transmission styles indicate similarities among transmission types and infection statuses. My research has expanded the basic knowledge underpinning the complex and dynamic relationship between thrips vectors and the plant viruses they transmit. Thrips response to TSWV infection is development stage dependent with transcriptomics of each stage providing a fine resolution of the interaction between virus movement and thrips development. Furthermore, description of the intricacies of stage-specific conserved responses provides a novel path towards development of control strategies effective against a wide array of vector-borne diseases.

Figures and Tables

Table 1.1 Global differential expression categories in insect vectors transmitting viruses

Insect	Insect Species	Virus	Transmission Type	Immune Categories	Author	Other Categories
Soybean Aphid	*A. glycines*	*Soybean mosaic virus* (SMV)	Non-circulative Stylet-borne	Autophagy, Caspases, Inhibitors of apoptosis, Peroxidases, Scavenger receptor, Serine protease inhibitors, TOLL	Cassone 2014a	Cellular respiration
Black-faced leafhopper	*G. nigrifrons*	*Maize chlorotic dwarf virus* (MCDV)	Non-circulative Semi-persistent	TOLL, Peroxidases, Superoxide dismutase, Scavenger receptor, Clip-domain serine protease, Peptidoglycan recognition proteins	Cassone 2014b	Proteolysis, Protein and energy metabolism
Pea Aphid	*A. pisum*	*Pea enation mosaic virus* (PEMV)	Circulative Non-propagative	None	Brault 2010	Cuticle protein, cytoskeleton, vesicles, signal transduction, Translation, Protein degradation, Stress and defense
Whitefly	*B. tabaci*	*Tomato yellow leaf curl China virus* (TYLCCNV)	Circulative Non-propagative	Autophagy, Lysosome, Complement and Coagulation, Apoptosis, Antimicrobial peptide, Melanization	Laun 2011	Ubiquitin-proteasome pathway, Cell cycle, Metabolism, Signal transduction
White backed planthopper	*S. furcifera*	*Southern rice black-streaked dwarf virus* (SRBSDV)	Circulative Propagative	RNAi, Autophagy, Lysosome, Antimicrobial peptide, Melanization	Xu 2012	Ubiquitin-proteasome pathway, Cell cycle, Protein metabolism, Lipid metabolism
Black-faced leafhopper	*G. nigrifrons*	*Maize fine streak virus* (MFSV)	Circulative Propagative	TOLL, Peroxidases, Superoxide dismutase, Scavenger receptor, Clip-domain serine protease, Peptidoglycan recognition proteins, JNK	Cassone 2014b, Chen 2012	Proteolysis, Protein and energy metabolism

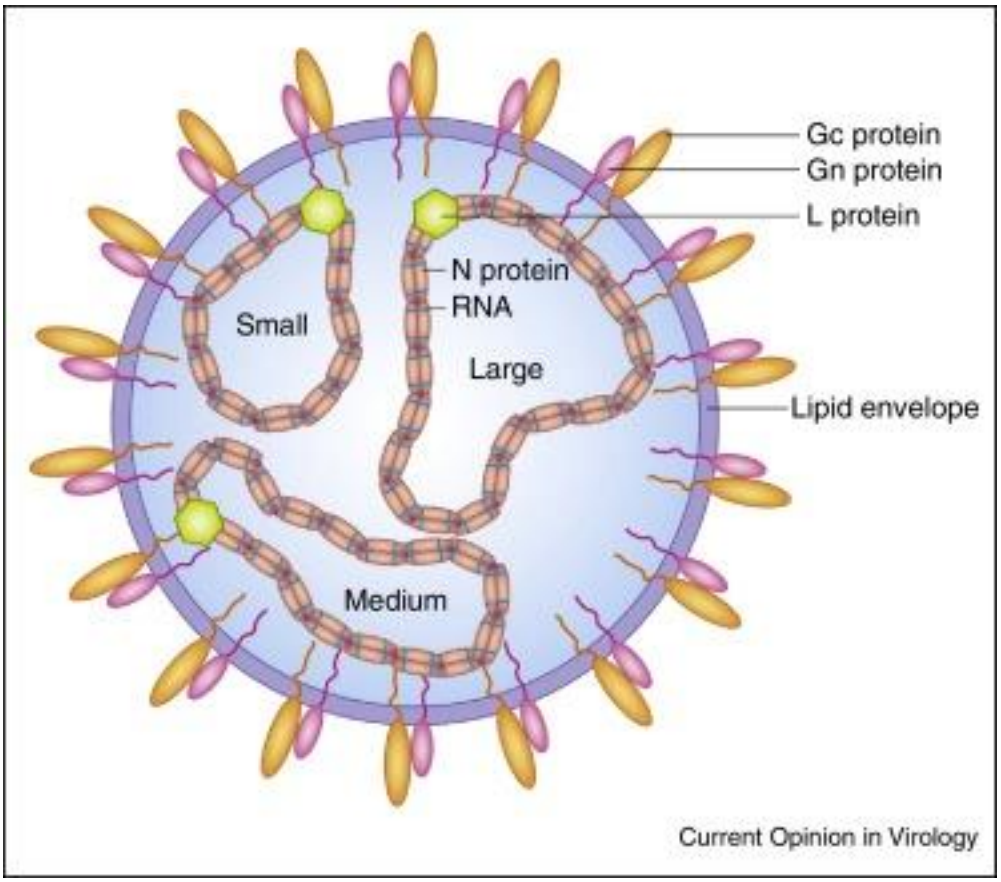

Figure 1.1 Diagram of TSWV virion.

The virus genome in comprised of three negative sense RNA segments: Small (S), Medium (M), and Large (L). The RNA genome is encapsulated by the nucleocapsid protein (N) to form ribonucleoprotein (RNP) and is protected by a phospholipid bilayer with embedded glycoproteins (Gn and Gc). The RNA-dependent RNA polymerase (RdRp) is associated with the RNPs (Rotenberg et al., 2015).

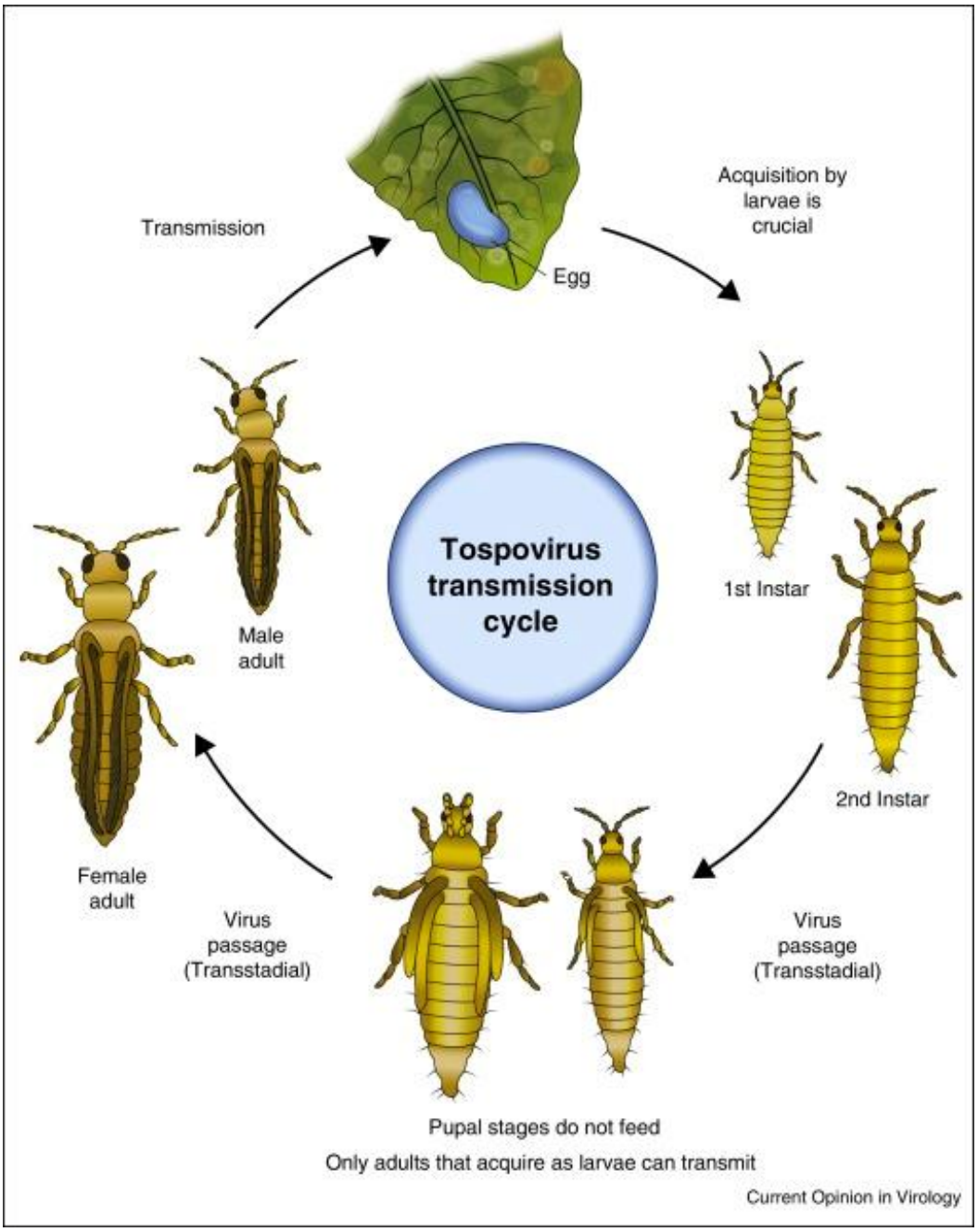

Figure 1.2 TSWV transmission cycle.

Transmission as adults only occurs by adult thrips that acquired TSWV during larval stages. Thrips hatch from eggs oviposited by adult female thrips and develop into first instar larvae. They acquire TSWV by feeding on infected plant tissue and the virus persists transstadially to the adult winged form. Adults disperse the virus by inoculating plants (Rotenberg et al., 2015).

Chapter 2 - Thrips developmental stage-specific transcriptome response to *Tomato spotted wilt virus* during the virus infection cycle in *Frankliniella occidentalis*, the primary vector[1]

[1]This chapter was published in 2017 in *Virology* as: Schneweis, D. J., Whitfield, A. E., and Rotenberg, D. 2016. Thrips developmental stage-specific transcriptome response to *Tomato spotted wilt virus* during the virus infection cycle in *Frankliniella occidentalis*, the primary vector. Virology 500 (2017) 226–237. (j.virol.2016.10.009).

Abstract

Tomato spotted wilt virus (TSWV) is transmitted by *Frankliniella occidentalis* in a circulative-propagative manner. Little is known about thrips vector response to TSWV during the infection process from larval acquisition to adult inoculation of plants. Whole-body transcriptome response to virus infection was determined for first-instar larval, pre-pupal and adult thrips using RNA-Seq. TSWV responsive genes were identified using preliminary sequence of a draft genome of F. occidentalis as a reference and three developmental-stage transcriptomes were assembled. Processes and functions associated with host defense, insect cuticle structure and development, metabolism and transport were perturbed by TSWV infection as inferred by ontologies of responsive genes. The repertoire of genes responsive to TSWV varied between developmental stages, possibly reflecting the link between thrips development and the virus dissemination route in the vector. This study provides the foundation for exploration of tissue-specific expression in response to TSWV and functional analysis of thrips gene function.

Introduction

Frankliniella occidentalis (Pergande), commonly known as the Western flower thrips, is a member of the insect order Thysanoptera (family Thripidae) and classified taxonomically in the hemipteroid assemblage with the orders Hemiptera, Pscocoptera, and Phthiraptera. Thrips are herbivorous, polyphagous insect pests that feed on a wide array of plant species, causing crop losses worldwide (Reitz, 2009). In general, thrips have a high reproductive capacity and develop rapidly from egg to adult within 14 days under constant conditions (23°C at 16h:8h light:day) (Moritz et al., 2004)The lifecycle of *F. occidentalis* includes the egg, two actively feeding larval stages (L1 and L2), quiescent prepupal (P1) and pupal (P2) stages and a sexually dimorphic adult stage. Post-embryonic development of thrips is intermediate between hemi- and holometabolism (Lewis, 1973) whereby the larval stages resemble adults (hemi-) and the pupal stages undergo major dissolution of various imaginifugal structures (late L2 stage) and reformation of internal anatomical structures (holo-), including those of the reproductive organs, sensory organs and digestive tract (Moritz, 1995). As such, this type of metamorphosis in thrips has been referred to as 'remetaboly' (Takahashi, 1921) with the suggested classification of thysanopterans with Coccina and Endopterygota in a group called 'Holometamorpha' (Moritz, 1995).

Frankliniella occidentalis is one of the most efficient thrips vectors of tospoviruses, transmitting seven of the 28 currently approved or described Tospovirus species (Oliver and Whitfield, 2016, Rotenberg et al., 2015). *Tomato spotted wilt virus* (TSWV) (family *Bunyaviridae*), the type member of the genus *Tospovirus*, is considered one of the ten most economically important plant pathogenic viruses worldwide (Riley et al., 2011). TSWV is a membrane-bound, single-stranded negative-sense RNA virus with a genome comprised of three

RNA segments encapsulated in nucleocapsid protein (N) and enclosed in a host-derived virion envelope. The virus is transmitted in a circulative propagative manner by permissive thrips vectors.

The TSWV route of dissemination and accumulation from the midgut to the salivary gland in the thrips vector is tightly linked to insect development. TSWV is acquired during feeding by larval stages (L1 and L2), persists through pupal development (P1 and P2) and accumulates in the salivary glands of adults (Nagata et al., 2002). Newly emerged L1s are the most efficient stage at acquiring the virus and efficiency declines as the larvae age(Moritz et al., 2004)Only adults that had fed on infected plants as larvae can inoculate plants and are the primary plant-to-plant transmitting stage because they are winged and highly mobile. Naïve adult thrips that feed on infected tissue can acquire virus, but are refractory to inoculating the virus to the plant host. TSWV is not transmitted transovarially (Wijkamp et al., 1996a) larvae must emerge from infected tissue and feed to establish the next generation of inoculative adults. Virions ingested with infected plant tissues bind and enter the epithelium of the anterior region of the midgut, the primary barrier to virus acquisition (Whitfield et al., 2005b) where it then replicates and disseminates to the surrounding visceral muscle cells. Replication occurs in the visceral muscle cells and the principal salivary glands of the insect (Montero-Astúa et al., 2016, Ullman et al., 1993, Ullman et al., 1995, Wijkamp et al., 1995) and more recently it was documented that virus accumulated in the tubular salivary glands of adult *F. occidentalis* and that the extent of infection/accumulation of virus in the principal salivary glands was greater in adults compared to other tissue systems (Montero-Astúa et al., 2016). In addition, the ability (Montero-Astua et al., 2014) and capacity (Rotenberg et al., 2009b) of *F. occidentalis* to inoculate plants appears to be virus dose-dependent, *i. e.*, relative abundance of TSWV

nucleocapsid N used as a proxy for virus titer was correlated positively with efficiency (proportion of transmitting adults) and frequency (number of transmission events per individual) of transmission, respectively. Characterizing the molecular interplay between virus and vector across the insect lifecycle can provide greater understanding of the factors modulating the success of the transmission process.

The roles of TSWV proteins in virus replication, infection and movement within the plant host has been defined to some extent, however there is little known about thrips molecules and their role in the virus transmission cycle. During viral replication and movement in the insect host there are likely myriad interactions that culminate into successful transmission. Previous work comparing proteomes of infected and non-infected L1s of *F. occidentalis* resolved a subset of proteins that were differentially-expressed due to TSWV infection (Badillo-Vargas et al., 2012) and one study examined global expression (*de novo* RNA-seq analysis) on a single combined pool of developmental stages to provide a generalized description of transcriptome-wide response of *F. occidentalis* to TSWV infection (Zhang et al., 2013). To describe the dynamic and complex molecular interaction between TSWV and *F. occidentalis* over the course of development, this study examines transcriptome-wide expression of three developmental stages that mark key points in dissemination of virus in the vector body and illustrates the utility of a *F. occidentalis* genome as a reference for RNA-seq analysis. Assembled stage-specific transcriptomes were used to infer ontologies of responsive transcripts, in turn providing hypotheses for unraveling the roles of these thrips molecules in thrips-TSWV interactions.

Results

Virus infection status of independent cohorts of insects selected for RNA-sequencing

To ensure the basis of comparison between virus-infected and non-infected cohorts of insects, infection rates (proportion of infected L1s of 10 individuals subsampled from each cohort) and an estimate of group virus titers (*i. e.*, normalized abundance of TSWV-N RNA for each cohort as measured by real-time qRT-PCR) were determined for the four biological replications entering the RNA-seq experiment. Percent infection rates of L1s sampled 21-hours (L1-21h) after a 3-hour AAP on TSWV-infected tissue ranged from 80% - 100%, an indication that each biological sample included in the virus-exposed treatment was significantly enriched for virus-infected individuals. Cohort titers were significantly lower ($P < 0.0001$) during early infection events of the L1 thrips (2 hours after a 3-hr AAP) compared to the ensuing developmental stages (Figure 2.1, $P < 0.0001$), and titers were not significantly different between L121h, P1 and Adult cohorts ($P = 0.19 – 0.92$)

Raw read and transcriptome assembly statistics

Illumina RNA sequencing of 24 RNA-Seq libraries representing three developmental stage-times (L1-21, P1, Adult-24), two treatments (+/- virus), and four biological replications of the time course experiment (Figure 2.1) yielded 878,175,618 raw reads (100 bp reads) of 68,441 Mb of sequence. On average across libraries, 78.2% of the raw reads passed the filter with a mean Phred quality score of 33.86 (Table S2.2). Genome-reference assembly of the three development stage transcriptomes resulted in comparable numbers of contigs (~40,000), mean contig length and contig N50s (Table 2.1).

Differential gene expression associated with virus infection

A total of 178, 181, and 127 transcripts were differentially expressed due to TSWV infection during L1-21h, P1, and Adult-24h developmental stage-times, respectively (Table S2.3). The majority (90%) of the differentially expressed transcripts for L1-21h were down regulated due to virus exposure (17/161, Up/Down), while comparable numbers of transcripts were up and down-regulated in the P1 (92/89, Up/Down) and Ad-24 (59/68, Up/Down) stages (Figure 2.2). The average fold change of these TSWV-responsive transcripts was 2.54, 2.33, and 2.69 for L1-21, P1, and Ad-24, respectively. However, 10% of transcripts exhibited fold changes ranging from 3.56-17.86 in the 90^{th} percentile of the dataset (Figure 2.3). The top ten most responsive transcripts in each stage and their Blastx annotations are shown in Table 2.2. Within the top ten responding to virus infection, all were down-regulated in L1-21, while the majority were up-regulated in the P1 and adult stages.

Non-annotated transcripts responsive to virus infection

A significant proportion of DE transcripts were non-annotated at the Blastx cut-off of $E < 10^{-3}$ (Table S2.3), including some of the most responsive to virus (Table 2.2). Specifically, non-annotated transcripts comprised 33% (P1), 48% (L1-21) and 65% (Ad-24) of the collection of DE transcript sequences per stage, and this trend was reflected in top-ten responding transcript sequences for the pre-adult stages (Table 2.2). Translated sequence of 66% of the repertoire of DE non-annotated transcripts contained predicted functional domains (Interpro), indication that these transcripts have a conserved functional domain but have diverged significantly and may have unique roles in thrips biology and/or thrips-tospovirus interactions.

Unique and shared differentially-expressed transcripts between developmental stages

Cross-development stage comparisons of TSWV-responsive genes were performed to determine if virus infection had a universal effect on genes based on sequence or sequence-inferred function. Two- and three-way comparisons of sequences (Figure 2.4A) or Blastx gene descriptions (Figure 2.4B) revealed that the effect of the virus on the thrips transcriptome was largely unique to each developmental stage, *i.e.*, less than 1% and 1.5% of the virus-responsive transcript sequences or gene descriptions, respectively, were shared by all three stages and likewise, less than 11% and 10% were shared between two stages. Examination by stage revealed that the P1 stage had a greater proportion of unique transcripts altered by virus (83%, Figure 2.4A) compared to L1-21 (68%) and Ad-24 (78%), and this uniqueness was also reflected in the annotations of the altered transcripts (82% vs 71% (Ad-24 or L1-21), Figure 2.4B). Two of the three 3-way-shared transcripts were in the top ten responsive transcript sequences for the P1 sequence collection (FOCC009158-RA and FOCC016444-RA) (Table 2.2), both with no significant Blastx annotation (NA). The other transcript shared by all stages was annotated as an endonuclease that cleaves DNA (i.e. Deoxyribonuclease I, FOCC007280). With regards to two-way comparisons, the subset of responsive transcripts and annotations shared by L1-21 and the other two stages was larger than the set shared between the P1 and Ad-24 stages. Within the 16 transcripts shared between L1 and P1, multiple genes were predicted to be involved in oxidative stress response and starvation response, including apolipoprotein d, protein takeout, peroxiredoxin 6, and cytochrome p450-4c3. The genes shared by the feeding stages (larva and adult) was a smaller subset of 7 total including three genes known to encode salivary gland and gut digestive enzymes (endoglucanase, beta-glucosidase 3-like isoform x1, and pancreatic

triacylglycerol lipase-like) in other insect species(Watanabe and Tokuda, 2010)including hemipterans (Campbell and Dreyer, 1985, Harmel et al., 2008). Similar annotated transcripts were identified in a transcriptome of the principal salivary glands of *F. occidentalis* (Stafford-Banks et al., 2014)

A total of six virus-responsive transcripts were shared between all three developmental stages based on exact sequence identity and gene descriptions. Deoxyribonuclease I, an endonuclease that cleaves DNA, (i.e. FOCC007280) was differentially expressed across all three stages and could potentially play a role in apoptosis(Enari et al., 1998)as well as myrosinase like-1, a glycoside hydrolase that plays an ecological role in volatile-mediated communication among insects(Bridges et al., 2002, Hopkins et al., 2009)The two other shared transcripts did not receive a significant blast annotation. Using eukaryotic linear motif prediction (Dinkel et al., 2016) FOCC016444-RA has a high incidence of GSK_3 phosphorylation sites near the 5' end in frame 1. They are suggested to act in an inhibitory manner in many different biochemical pathways. CK_1 phosphorylation sites are also prevalent near the 5' end in frame 1 and they are known to play a role in cell division, DNA repair, and glycogen metabolism. Finally, the 3' end in frame 1 has multiple forkhead-associated (FHA) domains that are known to act as signal transduction modules. They are important in cell cycle checkpoints, DNA repair, and transcriptional regulation. FOCC01644-RA might function as an inhibitor important during cell cycling. The second NA transcript, FOCC009158-RA, has FHA domains and WDR5 WD40 repeat-binding ligand domains towards the 3' end of frame 1. The combination of the two domains listed above indicates function in post-translational modification of histones and potentially control of gene transcription, cell cycle progression, and DNA repair.

Validation of RNA-Seq expression analysis

Of the 21 possible comparisons of target expression levels between virus-infected and non-infected samples (7 transcript targets x 3 stages), real-time qRT-PCR confirmed 71% at a statistical level of significance (Kruskal Wallis, $P < 0.05$, n = 3 biological replications) (Table 2.3). Based solely on the direction of change in response to virus, 85% of the comparisons were concordant between RNA-Seq (FPKM fold change) and real-time qRT-PCR (relative expression) estimation of transcript abundance.

Distribution and enrichment of TSWV-responsive thrips transcripts into gene ontologies (GOs)

A concatenated Blast2Go file comprised of non-redundant DE transcript sequences in the three stage datasets was analyzed to classify the sequences into a combined set of biological processes and molecular functions (Figure 2.5). Of the 254 TSWV-responsive transcript sequences with significant Blastx matches (54.4%), 207 had mapped GO IDs (GO terms). Classification of DE transcript sequences into 16 GO categories revealed developmental stage-related trends (Figure 5, Table S2.4). The most enriched category of 'structural constituent of cuticle' comprised 23.7% (45 non-redundant between stages) of the GO sequences, of which 75% and 22.4% were virus-responsive in the L1 and P1 stages, respectively. Similarly, sequences classified in the 'chitin-based cuticle development' and 'chitin process' categories were overrepresented in the pre-adult stages. In the two 'cuticle' GO categories ('structural constituent of cuticle' and 'chitin-based cuticle development'), 57 non-redundant transcript sequences were responsive to virus of which 39 were annotated as various cuticular proteins, 13 as endocuticular structural glycoproteins, and 5 as other cuticle-associated proteins (*e. g.*,

proline-rich extensin-like protein epr1). These cuticle-associated proteins were largely (85%) down-regulated in response to virus. Also apparently unique to the pre-adult stages were DE sequences associated with intracellular transport (6.8% of GO sequences). Sequences classified in the five categories: 'ion binding', 'transferase activity', 'transcription/translation', 'nervous system process' and 'receptor activity' were specific to P1 and adult stages, collectively comprising 11.6% of the GO sequences. With regards to direction of change in response to virus, 90% of the L1-associated GO sequences were down-regulated, mirroring the overall direction of change with regards to all DE transcripts for this stage (Figure 2.2) including those with no apparent orthology to other sequences (non-annotated).

Innate immune genes

The suite and number of putative innate immune genes responsive to TSWV varied across the three thrips developmental stages (Table 5). With the fewest number of matches, TSWV infection of L1s 24 hours after exposure resulted in downregulation of transcripts known to be associated with proteolysis (serine type endopeptidase) and anti-oxidant defense (peroxiredoxin). With a more diverse repertoire of matches, TSWV infection during the P1 stage resulted in downregulation of transcripts known to be associated with Toll activation or hemolymph coagulation and melanin production in response to pathogen infection (CLIP serine proteases), Toll signaling (spaetzle, Toll-binding ligand), proteolysis (serine type endopeptidase), cellular immunity (scavenger receptor croquemort, hemolymph), and inhibition of apoptosis (IAP). In addition, the P1 stage revealed up-regulation of transcripts consistent with detoxification (UDP-glucuronosyl/UDP-glucosyltransferase), oxidative stress (peroxidasin homolog), and proteolysis (peptidases). Unique to the emergent viruliferous adult thrips, 75% of

the innate immune protein matches were annotated as hexamerins, insect larval and pupal storage proteins (Telfer and Kunkel, 1991) that have been also shown to be inducible by juvenile hormone (Zhou et al., 2006) and 20H ecdysone (Manohar et al., 2010) and associated with humoral immunity (Burmester, 1999) namely pro-phenol oxidase (PPO)-activating immunity in arthropods (hemolymph melanization and coagulation).

Discussion

The central hypothesis of this study is that the culmination of TSWV processes that occur in the permissive thrips vector perturbs gene expression and/or accumulation of transcripts, and that the virus effect varies over the course of development. We documented the differential effect of virus on the transcriptomes of the three thrips developmental stages that mark key changes in thrips morphology (Moritz, 1989, Muller, 1926) and tissue tropism of TSWV (Montero-Astúa et al., 2016, Ullman et al., 1992c). This stage-dependent effect was evident by the direction of change in expression, the high proportion of DE transcript sequences unique to a particular stage, inferred ontologies of these sequences, and the varying proportions of non-annotated, and possibly thrips-unique responsive transcripts. Most apparent was the nearly universal (90%) down-regulation of virus-responsive transcript sequences in the first instar larvae during early infection (Figure 2.2). This finding corroborates a previous proteomics study that used the same strain of TSWV, *F. occidentalis* isolate and acquisition access period (3 hours) and reported the down-regulation of 62% of the resolved DE proteins in infected L1s (Badillo-Vargas et al., 2012). Previous microscopic observations of immunolabeled TSWV proteins in *F. occidentalis* report that virus infection is restricted to the midgut tissues during L1-21 stage-time (Montero-

Astúa et al., 2016, Ullman et al., 1992c) a time at which the relative abundance of viral N RNA increased 14 fold from the L1-2h time point (Figure 2.1).

While TSWV significantly altered expression of a diverse repertoire of thrips genes, the effect was subtle in magnitude (fold change in expression) and richness (numbers of responsive genes), with less than 1% of the transcript sequences differentially-abundant in response to virus. This subtlety may point to a dilution effect of using whole bodies and furthermore, pools of insect bodies when only a few tissues/cells may be responding to virus along the route of dissemination. It may also underscore our attempt to examine the direct effect of the virus on the vector by limiting persistent exposure to virus-infected plants (3 hour AAP, then reared on green bean pods), thus eliminating infected plant-mediated indirect effects on transcript abundance which others have documented to play a substantial role in vector transcriptome response (Cassone et al., 2014b). Regardless of the number of responsive genes in the present study, the differential effect of virus infection during thrips development warrants further investigation of refined temporal and spatial (tissue-specific) analysis of gene expression to understand the basis of the molecular interaction between virus and vector. Furthermore, research is also needed to describe the functions of the numerous TSWV-responsive non-annotated (NA) transcripts with predicted protein functional domains identified that may be unique to thrips-tospovirus interactions.

Variation in virus titer and transmission is often observed at the individual insect level and between replicated experiments (biological replication) even under controlled conditions (Montero-Astúa et al., 2016, Rotenberg et al., 2009b). This biological variation and innate experimental variation in the present study appeared to influence statistical resolving power. It was evident that while a robust set of transcripts formed the core of the virus effect in each

developmental stage, removal of one apparently disconcordant biological replicate increased the number of responsive transcript sequences by 2.6 fold and average fold change by 9%. This finding underscores the natural variation in the complex system of virus, vector and rearing conditions of these types of experiments and highlights how influential biological replications can be in determining outcomes of analyses as sensitive as RNA-seq (Robles et al., 2012). As such, it is not surprising that a previous RNA-Seq analysis of one un-replicated pool of mixed stages of *F. occidentalis* exposed to TSWV reported 1,454 virus-responsive 'unigenes' (Zhang et al., 2013).

The developmental stage-associated changes due to virus infection may highlight the tightly-coordinated link between thrips development and tissue tropism. For example, the repertoire of differentially-abundant putative innate immune gene transcripts supports this hypothesis. During a time when virus infection is known to be limited to the midgut (L1), there was a downregulation of transcripts that encode proteins associated with proteolysis and detoxification in response to microbial infection and oxidative stress in other insect systems. This finding corroborates the previously reported downregulation of similar types of innate immune associated proteins, namely cytochrome b-c1 complex subunit 2, peroxiredoxin 1-like, and phospholipid hydroperoxide glutathione peroxidase, in TSWV-infected L1 thrips using a proteomics approach (Badillo-Vargas et al., 2012). In the present study, we documented a concerted upregulation of transcripts putatively associated with detoxification, oxidative stress, proteolysis and inhibition of apoptosis in P1 thrips. While thrips belong to the hemipteran assemblage, which includes aphid and other hemipteran vectors of plant viruses, thysanopterans undergo unique post-embryonic development whereby transformation proceeds from a larval stage to at least two pupal (quiescent) stages and some of the organs and tissues that exist

exclusively in the larval stage (imagifugal) are dissolved during transformation into adults (Moritz, 1989). The apparent 'clearing' of virus from midgut tissues prior to entering P1 (Montero-Astúa et al., 2016, Nagata et al., 1999) and during pupation (Tsuda et al., 1996) presents a unique strategy for modulating and sustaining a persistent infection necessary for successful transmission to the plant host by adult thrips. During a time when the virus begins to accumulate in the early adult stage, the majority of differentially-abundant transcript sequences matched hexamerin proteins, multi-subunit insect storage proteins that have been found in high concentrations in the hemolymph prior to metamorphosis (Burmester, 1999, Telfer and Kunkel, 1991) and have been implicated in humoral immune response to pathogen invasion (Beresford et al., 1997, Phipps et al., 1994, Tang et al., 2014, Wang et al., 2010).

One highly enriched category of DE transcripts, most notably unique to L1 and P1 thrips and for the most part downregulated in response to TSWV, encode proteins putatively associated with insect cuticles. These included proteins involved in cuticle structure (cuticular proteins (CPs), endocuticle structural glycoproteins, and extracellular matrix protein), chitin-based cuticle development (cuticular proteins, proline-rich extensin) and chitin metabolism (probable chitinase 3, collagen alpha-1 chain-like, chondroitin proteoglycan-2-like). In insects, cuticle and its primary biopolymer components, cuticular proteins and chitin, are periodically turned-over and new cuticle is secreted by the insect epidermis during ecdysis (molting) to accommodate the rapid growth and expansion of the body, and it is thought that temporally and spatially-dynamic epidermal expression of diverse cuticular and endocuticle proteins occurs to support the structure of different hard and soft cuticles of insect body parts during development (Willis, 2010). It is known that cuticles also line foregut and hindgut regions of the alimentary canal (Chapman, 2013, Maddrell and Gardiner, 1980). The midgut of the majority of insects is lined with a

proteinaceous and chitin-containing peritrophic matrix (Zhu et al., 2016) while in thysanopterans and hemipterans, the epithelial microvilli are instead surrounded by a double-lipid perimicrovillar membrane (PMM) (Cristofoletti et al., 2003, Silva et al., 2004) derived from Golgi membranes (Silva et al., 1995). In blood-feeding hemipterans, the PMM has been chemically-characterized and was determined to contain lipoproteins, glycoproteins and carbohydrate-binding molecules (Albuquerque-Cunha et al., 2009, Gutierrez-Cabrera et al., 2014).

The concerted down-regulation of CP and endocuticular glycoproteins in the pre-adult stages of *F. occidentalis* under TSWV infection may signify a delay in molting or turnover of cuticle-associated proteins. In the case of the P1 stage, downregulation of cuticle-associated transcripts may indicate viral infection of cuticle-lined regions of the accessory or primary salivary gland ducts (Ullman et al., 1992a) during the late L2 stage. In the case of the L1 stage 24 hours after initial exposure to the virus, the extent of infection is the midgut epithelium, so a delayed effect on exo-cuticle development would be suggestive of a systemic effect of gut infection on the whole body or body parts distant from the site of virus infection. Alternatively, one hypothesis is that CPs and endoC-GPs transcripts are expressed in the alimentary canal of *F. occidentalis*, and expression is altered during epidermal cell infection by TSWV. Analysis of localization of endocuticle glycoprotein expression in L1 *F. occidentalis* has revealed that it is expressed in the midguts and salivary glands (Catherine Stewart and Anna Whitfield, unpublished data). A study with a Tenuivirus found that a planthopper cuticle protein interacts directly with the nucleocapsid protein and knockdown of the transcript using RNAi resulted in reduced virus abundance and transmission efficiency (Liu et al., 2015). One study reported a similar coordinated down-regulation of six of seven CP transcript sequences of the pest moth

species *Plodia interpunctella* (Indian meal moth) 24 hours after exposure to the baculovirus *Plodia interpunctella* Granulosis Virus (PiGV)(McTaggart et al., 2015). The authors hypothesized that infection suppressed activities of cuticular proteins embedded in the peritrophic matrix, a structural barrier to pathogen attack (Kato et al., 2008, Levy et al., 2011) however they alternatively offered the possibility that the pathogenic virus may also negatively affect molting. While it has been shown that the PMMs of plant-feeding hemipterans and thrips species, including *F. occidentalis*, contain significant levels of membrane-bound α-glucosidase (Silva et al., 2004) it remains to be determined whether endocuticular glycoproteins or cuticular proteins serving functions beyond structure occur in the PMM of thysanopterans.

Virus-responsive transcripts that encode proteins that hydrolyze complex plant carbohydrate-containing compounds (e.g., glycosides and pectins) were most prevalent in the two feeding stages with a few exceptions. Differential abundance of these types of transcripts may indicate that tospovirus infection modulates extra-oral (salivary gland) and gut digestive processes in thrips. One of the few DE transcript sequences common to the three infected developmental stages was myrosinase-1, a thioglucosidase (glycoside hydrolase) that can be expressed by both plants (primarily *Brassicaceae*) and insects. Plant and insect-expressed myrosinases serve a similar ecological purpose, however with different outcomes. In plants under attack by herbivores, myrosinase hydrolyzes plant glucosinolates to produce byproducts, such as isothiocyanates (ITC), which are toxic to metazoans and therefore protect the plant from further consumption (Hopkins et al., 2009). Some aphid species have the capacity to sequester plant glucosinolates to render them ineffective (Bridges et al., 2002, Hopkins et al., 2009). During attack by predators, however, insect-expressed myrosinase comes in contact with released glucosinolates during predation to produce ITC, a volatile that has been described to

serve a role in communication of warning signals between insect members under attack by predation (Bridges et al., 2002). Isothiocyanates have been shown to act synergistically with the alarm pheromone E-β-farnesene (Dawson et al., 1987). While there did not appear to be a discernible pattern to the direction of expression of the various transcript isoforms in the feeding stages, the two pupal stage myrosinase sequences were both down-regulated under infection. Interestingly, (Belliure et al., 2008) found that thrips predation was decreased in TSWV-infected insects. Establishing a link between myrosinase expression and thrips performance will be an area of study in the future and it will help to describe the dynamics observed during TSWV infection.

Transcripts that encode proteins associated with inter- and intracellular transport of molecules were virus-responsive in the pre-adult stages. Based on GO annotation, three down-regulated transcripts (alpha-tocopherol transfer isoform 1 and isoform 2, potassium channel subfamily k member 9) are involved in retention of membrane potential. Gene expression dynamics in membrane potential might be indicative of responses to the virus infection route. Bunyaviruses have been shown to require potassium channels for successful infection of host cells. The requirement of potassium channels appears to be early in bunyavirus infection of a host cell and the interaction between the potassium channels and virus is proposed to contribute to early events in the virus life cycle related to uncoating and/or formation of RNA replication factories (Hover et al., 2016). Further evidence of transport gene expression changes arises from knowledge that virus infection can also affect microtubule dynamics such as depolymerization and stabilization (Dohner and Sodeik, 2005, Ramanathan and Jonsson, 2008). Using animal cell lines, a study of the bunyavirid Crimean-Congo hemorrhagic fever virus (CCHFV) found that CCHFV RNA and progeny virus levels were reduced by depolymerization of microtubules. It

was hypothesized that depolymerization of microtubules during early infection inhibited virus movement along microtubules and reduced capacity to reach a site of viral transcription (Simon et al., 2009). Two GTP binding transcripts (*i.e.* tubulin beta-4b chain and tubulin alpha chain-like) displayed over two fold down regulation in the pre-pupa stage. Through sequence similarity annotations, both transcripts are involved in microtubule formation. Building upon the previous studies, down regulation of key components for microtubule formation and membrane potential in infected pre-pupa might be indicative of an attempt by the host to restrict virus cellular movement prior to the second cycle of accumulation during the adult stage.

Comparison of findings documented in the present study to two other global expression studies for *F. occidentalis* revealed a few commonalities with regards to types of TSWV-responsive genes and processes. For example, in addition to negative regulation of a few innate immunity-associated proteins in L1 thrips, Badillo-Vargas et. al. (2012) documented the differential expression of proteins that play roles in transport (*i.e.* vitellogenin and apolipoprotein d), indicating that cellular trafficking may be perturbed during TSWV infection. In that study, multiple proteins involved in cytoskeletal and cellular structure were also found to change in abundance under infection, providing additional evidence for virus utilizing or disrupting movement of molecules in the insect-host cells. A total of nine proteins were identified as putatively involved in localization, membrane-associated, and transport at the L1 stage, and these gene ontology terms were common across transcripts determined to be differentially expressed in the present study. As one might expect, the magnitudes of differentially-abundant proteins (Badillo-Vargas et al., 2012) and transcripts (present study) of shared DE genes were not correlated (Vogel and Marcotte, 2012). Comparison to another RNA-Seq study revealed relatively few shared DE transcripts (9%) based on gene descriptions of a pathway enrichment

analysis (Zhang et al., 2013) whereby the authors used a *de novo*- assembled transcriptome of *F. occidentalis* and an un-replicated single sample of mRNA pooled from mixed stages infected with TSWV. Similar to the present study, the authors performed a GO-enrichment analysis and found that TSWV-responsive transcripts were enriched in 'structural constituent of cuticle.' However, gene descriptions for this group of cuticle-associated transcripts were not reported which precludes direct comparison with the relatively large proportion of CPs, endoC-GPs and other cuticle-associated proteins determined to be responsive to TSWV in pre-adult stages reported here. Furthermore, since all stages were essentially combined into one sample for sequencing in the published study, it could not be determined if this category was enriched in the pre-adult stages as determined in the present study. In total, our study provides new insight into the transcriptome-wide effect of virus infection over the course of insect vector development.

Materials and Methods

Thrips colony and TSWV source

A colony of *Frankliniella occidentalis* (Pergande) originating from Kamilo Iki Valley, Oahu, Hawaii, was maintained on green bean pods (*Phaseolus vulgaris*) as described previously (Ullman et al., 1992c). TSWV (isolate TSWV-MT2) was maintained on *Emilia sonchifolia* by thrips-transmission as described previously (Meister and Tuschl, 2004). The source of virus for experiments was symptomatic leaves from young *Emilia* plants 12 days post mechanical inoculation with leaf sap from an approximately one-month-old thrips-inoculated TSWV culture using methods described previously (Badillo-Vargas et al., 2012).

Virus acquisition by larval thrips

Colony bean pods impregnated with eggs were brushed to remove newly hatched thrips and incubated for 17 hr at 25^{o}C to generate a synchronized group (0 – 17-hr-old) of young first instar larvae (L1). Half of the young L1s were brushed onto bouquets of TSWV-infected *Emelia* leaves and the other half onto bouquets of healthy *Emilia* leaves as previously described (Badillo-Vargas et al., 2012) to achieve two experimental treatments: virus-infected (V) and non-infected (NV) thrips. The L1s were given a 3-hr AAP on the *Emilia* bouquets, then the larvae were gently brushed off and leaf tissue replaced by healthy green bean pods, allowing the insects to be reared in the absence of continued exposure to infected plant tissue.

Biological samples for analysis of virus accumulation and transcriptome-level response to virus

Four biological replications of a time-course experiment were conducted to determine virus titers in developing thrips, which provided the source of developmental stage-time samples for RNA-seq analysis of thrips gene expression in response to TSWV. Following the 3-hr AAP on infected and non-infected bouquets, cohorts of thrips were sampled during the L1 stage (two and 21 hours after exposure), the P1 stage (when ~ 90% were observed at this stage with the use of a stereoscope), and adult stage comprising females and males (24 hours post eclosion). For each treatment-sampling time point, one cohort of 75 – 100 insects was collected into a 1.7 ml microfuge tube using separate fine paintbrushes, then immediately flash-frozen in liquid nitrogen and stored at -80^{o}C. Total RNA was isolated from each sample using TRIzol reagent (Invitrogen, Carlsbad, CA) using methods described previous (Badillo-Vargas et al., 2012). RNA yields determined using the Nanodrop spectrophotometer (Agilent, Inc, Santa Clara, CA, USA) ranged

from 340-461 ng μl^{-1} for L1, 515-710 ng $\mu l^{-1}$for P1, and 669-679 ng $\mu l^{-1}$for adults. Aliquots of each sample were stored at -80ºC for virus titer determination and subsequent RNA sequencing.

To estimate virus titer per cohort, previously described methods for normalized real-time qRT-PCR quantification of TSWV nucleocapsid (N) RNA were followed (Badillo-Vargas et al., 2012, Rotenberg et al., 2009b). Briefly, cDNA was synthesized from 1µg of total RNA using Verso^{TM} cDNA kit (Thermo Scientific, Wilmington, DE, USA), then cDNA reaction volumes were diluted 10-fold with DEPC-treated ddH_2O. Real-time qRT-PCR was performed on two technical replicates of 20 µl-reaction mixtures containing 200 nM each of TSWV nucleocapsid (N) and thrips internal reference gene RP49 primers, iQ SYBER Green Supermix (Bio-Rad, Hercules, CA, USA). Reactions were run on the iCycler iQ Thermal Cycler with a 96 x 0.2 ml reaction module with iCycler iQ software (Bio-Rad). The internal reference RNA (RP49) was used previously for normalized real-time qRT-PCR quantification of TSWV titer in L1 thrips (Badillo-Vargas et al., 2012) and in the present study, the coefficient of variation in Ct values for RP49 between treatments within stage was at most 2%, indicating that it is invariant to virus treatment and can serve as a reliable reference for normalized expression analysis within stage. The 2-step amplification and melt protocol was run using the following cycling parameters: 95ºC for 3 mins, then 40 cycles of 95ºC for 1 min and 55ºC for 45s; then melt protocol of 55ºC for 1 min then 80 cycles of 10 seconds each with 0.5ºC increase in temperature at each cycle. The normalized abundance of TSWV-N RNA to RP49 RNA was calculated for each developmental-stage time point using the equation: $E_{RP49}^{Ct(RP49)}/E_N^{Ct(N)}$ (Pfaffl, 2001) where E = PCR efficiency of a primer pair, and C_t = the fractional amplification cycle number at which florescence emitted during the reaction first exceeds background fluorescence. To compare virus titers per cohort between developmental stage-time points, normalized abundance data were analyzed statistically

using SAS v.9.3 (SAS Institute, Cary, NC). The SAS procedure GLIMMIX was used to determine the best fit of data and residuals to perform Type III tests of fixed effects (F-tests). LSMEANS and p-values were computed post hoc to determine the statistical difference ($P < 0.05$) between pairwise developmental stage-time points. GLIMMIX analysis determined that the best fit of the normalized abundance data and accompanying residuals was lognormal distribution (link function = identity).

To determine the efficiency of acquisition for each biological replicate, ten individuals were arbitrarily collected from both treatments at the L1 21-hr time point for endpoint reverse transcriptase-PCR of TSWV N RNA using previously described methods (Badillo-Vargas et al., 2012). All insects sampled from the NV treatment (negative control) were determined to be PCR-negative for the virus.

RNA sequencing

Three developmental stage-time samples per treatment per biological replicate (*i.e.*, 24 RNA samples in total) were selected for sequencing based on temporal trends determined for virus accumulation, thrips developmental biology and key steps in the infection/transmission cycle of TSWV. The L1-21 stage (24 hours after larvae first exposed to infected tissue) was chosen because we consistently measure an early and significant increase in virus accumulation from five hours to 24 hours after exposure to infected plant tissue (Badillo-Vargas et al., 2012) which was also apparent for the present study (Figure 2.1), and it is during the young L1 stage that the vector is most efficient at acquisition (van de Wetering et al., 1996). The P1 was chosen because the virus has reached the salivary glands by the time it enters the pre-pupal stage (Montero-Astúa et al., 2016) and P1s undergo marked tissue differentiation, re-organization and

dissolution of some larval structures (Muller, 1926) including the gut epithelium (Moritz, 1989, Muller, 1926). The adult stage 24 hours after eclosure (Ad-24) from pupae was chosen because it efficiently transmits the virus at this stage-time (Rotenberg et al., 2009b).

Prior to RNA-seq sample preparation, the selected 24 RNA samples were subjected to a rigorous DNAse treatment using the Turbo DNA-free kit (Ambion, Foster City, CA) following manufacturer's instructions. Ten microliters of each sample received 1µl of Turbo DNAse, then samples were incubated at 37ºC for 30 min followed by a second 1 µl DNAse treatment for an additional 30-minute incubation period. RNA concentrations were determined using a NanoDrop spectrophotometer (NanoDrop Technologies, Wilmington, DE, USA) and quality was evaluated by the 2100 Bioanalyzer using Nanochip technology (Agilent Technologies, Inc., Palo Alto, CA, USA). All RNA samples were of high quality (no evidence of degradation).

RNA samples were submitted to the DNA Core facility at the University of Missouri for RNAseq library preparation with 800 ng of RNA using TruSeq chemistry (Illumina TruSeq RNA-Seq library prep kit version 2, San Diego, California) and multiplex single-end sequencing of indexed RNAseq libraries using Illumina Hi-Seq 2000. Each of the four biological replications of the experiment, *i.e.*, six RNAseq libraries consisting of two treatments (+/- TSWV exposure) and three developmental stages, was sequenced in separate lanes. Table 2.5 provides the quality indices and raw read summary statistics for the 24 libraries.

i5K Frankliniella occidentalis genome reference

The *F. occidentalis* draft genome was sequenced, assembled, and computationally-annotated by the Baylor College of Medicine, Human Genome Sequencing Center (BCM-HGSC, Houston, TX, USA) as part of a pilot project of the i5k Genome Sequencing Initiative for

Insects and Other Arthropods (http://arthropodgenomes.org/wiki/i5k). The biological sample prepared for sequencing was a cohort of females from a 10^{th} generation sibling-sibling breeding line generated from our lab colony. Preliminary sequence data was obtained from the BCM-HGSC website at https://www.hgsc.bcm.edu/arthropods/i5k. Illumina sequencing produced 532 million reads that were assembled and represented 263.8 Mb of sequence (contigs) at 158.7X coverage of the genome (size = 415 Mb of scaffold sequence including gaps). This draft genome assembly was used as the reference for differential expression analysis and consisted of 6,263 scaffolds (N50 = 948 Kb) and 17,553 Maker-predicted gene models.

Read-alignment, stage-transcriptome assembly, and differential expression analysis

The Tuxedo pipeline (Trapnell et al., 2012) was used for genome reference-based alignment and assembly of the RNA-seq reads for each developmental stage using the cloud computing resource of the iPlant Collaborative Discovery Environment (currently CYVERSE, http://www.cyverse.org). Raw reads (multiplex indices removed) for each treatment (V and NV) were aligned to the genome (scaffold fasta) by stage with TopHat v.2.0.9. The average percent of mapped reads ($\pm$ standard deviation) across the 24 RNA-seq libraries was 65.6 $\pm$ 6.3% (Table S2.2). Each stage transcriptome was assembled with the mapped-read BAM files of both treatments and all biological replicates (8 files) and the genome reference using Cufflinks v.2.1.1, and Cuffmerge v.2.1.1 was used to merge the eight assemblies and genome annotation file (gtf) into a single assembly per stage (L1, P1, and Ad). Transcript sequences were extracted from the Cuffmerge (gtf) files for each stage assembly with the Cufflinks "gffread" function. Using the mapped reads for each treatment and the corresponding stage, differential expression analysis was performed using Cuffdiff v.2.1.1 on geometrically-normalized count data per

transcript (fragments per kilobase of transcript per million mapped reads, FPKM) and FPKM fold change values were tabulated for differentially-expressed (DE) transcripts (FDR cutoff = 0.05, Benjamini-Hochberg multiple test correction). Visualization of DE data generated from Cuffdiff was performed using CummeRbund v. 2.6.1 (Trapnell et al., 2012) in the R statistical computing environment (R studio v0.98.945, Boston, MA). Visual inspection of tabulated FPKM values and subsequent manual fold change calculations for each biological replication revealed an apparent disconcordance in direction of change among replications. It was determined that the fourth biological replicate produced the largest proportion of disconcordant DE transcripts among the four replicates for two of the three stages (L1=48% and Ad=39%). Removal of this outlying replicate and a second iteration of Cuffdiff analysis with the remaining three biological replicates retained up to 93% of original set of DE transcripts, plus an additional 151 (L1), 114 (P1) and 69 (Ad) DE transcripts across the three stages. The reduced DE transcript dataset (Bioreps 1, 2 and 3) was used for all subsequent analyses and interpretations herein. Transcript identifiers were used to extract sequence text from the assembled stage-transcriptome fasta files for downstream analyses.

Innate immune genes

For each developmental stage, local Blastx analyses were performed using Blast 2.2.28+ on the set of DE transcripts (queries) against a subject database of innate immunity-associated protein sequences obtained from http://cegg.unige.ch/Insecta/immunodb (Waterhouse et al., 2007). The generated subject database (Dec 01 2015) was comprised of 7,017 sequences from 362 orthologous groups from the Class Insecta and represented various canonical innate immune signaling pathways (recognition, modulation, signal transduction and effector production) and

other defense-associated functions (*e.g.*, apoptosis, anti-oxidation). An alignment cut-off value of $E < 10^{-15}$ was used to select the most significant database match for each thrips transcript sequence.

Provisional assignment of differentially-expressed transcripts into gene ontologies (GO)

To map and assign gene ontologies ($E < 10^{-3}$) to DE transcript sequences, Blast2Go Basic (https://www.blast2go.com) (Conesa et al., 2005) was run locally in windows on a concatenated file containing 450 non-redundant sequences across the three stages. To determine the number and distribution of sequences into functional GO categories, GO-annotated sequences were assigned to 16 bioprocess and molecular function GO categories according to their most specific GO terms.

Real-time quantitative reverse transcriptase-PCR validation of RNA-seq expression analysis

Seven transcript sequences were selected for validation of differential expression in response to virus in the three developmental stages. Total RNA isolated from the same three biological replications (*i.e.*, two conditions (+/- TSWV), three developmental stages, and biological replicates 1-3) that were subjected to RNA-seq analyses served as templates for cDNA synthesis. Primers were designed using Beacon Designer 7.0 software (Premier Biosoft International, Palo Alto, CA) and tested for PCR efficiency (Table 2.5). The same cDNA synthesis and real-time qRT-PCR methods, internal reference gene (Rp49), reaction components and conditions were used as described above for determination of normalized abundance of

TSWV N RNA (virus titer) in thrips, with the exception that real-time qRT-PCR reactions were performed in 10 μl volumes using Biorad CFX96 thermocycler and Bio-Rad CFX Manager™ v.3.1 software to generate quantification cycle (Cq) data for target gene expression analyses. The normalized abundance of target RNA to Rp49 RNA was calculated for each condition within stage and analyzed using Kruskal-Wallis median test (Minitab v.14, State College, PA, USA) to determine if the virus effect on transcript abundance was statistically significant (alpha < 0.05). The relative expression ratio (target gene expression in the virus condition relative to the no-virus condition) for each transcript target was calculated to determine the direction of fold change (Pfaffl, 2001).

Figures and Tables

Table 2.1 Genome-reference assembly[a] statistics for three developmental-stage transcriptomes for *Frankliniella occidentalis*

	L1-21	P1	Ad-24
[b]Number of assembled contigs (transcripts)	39,954	42,398	41,424
Mean contig length (bp)	3,129	3,286	3,062
Max/Min contig length (bp)	34,576/86	42,317/86	33,170/86
Contig N50	4,914	5,364	4,864
No. of contigs with N's	3,030	3,564	3,048

[a]Illumina RNAseq reads from four biological replicates of two treatments (insects infected with *Tomato spotted wilt virus* or non-infected) were assembled together using Cufflinks (Trapnell et al., 2012) for each developmental stage separately. L1 = first instar larvae allowed a 3-hr acquisition access period on infected tissue, then reared on green bean pods for 21 hr prior to sampling; P1 = pre-pupal stage; Ad-24 = adults sampled 24 hr after eclosure. [b]Includes transcripts assembled to predicted gene models, isoforms or variants of gene models, and novel contigs assembled to scaffold regions with no predicted gene model; contig statistics generated with Prinseq (Schmieder and Edwards, 2011a).

Table 2.2 The top ten most differentially-abundant transcript sequences in each of the three developmental stages of *Frankliniella occidentalis* in response to tomato spotted wilt virus (TSWV) infection

[a]Stage-time (hr)	[b]Transcript sequence identifier	Fold change	Direction	Gene description (Blastx)	Similarity mean (%)	*E*-value (top hit)	Interpro domain present
L1-21	TCONS_00000948	9.44	DOWN	NA			NO
	FOCC004194-RA	8.22	DOWN	ejaculatory bulb-specific protein 3	77.4	2.3e-41	NO
	FOCC001757-RA	7.15	DOWN	NA			YES
	FOCC015675-RA	5.27	DOWN	NA			NO
	FOCC006231-RA	5.04	DOWN	trypsin 1	59.4	8e-56	NO
	CUFF.6108.1	4.93	DOWN	alpha-tocopherol transfer isoform x2	70.8	1.1e-97	YES
	FOCC013331-RA	4.80	DOWN	NA			YES
	FOCC002780-RA	4.78	DOWN	peroxiredoxin-6-like	85.1	1.1e-124	NO
	FOCC010934-RA	4.51	DOWN	endocuticle structural glycoprotein bd-1-like	62.2	2.3e-23	NO
	TCONS_00028224	4.51	DOWN	cysteine sulfinic acid decarboxylase	77.4	0	YES
P1	TCONS_00003267	17.86	UP	NA			YES
	TCONS_00012780	8.21	UP	NA			NO
	TCONS_00024666	7.85	DOWN	NA			NO
	FOCC009158-RA	5.78	UP	NA			YES
	FOCC016444-RA	5.30	UP	NA			NO
	CUFF.731.2	5.25	UP	glucose dehydrogenase	53.1	1.1e-88	YES
	TCONS_00015869	4.60	DOWN	protein qil1-like isoform x2	52.1	1.8e-06	NO
	FOCC010472-RA	4.55	UP	trypsin-like serine protease	47.8	7.2e-21	YES
	CUFF.7847.2	4.16	UP	uncharacterized protein LOC105690123	45.5	1.2e-27	YES
	FOCC008254-RA	4.14	DOWN	zinc finger mym-type protein 1-like	51.8	2.7e-126	YES

Ad-24	FOCC017110-RA	15.38	UP	NA			YES
	FOCC003013-RA	13.31	UP	hemocyanin subunit type 1 precursor	56.8	1.1e-166	YES
	FOCC012829-RA	8.87	UP	hexamerin, arylphorin subunit alpha	53.1	3.9e-168	YES
	FOCC004760-RA	8.64	UP	hexamerin	57.6	2.2e-110	NO
	TCONS_00001377	8.61	UP	NA			NO
	TCONS_00029033	6.21	UP	arylphorin subunit c223-like	57.7	5.3e-8	NO
	FOCC016855-RA	6.14	UP	hexamerin	64.2	3.9e-60	NO
	TCONS_00029451	5.58	DOWN	NA			NO
	CUFF.13055.2	4.79	UP	probable chitinase 3	72.1	0	YES
	FOCC009367-RA	4.20	UP	hexamerin	54.3	1.3e-61	YES

[a]L1 = first instar larvae allowed a 3-hr acquisition access period on -infected tissue, then reared on green bean pods for 21 hr prior to sampling; P1 = pre-pupal stage; Ad-24 = adults sampled 24 hr after eclosure. [b]FOCC (transcript assembled to Maker-predicted gene models), CUFF (assembled transcript in close proximity or partially overlaps Maker-predicted gene model, *i.e.*, isoforms or variants), TCONS (novel contig (transcript fragment) on scaffold with no Maker-predicted gene model).

Table 2.3 Real-time quantitative reverse-transcriptase PCR (qRT-PCR) validation of RNAseq normalized count (FPKM) data

Transcript ID	Gene description (Blastx)	Stage-time (hr)	Fold change (total FPKM, V:NV)	[a]Relative expression (V:NV) by qRT-PCR
FOCC006231-RA	trypsin-1	L1-21	**[b]0.20**	[c]0.69 ± 0.12
		P1	0.57	0.80 ± 0.39
		Ad-24	3.77	**2.16 ± 0.66**
FOCC014449-RA	beta-glucosidase 3-like isoform x1	L1-21	**2.27**	**3.35 ± 1.57**
		P1	[d]0.00	**2.81 ± 0.76**
		Ad-24	0.53	0.73 ± 0.25
FOCC010934-RA	endocuticle structural glycoprotein bd-1-like	L1-21	**0.23**	**0.33 ± 0.18**
		P1	0.58	0.82 ± 0.40
		Ad-24	1.34	2.65 ± 1.14
FOCC002031-RA	venom peptide isomerase heavy chain-like	L1-21	1.04	1.56 ± 0.32
		P1	**3.27**	2.27 ± 0.48
		Ad-24	1.15	1.34 ± 0.27
FOCC010472-RA	trypsin-like serine protease	L1-21	0.96	1.18 ± 0.11
		P1	**4.55**	**4.17 ± 0.14**
		Ad-24	1.17	1.43 ± 0.11
FOCC012829-RA	arylphorin subunit alpha	L1-21	1.04	1.34 ± 0.06
		P1	1.06	**2.22 ± 0.62**
		Ad-24	**8.87**	**1.83 ± 0.43**
FOCC009367-RA	hexamerin a	L1-21	1.11	1.22 ± 0.11
		P1	1.12	0.88 ± 0.38
		Ad-24	**4.20**	4.11 ± 2.80

[a]Relative expression of FOCC target sequence RNA in infected thrips (V) calibrated to non-infected thrips (NV) and normalized to internal reference RNA (rp49). Kruskal-Wallis tests of significance was performed on normalized abundance of target RNA to internal reference RNA to compare medians of the two conditions (V vs. NV) for a given FOCC transcript sequence. [b]RNAseq

differential expression analysis of total normalized read counts (FPKM) by Cuffdiff to compare the two conditions (V vs. H) for three biological replications of virus accumulation experiment; [c]mean ± standard error of n = 3 biological replications; [d]zero FPKM counts for the virus condition. Values in **bold** indicate statistically-significant differences (total FPKM (Cuffdiff): $q < 0.01$; Kruskal-Wallis: $p < 0.05$) between the two conditions for a given developmental stage (L1-21 = 1st instar larvae, 21 hr after 3-hr AAP, P1 = pre-pupae, AD = adults 24 hr after eclosure).

Table 2.4 Differentially-expressed putative innate immune-related transcripts in *F. occidentalis* in response to tomato spotted wilt virus infection

Stage-time (hr)	Sequence ID	Top ImmunoDB match	Gene description	Process	% Identity	Length of match (a.a.)	*E*-value	Direction, Magnitude of change
L1-21	FOCC002780-RA	FBgn0220008	Peroxiredoxin C-terminal; thioredoxin-like	Anti-oxidation	75.9	220	$1x10^{-125}$	Down, 4.78
	FOCC006231-RA	AGAP004570-PA	Peptidase S1/S6, chymotrypsin/Hap	Proteolysis	35.3	224	$3x10^{-36}$	Down, 5.04
P1	FOCC004567-RA	PHUM345810-PA	NF-kappa-B inhibitor alpha, putative	Humoral signaling (Toll pathway)	31.3	166	$2x10^{-12}$	Down, 1.95
	CUFF.10010.1	FBgn0115643	protein binding, cysteine-knot cytokine (spaetzle 3A)	Humoral signaling (Toll binding)	56.7	319	$2x10^{-107}$	Down, 1.59
	FOCC017389-RA	NV17949-PA	Disulfide knot CLIP, serine protease	Humoral and cellular signaling	34.7	265	$1x10^{-32}$	Down, 2.71
	TCONS_00028705	TcGLEAN_13326	Disulfide knot CLIP, serine protease	Humoral and cellular signaling	45.6	364	$1x10^{-95}$	Down, 2.05
	FOCC006231-RA	AGAP004570-PA	Peptidase S1/S6, chymotrypsin/Hap	Proteolysis, serine-type endopeptidase	35.3	224	$3x10^{-36}$	Down, 1.76
	CUFF.7837.2	TcGLEAN_15295	Peptidase S1/S6, chymotrypsin/Hap; CYP450	Proteolysis, serine-type endopeptidase	27.1	229	$3x10^{-17}$	Down, 2.48
	CUFF.6664.2	PHUM569120-PA	Protein croquemort (scavenger receptor)	Pathogen recognition receptor; cell adhesion	48.1	316	$3x10^{-103}$	Down, 2.25
	FOCC014902-RA	NV14467-PA	Proteinase inhibitor I32,	Inhibitor of apoptosis	40.6	352	$4x10^{-75}$	Down, 1.94

	FOCC014201-RA	GB17129-PA	Proteinase inhibitor of apoptosis	Inhibitor of apoptosis	36.3	361	$1x10^{-78}$	Down, 1.94
	FOCC003406-RA	FBgn0156974	Haem peroxidase, animal; UDP-glucuronosyl/UDP-glucosyltransferase	Response to oxidative stress, detoxification	30.1	435	$1x10^{-53}$	Up, 2.22
	FOCC017438-RA	TcGLEAN_05493	Haem peroxidase, animal; UDP-glucuronosyl/UDP-glucosyltransferase	Response to oxidative stress, detoxification	55.2	1018	0	UP, 1.6
	CUFF.9922.2	AGAP004570-PA	Peptidase S1/S6, chymotrypsin/Hap	Proteolysis, serine-type endopeptidase	41.3	247	$4x10^{-46}$	Up, 1.55
	FOCC002031-RA	GB14654-PA	Peptidase S1/S6, chymotrypsin/Hap	Proteolysis, serine-type endopeptidase	31.7	268	$1x10^{-32}$	Up, 3.27

Table 1.4 continued

Stage-time (hr)	Sequence ID	Top ImmunoDB match	Gene description	Process	% ID	Length of match (a.a.)	E-value	Direction, Magnitude of change
P1	CUFF.1766.1	TcGLEAN_15295	Peptidase S1/S6, chymotrypsin/Hap; CYP450	Proteolysis, serine-type endopeptidase	27.3	403	$5x10^{-42}$	Up, 1.72
	FOCC010472-RA	FBgn0124926	Proteinase, regulatory CLIP domain	Humoral and cellular signaling	26.5	245	$3x10^{-17}$	Up, 3.27
	FOCC003634-RA	TcGLEAN_09089	serine-type endopeptidase activity	Proteolysis	29.1	251	$3x10^{-23}$	Up, 1.72
	CUFF.10419.1	CPIJ012305-PA	zinc finger protein 8	DNA-binding transcription factor	39.6	101	$3x10^{-14}$	Up, 1.57
Ad-24	CUFF.4937.1	AGAP005717-PA	Glycoside hydrolase, Lysozyme-like	Anti-bacterial	36.1	180	$1x10^{-28}$	Down, 1.89
	CUFF.7388.2	PHUM540850-PA	Sushi/SCR/CCP; C-type lectin	Pathogen	88.0	75	$1x10^{-38}$	Down, 2.32

			recognition receptors, cell adhesion				
CUFF.12585.1	FBgn0156974	Haem peroxidase, animal; UDP-glucuronosyl/UDP-glucosyltransferase	Response to oxidative stress, detoxification	30.5	430	$1x10^{-46}$	Up, 3.67
FOCC003013-RA	AAEL013981-PA	Hemocyanin, C-terminal, N-terminal, copper-containing	Phenoloxidase activity in melanogenesis	33.6	699	$1x10^{-125}$	Up, 13.31
FOCC004760-RA	AAEL013981-PA	Hexamerin 2 B	Humoral and cellular immunity; prophenoloxidase -activating	35.8	466	$1x10^{-81}$	Up, 8.64
FOCC009367-RA	AGAP005768-PA	Hexamerin 2 B	Humoral and cellular immunity; prophenoloxidase (PPO)-activating	38.7	282	$3x10^{-54}$	Up, 4.20
FOCC016855-RA	AAEL013983-PA	Hexamerin 2 B	Humoral immunity; PPO-activating	30.4	178	$2x10^{-13}$	Up, 1.60
FOCC017274-RA	AAEL013981-PA	Hexamerin 2 B	Humoral immunity; PPO-activating	35.1	251	$1x10^{-43}$	Up, 6.14
FOCC012829-RA	AAEL013983-PA	Hexamerin 2 B	Humoral immunity; PPO-activating	35.2	685	$4x10^{-124}$	Up, 4.20
FOCC014595-RA	PHUM538080-PA	Thyroid peroxidase precursor, putative	Response to oxidative stress	34.8	739	$9x10^{-118}$	Up, 8.87

Table 2.5 Real-time quantitative reverse-transcriptase PCR (qRT-PCR) primers designed for validation tests

Target sequence ID	Primer sequence (5'-3', forward/reverse)	[a]PCR efficiency	[b]Amplicon length (bp)
FOCC006231-RA	ATCTTCGTTGGAATGCAAGTC/ GATGGGAATGTTTGGAAGGT	1.95	75
FOCC014449-RA	CCTTATAGTCTGGAGAAGA/ CGTATGTTGTGAAGAGAA	1.90	94
FOCC010934-RA	CACTTTCCTCTCCTTTGC/ TACGAATACCTTGGCGAT	2.04	75
FOCC002031-RA	CTACAACGAATGGATCAACTTG/ GCACAAATAGCGACAAATAGT	1.97	93
FOCC010472-RA	CACAACATCTTTATCGGTAA/ GAAGGTCTTCAGGAACTC	1.90	108
FOCC012829-RA	CCTACTTCTACTTCTATGG/ ATCACTGACTTCTTCTTC	1.94	113
FOCC009367-RA	TCATCTTCCACAAGGACT/ CGTTATCGAAATCGTTGAC	1.96	75

[a]Calculated efficiency (Pfaffl, 2001) = $10^{(-1/slope)}$; slope = slope of real-time PCR titration curve of 5-fold dilutions of cDNA template

[b]Predicted length by Beacon Designer v. 8.02.

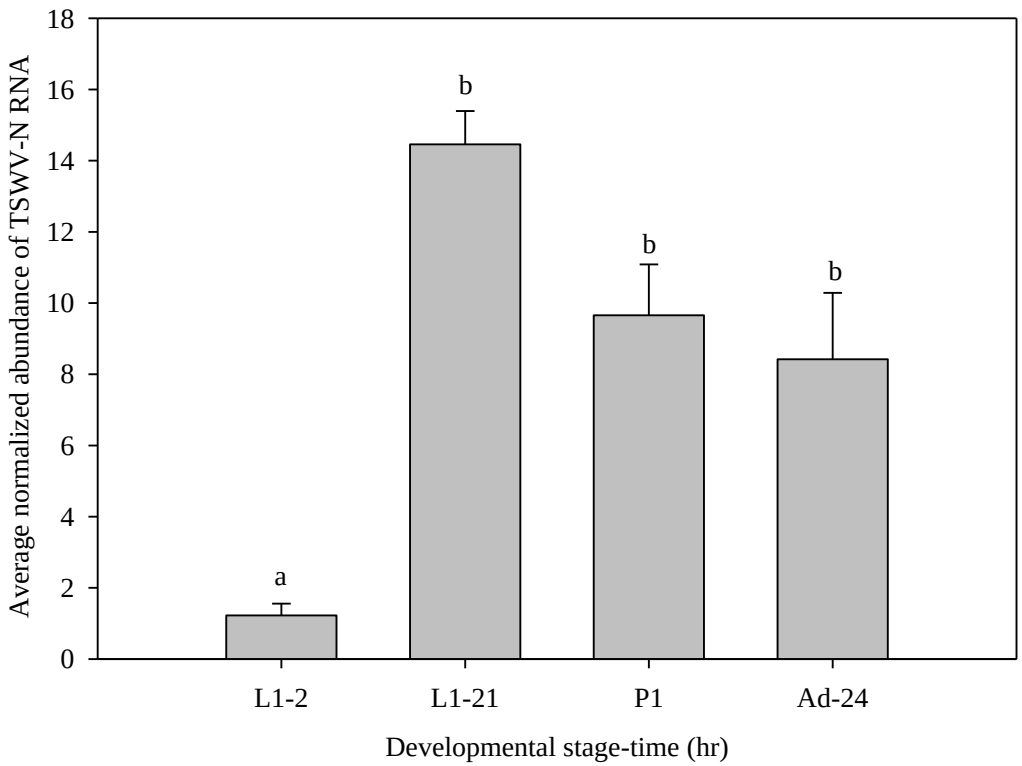

Figure 2.1 Tomato spotted wilt virus (TSWV) accumulation during thrips development. L1 = first instar larvae allowed a 3h acquisition access period (AAP) on TSWV-infected tissue, then reared on healthy green bean pods for 2 hr and 21 hr prior to sampling; P1 = pre-pupae stage; Ad = adults sampled 24 hr after eclosure. Real-time qRT-PCR of nucleocapsid (N) RNA was used to estimate virus titer. The normalized abundance of TSWV N relative to an internal standard was calculated using the equation: $((E_{RP49})^{(CtRP49)}/(E_{TSWV\text{-}N})^{(CtTSWV\text{-}N)})$ (Pfaffl, 2001) where E = PCR efficiency of a primer pair, and Ct = the amplification cycle number at which fluorescence emitted during the reactions first exceeds background fluorescence and is inversely related to the initial template concentration in the PCR reaction. Each bar represents four biological replications $\pm$ standard error. Bars headed by different letters indicate statistical differences between pairwise means after Tukey multiple comparisons (adjusted $P < 0.05$).

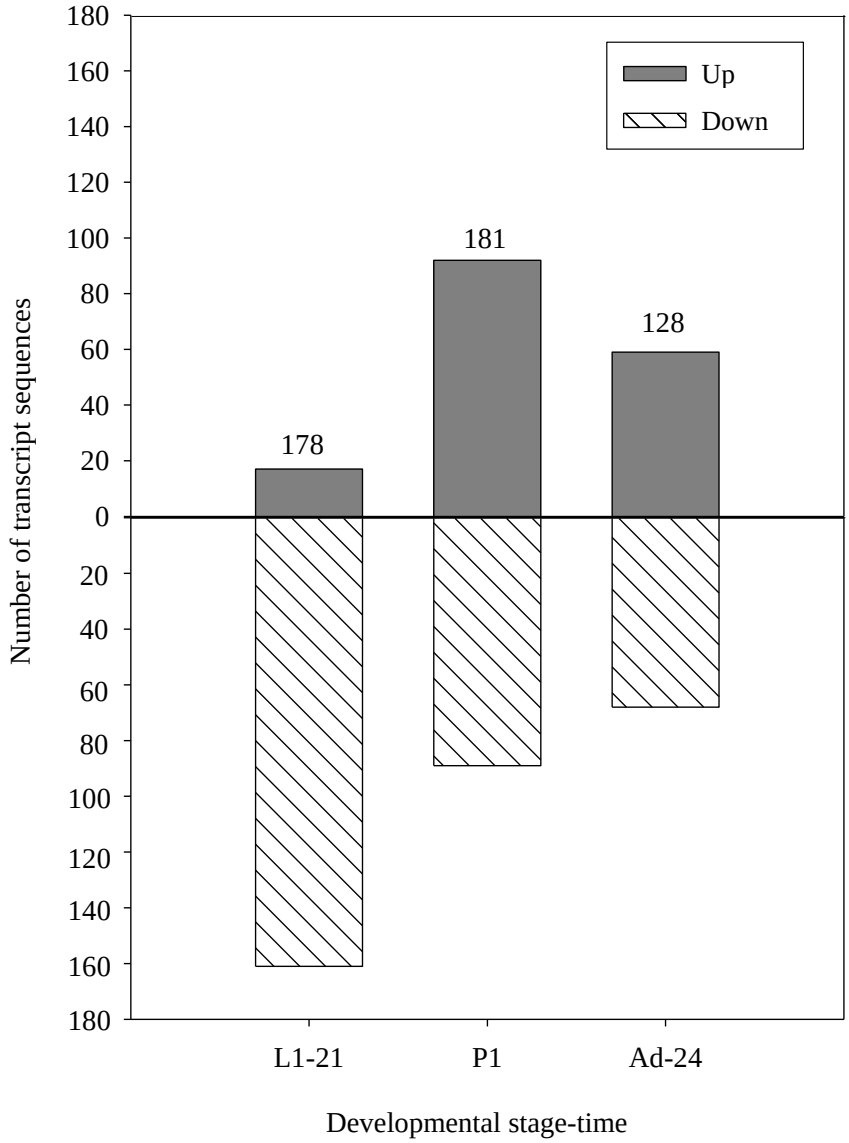

Figure 2.2 Number and direction of change of differentially-expressed transcript sequences of *Frankliniella occidentalis* in response to tomato spotted wilt virus (TSWV) infection.

L1 = first instar larvae allowed a 3-hr acquisition access period on TSWV-infected tissue, then reared on healthy green bean pods for 21 hr prior to sampling; P1 = pre-pupal stage; Ad-24 = adults sampled 24 hr after eclosure.

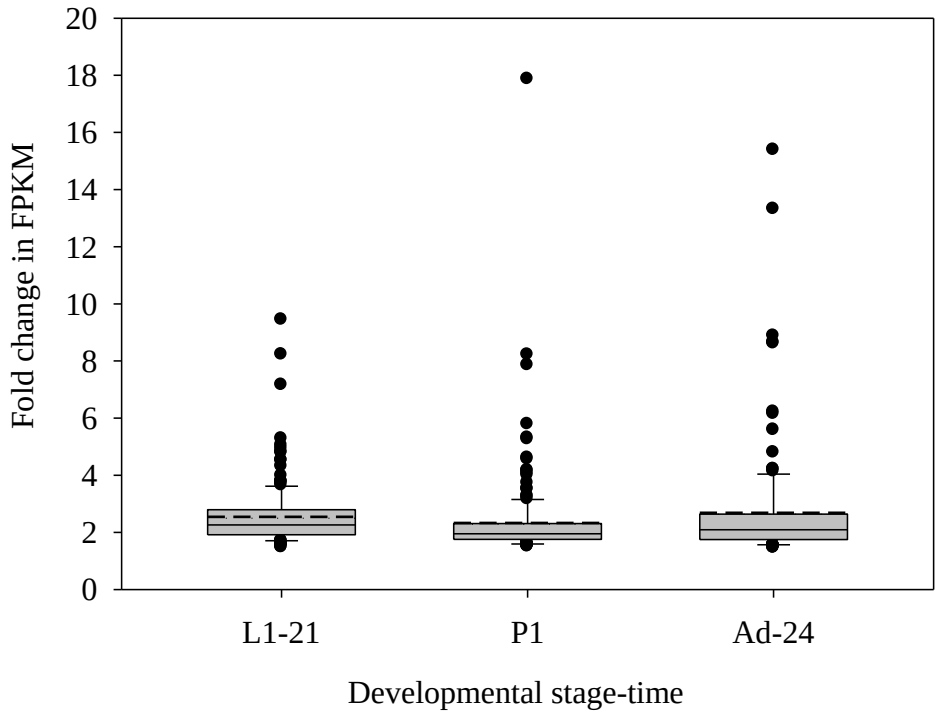

Figure 2.3 Distribution of fold change in FPKM values between the non-infected and tomato spotted wilt virus (TSWV)-infected *Frankliniella occidentalis* treatments for three developmental stage-time samples determined separately.

Magnitude of fold change in FPKM = larger FPKM value/smaller FPKM value between the two treatments. Each treatment included three biological replications of a virus accumulation time course experiment. L1 = first instar larvae allowed a 3-hr acquisition access period on TSWV-infected tissue, then reared on healthy green bean pods for 21 hr prior to sampling; P1 = pre-pupal stage; Ad-24 = adults sampled 24 hr after eclosure. SigmaPlot v.10.0 standard method was used to compute box boundaries (25^{th} and 75^{th} percentile), the median and mean represented as a solid and dashed line, respectively, within the box. The whiskers (error bars) represent the 10^{th} and 90^{th} percentiles and the outlying points are represented (solid dots).

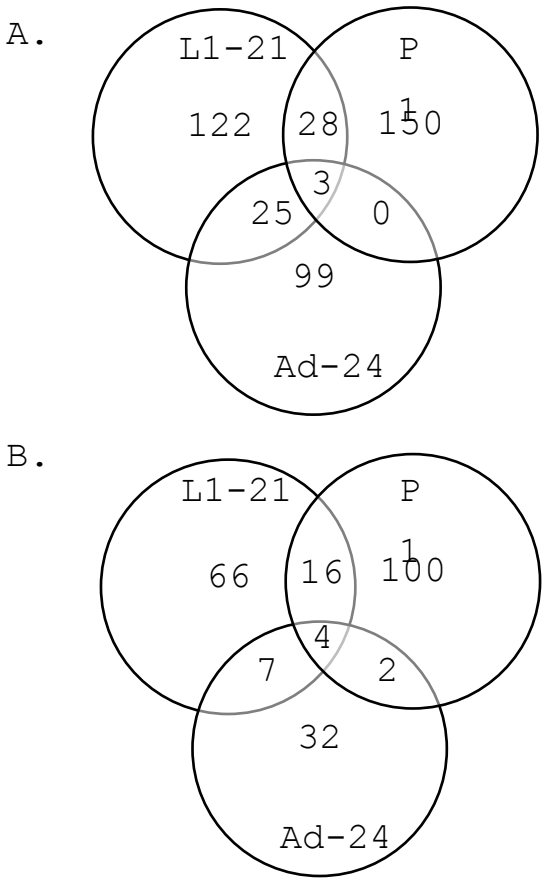

Figure 2.4 Venn diagrams depicting shared and unique differentially-expressed transcripts between the three developmental stages of *Frankliniella occidentalis* in response to tomato spotted wilt virus (TSWV) infection.

(A) Pair-wise sequence comparisons were based on Blastn matches (Blastn, e-value = 0, % identity = 100%) and (B) Blastx gene descriptions (Blastx) (excludes non-annotated sequences). L1 = first instar larvae allowed a 3-hr acquisition access period on TSWV-infected tissue, then reared on healthy green bean pods for 21 hr prior to sampling; P1 = pre-pupal stage; Ad-24 = adults sampled 24 hr after eclosure.

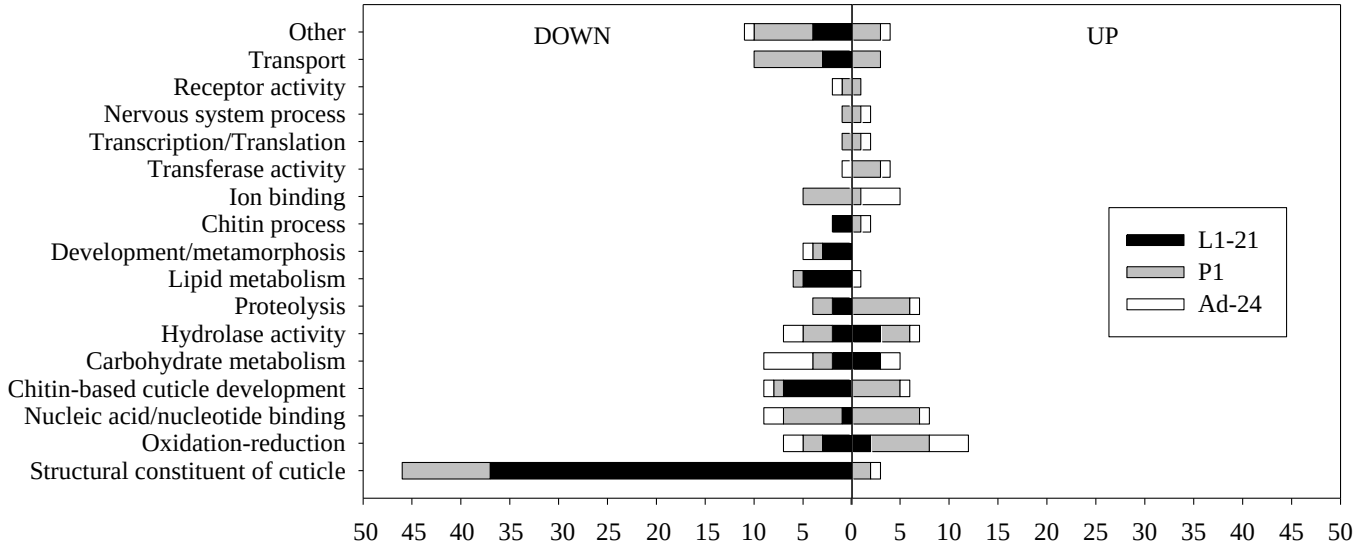

Figure 2.5 Number and classification of differentially-expressed transcript sequences of tomato spotted wilt virus (TSWV)-infected *Frankliniella occidentalis* into gene ontologies (GO) associated with biological processes and molecular functions.

L1 = first instar larvae allowed a 3-hr acquisition access period on TSWV-infected tissue, then reared on healthy green bean pods for 21 hr prior to sampling; P1 = pre-pupal stage; Ad-24 = adults sampled 24 hr after eclosure.

Chapter 3 - Silencing of two key RNAi transcripts Dicer-2 (DCR2) and Argonaute-2 (AGO2)

Abstract

TSWV is transmitted by *F. occidentalis*, the Western flower thrips, in a circulative and propagative manner, infecting and replicating in several tissue types with no apparent pathogenic effect on the insect vector. My research goal for this study was to investigate and develop an understanding of the molecular basis of thrips innate immune response to TSWV, specifically the small-interfering RNA (siRNA)-mediated antiviral pathway, well characterized for model insect systems but lacking for thrips. I hypothesize that the genes (Dicer-2 and Argonaute-2) associated with siRNA-mediated silencing of viral genomes are important modulators of the amount of TSWV harbored by the thrips vector. The specific objectives of my research were to 1) use RNA-Seq to measure the basal expression of Dicer-2 (pattern recognition receptor of double-stranded viral RNA) and Argonaute-2 (silencer of mRNA viral transcripts) during the first instar larva (L1), pre-pupa (P1) and Adult; 2) generate dsRNA molecules for thrips specific Dicer-2 and Argonaute-2 (AGO2); and 3) conduct a time-course experiment to determine the effect(s) of challenging TSWV-exposed and non-exposed thrips with dsRNAs of *F. occidentalis* Dicer-2 or AGO2 by hemocoel injection by quantifying i) the abundance of endogenous Dicer-2 and AGO2 transcripts and viral RNA (TSWV-N) in whole bodies at three time points post-injection, and ii) measuring insect fitness during the course of the experiment (mortality and viable offspring). I constructed a genome-reference-based transcriptome assembly from thrips coding RNA derived from sequence reads of Illumina RNA-Seq libraries from four independent biological

replications of TSWV-exposed and non-exposed thrips (Chapter 2 experimental analysis of differential expression). There was no apparent effect of TSWV infection of expression of Dicer-2 and AGO2 in whole bodies. Using the count data matrix obtained from my Illumina RNA-Seq analysis of transcript read counts across the three developmental stages (L1, P1, and Ad), it was determined that both Dicer-2 and AGO2 were significantly less abundant in the first instar larva (L1) when compared to both pre-pupa (P1) and adult (Ad), which may point to a more permissive environment during the early stages of gut infection in the L1 or a role in thrips development. Knock-down of Dicer-2 and AGO2 resulted in reduced insect survival and reduced production of larva.

Introduction

The primary antiviral defense pathway in insects and other invertebrates is the small-RNA-mediated gene-silencing pathways called the short interfering RNA (siRNA) pathway (Meister and Tuschl, 2004). The siRNA pathway is induced by double-stranded RNA (dsRNA). RNA viruses, like TSWV, produce dsRNA through replicative intermediates (*i.e.* double stranded replication). Virus (ssRNA) genomic stands are present at higher levels than antigenome stands during infection (Aliyari et al., 2008), but virus induced small interfering RNAs (vsiRNAs) map to genome and antigenome strands are present at similar levels and distribute across the entire viral genome (Gammon and Mello, 2015). Innate secondary structure within the RNA genome also generates vsiRNAs with examples of approximately 87% of vsiRNAs generated during infection of *Drosophila* cells with Drosophila C virus map to the genomic strand (Sabin et al., 2013). The pattern recognition receptor, Dicer-2 (DCR2), cleaves the dsRNA into small RNA duplexes of 21 nucleotides in length. These small RNA duplexes are

loaded into the RNA-induced Silencing Complex (RISC), a protein complex comprised of multiple enzymes. The central player in the RISC complex is Argonaute 2, another RNA binding endonuclease that uses the guide strand of the small RNA duplex to act as a guide for locating complementary single-strand RNA (ssRNA) sequence. Once complementary sequence is located, Argonaute 2 slices the viral RNA into small noncoding fragments rending the virus ineffectual (Hannon, 2002).

Viruses that establish persistent infections within insect vectors infect the midgut epithelium and disseminate through the insect. TSWV enters the thrips gut during feeding on infected plant tissue. Once the virus enters the host cell, the Gc protein is thought to provide membrane fusion within the endosome similar to other Bunyaviruses (Cifuentes et al., 2012, Whitfield et al., 2005a). The virus enters the host cell and begins replication providing the substrate for RNAi. A similar infection pattern is found when *Southern rice black streaked dwarf virus* (SRBSDV) infects the small brown planthopper, but the infection is restricted to the midgut. Knockdown of Dicer-2 in infected cells increased the ability of SRBSDV to propagate and disseminate from the midgut cells (Lan et al., 2016). This research indicates a threshold for midgut escape, and provides evidence that Dicer-2 and the RNAi system regulate virus level during persistent infection.

Viruses encode silencing suppressors to inhibit the RNAi pathway at different key steps. The NSs protein of TSWV has silencing suppressor activity during infection (Takeda et al., 2002b). It is known to suppress RNAi in *N. benthamiana* plants expressing high levels of GFP. Infection with TSWV provided complete reactivation of GFP expression, and the NSs gene was identified as responsible for RNA silencing-suppressing activity (Bucher et al., 2003). The NSs

protein appears to have affinity to both small double-stranded RNA molecules and long dsRNA molecules (Schnettler et al., 2010b).

Characterization of Dicer-2 and AGO2 is established in other insect-virus interaction studies indicating modulation of virus by the RNAi pathway. The insect innate immune response is in contrast to interferon-induced responses mediating innate host defense virus response in mammals (Kemp and Imler, 2009). Silencing of the RNAi pathway protein AGO2 resulted in a 16-fold increase of O'nyong-nyong virus (ONNV) titers when compared to control in *Anopheles gambiae* (Keene et al., 2004). Silencing the expression of Dicer-2, R2D2, and AGO2 in *Aedes aegypti* results in an increase in Dengue virus type 2 replication and a decrease in the incubation period needed for virus transmission (Sanchez-Vargas et al., 2009), while Sindbis virus (SINV) also increases in infectious titers following injection of dsRNAs for AGO2, Dicer-2, and TSN. Regulation of viral titer is apparent across the systems listed, and innate immune response appears to play a major role in insect defense against virus infection. Interestingly the expression of both AGO2 and Dicer-2 transcript RNA was unchanged during SINV infection with only TSN significantly increased when compared to controls (Campbell et al., 2008). The lack of expression differences in Dicer-2 and AGO2 transcripts indicates that both proteins are capable of silencing viral genomes without needing to elevate transcript expression for production of more protein. The RNAi pathway is known to remove the presence of a RNA virus genome in *Drosophila melanogaster* (Galiana-Arnoux et al., 2006, van Rij et al., 2006), and viral derived small interfering RNAs (vsiRNAs) have been observed in *Frankliniella fusca*, a closely related thrips species, when allowed to acquire TSWV (Fletcher et al., 2016). Processing of TSWV into 21 and 22 nucleotide siRNAs is direct evidence of viral genome processing within the thrips RNAi system.

Results

Two cycles of virus accumulation during thrips development

A temporal sampling strategy was used to determine the accumulation of virus in *F. occidentalis* through development to determine if virus titer is regulated. A fine scale description of virus accumulation was built to determine changes in viral load while insects develop so as to select and target stages for silencing of innate immunity. The time-course experiment consisted of nine sampling events over the thrips life, and four biological replicates of the experiment were performed. Generalized linear mixed model (GLIMMIX) analysis of the normalized abundance of TSWV-N RNA for each thrips developmental stage revealed two cycles of virus accumulation, *i.e.*, increase in titer, one occurring between the early stage of infection (L1-2) to the late L2 stage, and the other occurring from P1 stage through adulthood (Figure 3.1). Virus accumulation peaked during at the L2-72h stage, was markedly reduced during the pupal stages ($P < 0.0001$), and then significantly increased again as adults aged ($P < 0.0092$ for comparisons between adult 24 and older adults). As expected, titer was significantly lower ($P < 0.0001$) during early infection events of the L1 thrips (2 hours after a 3-hr AAP) compared to the other developmental stages. These TSWV-N abundance dynamics provided evidence for the hypothesis that TSWV is regulated differently at each stage during infection of the thrips vector. The continual rise in TSWV-N abundance provided a time-point to target the RNAi pathway and reduce viral silencing during the secondary increase. Targeting this time-point enabled descriptions of changes in TSWV abundance during an increase curve.

Phylogenetic tree topology and domain architecture of *F. occidentalis* Dicer-2 and AGO2

Clustering both Dicer-2 (Dcr-2) and Argonaute 2 (AGO2) with other insect species and varying forms provided the detailed information needed to determine targeting of the correct target. The Dicer-2 amino acid sequence of *F. occidentalis* clusters with Dicer-2 sequences of the other nine insect species included in the analysis, is basal to the hemipteran species, and branches with a newly annotated Dicer sequence for *P. humanus corporis* on a collective branch indicating a likelihood for this novel sequence to be Dicer-2 (Figure 3.2). The placement of *F. occidentalis* AGO2 as a branch from the larger group consisting of *A. glycines*, *A. pism*, *B.tabaci*, *N. lungens*, and *C. letularius* indicates uniqueness and agreement with hemipteran species. The placement of AGO3 appears to place *F. occidentalis* as an out-group to all the species, including hemipterans, indicating high divergence of this protein sequence (Figure 3.3). It clusters with *A. mellifera* AGO1A close to the larger AGO2 grouping, while *F. occidentalis* AGO1 clearly clusters in the AGO1 grouping. The relatedness of these selected protein sequences support evidence described in other complete transcriptome phylogenetic comparisons (Misof et al., 2014).

The domain architecture identified using InterPro (https://www.ebi.ac.uk/interpro/) for Dicer-2 and AGO2 in western flower thrips is conserved in similarity with domains of other species indicating a well-built gene model for the two proteins. Thrips Dicer-2 contains a dicer-dimerization domain commonly held across dicer proteins and two helicase domains important for un-winding double stranded RNA. The two RIBOc domains act to cut dsRNA into small RNAs with the double stranded RNA-binding domain (DSRM) acting to bind dsRNA. The

domain architecture for AGO2 was also conserved in thrips with N-terminal argonaute, Argonaute linker, Piwi Argonaut Zwille, and Piwi Argonaut-like domains commonly found in argonaute proteins (Figure 3.6).

Basal expression of Dicer-2 and AGO2 in *Frankliniella occidentalis* is reduced in younger development stages

Exploration of basal expression of targeted transcripts provided basic knowledge of transcript expression and the expression patterns present at each development stage. Global transcriptome counts were calculated for three development stages (Appendix A). Dicer-2 and AGO2 are significantly down-regulated (padj < 0.01) in L1s when compared to both P1 and Adult (Pairwise). Dicer-2 has a reduced log2FoldChange of 0.79 and 0.74 and AGO2 was 0.79 and 0.70 log2FoldChange in P1 and Adult, respectively (Figure 3.4).

Injection of Dicer-2 and AGO2 dsRNA results in reduced survivorship and reduced production of viable offspring

Injection of Dicer-2 dsRNA appeared to negatively impact the health of thrips and cause a higher morality when compared to controls. When compared to GFP dsRNA control, the injection of Dicer-2 dsRNA elicited a 54% reduction in survivorship two days post injection ($P < 0.05$) (Figure 3.6 Non-exposed). This reduction in survivorship was also observed in both non-exposed and TSWV-exposed thrips for day two, three, and four (Figure 3.6). Injection of water for day one had a high mortality due to a defect in the microinjection needle causing death from injection (data not shown).

Injection of AGO2 dsRNA also appeared to negatively impact the health of thrips and cause a higher morality when compared to controls. When compared to GFP dsRNA control, the injection of AGO2 dsRNA elicited a 34% reduction in survivorship two days post injection ($P < 0.05$) (Figure 3.6 Non-exposed). This reduction in survivorship was observed in both non-exposed and TSWV-exposed thrips for both day two and day three (Figure 3.6).

The production of offspring was calculated by observing living L1s and L2s two days after the last sampling date (day six post injection) making the timeline 8 days post injection. Marked reductions in production were observed for all treatments of dsRNA compared to water control. The DCR2 and AGO2 dsRNA treatments had significantly lower values (approximately 35-45% reduced) of offspring production for both non-exposed and TSWV-exposed conditions ($P < 0.05$) (Figure 3.7).

Silencing of AGO2 and Dicer-2 when challenged with dsRNAs

The abundance of DCR2 transcript was elevated initially at day one and then reduced at day six. Insects challenged with DCR2 and AGO2 dsRNA displayed elevated expression of DCR2 transcripts one day after microinjection ($P < 0.05$) (Figure 3.8). During the final time-point (Day 6), DCR2 abundance levels were reduced when challenged with both DCR2 and AGO2 dsRNA, and DCR2 abundance was significantly lower than day one when insects were injected with DCR2 dsRNA ($P < 0.05$) (Figure 3.8). There were no significant transcript abundance changes in the TSWV exposed condition, indicating a challenge for retention of TSWV infected insects that survive after the two day period.

The AGO2 was silenced at two time points when challenged with AGO2 dsRNA. AGO2 transcript abundance was significantly reduced (lowest level measured) at day one in TSWV

exposed thrips ($P < 0.05$) (Figure 3.9). Silencing was also observed at day six in non-exposed insects when challenged with AGO2 dsRNA ($P < 0.05$) (Figure 3.9). A time effect for AGO2 abundance was observed when insects were challenged with varying treatments with the abundance of AGO2 transcript significantly reduced in DCR2 dsRNA treated non-exposed insects at day 3 and GFP, DCR2, AGO2 dsRNA treated at day 6 when compared to day 1 ($P < 0.05$) (Figure 3.9).

AGO2 dsRNA injection reduces abundance of TSWV-N

TSWV-N abundance was measured using qRT-PCR for all individuals collected at each time point and from each treatment. Nine individuals were sampled for both water and dsGFP control and eleven individuals were sampled for DCR2 and AGO2 dsRNA treatments. Only four out of eleven (37%), and five out of eleven (45%) were infected with TSWV for the DCR2 and AGO2 dsRNA treatments respectively. Low numbers of infection reduced the power for statistical testing, and it also appears that individuals with higher titer were absent from the dsRNA treated individuals. The abundance of TSWV-N was higher in the H_2O injected controls when compared to AGO2 dsRNA treatment (Figure 3.12). No obvious association between viral RNA abundance and endogenous gene transcript abundance of DCR2 or AGO2 was measureable (Figure 3.13).

Discussion

We hypothesized that TSWV abundance is regulated by the siRNA innate immune pathway in thrips, providing permissibility to infection while also sustaining insect survival. Paramount to thrips vector competence is the passage, accumulation and persistence of TSWV through adulthood for inoculation of plants to occur. In this study, a robust two-cycle pattern of

viral N RNA accumulation during development (Fig. 1) was determined by real-time qRT-PCR, a method that has been used previously to estimate virus abundance in whole bodies of *F. occidentalis* (Margaria et al., 2015, Rotenberg et al., 2009b). The pattern of virus accumulation was similar to that reported for TSWV N protein abundance using ELISA (Montero-Astúa et al., 2016, van de Wetering et al., 1996). During adulthood and within the time-frame of my gene-knockdown experiment, I measured a significant increase in virus abundance at the Ad-96h and Ad-144h stages, a time that has been reported to support strong TSWV infection of principal salivary glands.

The abundance of TSWV-N is an indicator of virus titer (Rotenberg et al., 2009b), and we hypothesized that a reduction in DCR2 and AGO2 transcript presence would reduce expression of those proteins and ultimately provide an environment of increased viral genome abundance. Other similar studies in mosquito detail an increase in virus titer when the RNAi system in silenced using dsRNA (Campbell et al., 2008, Keene et al., 2004, Sanchez-Vargas et al., 2009). In a plant-virus-vector system, silencing of Dicer-2 in small brown planthopper increased the ability of a plant virus (SRBSDV) to propagate and disseminate (Lan et al., 2016). Interestingly, I found the opposite, where insects presenting TSWV infection tended to have lower titers when challenged with DCR2 and AGO2 dsRNA. This might be explained by the decrease in survivorship and our inability to sample dead adult thrips. It is possible that thrips challenged with DCR2 or AGO2 dsRNA and a high TSWV titer were compromised and quickly died around the day two and three sampling point (Figure 3.6). When observing DCR2 and AGO2 transcript abundance of living individuals exposed to TSWV, knock-down is no longer measurable past day one (Figure 3.10 and 3.11), and insects with TSWV infection presented lower TSWV-N abundance when challenged with AGO2 dsRNA. Taken together, evidence

indicates that insects with higher TSWV-N abundance (titer) challenged with DCR2 or AGO2 dsRNA resulted in mortality and subsequent absence from my measurements. This preliminary study provides the first glimpse at the deleterious effect of silencing DCR2 and AGO2 in thrips and further exploration of mechanism will provide novel description this virus-vector relationship.

Based on my findings herein, the two cycles of virus accumulation provided an indication of a coordinated process in which virus abundance is controlled by the thrips host during development. My study is the first to knock down key players in the thrips RNAi pathway (*i.e.* DCR2 and AGO2) providing the first opportunity to silence Dicer-2 and AGO2 genes with apparent effect on survivorship and production of offspring. Phylogenetic trees were constructed for comparative analysis within each RNAi pathway target (*i.e.* DCR2 and AGO2) spanning multiple insect species (Figure 3.2 and 3.3). Determination of correct transcript target was important for successful knock-down of intended target while reducing off-target effects (*e.g.* DC1, AGO1, and AGO3). While there was significant silencing of both DCR2 and AGO2 transcripts post injection in non-exposed insects (no TSWV infection), there was also an increase in DCR2 post-injection with either DCR2 or AGO2 dsRNA (Figure 3.8). This initial increase at day one may indicate a potentiated response of the insect immune system and it appears to be specific to injection of DCR2 and AGO2 dsRNA with a similar response not observed with GFP dsRNA (Figure 3.8). This initial increase of abundance and subsequent decrease indicates a dynamic response to the dsRNA molecules that perturb endogenous gene expression. Changes in abundance of DCR2 when challenged with AGO2 and DCR2 dsRNA indicate possible cross-talk between these two siRNA pathway components. Within the miRNA pathway, DCR deficient mouse embryonic stem cells present low levels of AGO2 protein, which can be rescued by

reintroduction of DCR cDNA (Martinez and Gregory, 2013). Further research is needed to explore siRNA internal pathway cross-talk.

My hypothesis that silencing RNAi genes, namely DCR2 and AGO2, in viruliferous thrips would result in increased TSWV titer and eventually death was not supported by my present findings. One unexpected finding that precluded fully addressing my hypothesis was that the survivorship and number of larvae produced by non-exposed thrips (no TSWV infection) injected with dsRNA of either RNAi transcript were equally affected (negatively) as the dsRNA-injected TSWV-exposed thrips (Figure 3.6 and 3.7). The timing and magnitude of the effect of silencing on TSWV accumulation may have been apparent if I had collected and assayed dying or dead individuals and sampled them earlier post-injection. Nonetheless, the finding that the non-exposed thrips responded to dsRNA of the two DCR2 and AGO2 transcripts points to the effect of these dsRNAs on another unaccounted factors related to insect health. Perhaps in thrips, DCR2 and AGO2 interact with other vital genes or innate immune-associated genes. This would be unusual given that silencing of these two genes in healthy insects of other species has been reported to have little to no effect on fitness (Lan et al., 2016). Another hypothesis generated from my findings is that the DCR2 and AGO2 silencing effect on insect fitness may be affecting other 'below-threshold' pathogenic insect viruses harbored by the thrips, if such viruses exist in thrips, ultimately compromising insect health. With the advancement of deep sequencing tools for insect genomes and transcriptome, others have discovered viromes of various insects (Feng et al., 2017).

Materials and Methods

F. occidentalis colony and TSWV maintenance

Franklinella occidentalis (Pergande) originally obtained from Kamilo Iki Valley, Oahu, Hawaii, was maintained on green bean pods (*Phaseolus vulgaris*) in 16-oz clear plastic deli cups with lids adapted for air transfer using thrips-proof mesh. The colony was maintained at room temperature and as described previously (Ullman et al., 1992c). TSWV (isolate TSWV-MT2) was maintained on *Emilia sonchifolia* by thrips-transmission as described previously (Meister and Tuschl, 2004). The source of TSWV for thrips acquisition was symptomatic leaves from *Emilia* plants 12 days old post mechanical inoculation with leaf sap from a one-month-old thrips-inoculated TSWV culture as described previously (Badillo-Vargas et al., 2012).

Biological samples for analysis of virus accumulation spanning development

Four biological replications of a time-course experiment were conducted to determine virus titers in developing thrips. Following the 3-hr AAP on infected and non-infected bouquets, cohorts of thrips were sampled during the L1 stage (two and 21 hours after exposure), L2 stage (47 and 72 hours after exposure), the P1 and P2 stages (when ~90% were observed to present for each stage with the use of a stereoscope), and adult stage comprising females and males (24, 96, and 144 hours post eclosion). For each treatment-sampling time point, one cohort of 75-100 insects was collected into a 1.7ml microfuge tube using separate fine paintbrushes, then immediately flash-frozen in liquid nitrogen and stored at -80^{O}C. Total RNA was isolated form each sample using TRIzol reagent (Invitrogen, Carlsbad, CA) using methods described previous (Badillo-Vargas et al., 2012). To estimate virus titer per cohort, previously described methods for normalized real-time qRT-PCR quantification of TSWV nucleocapsid (N) RNA were followed (Badillo-Vargas et al., 2012). Briefly, cDNA was synthesized from 1ug of total RNA using

Verso^{TM} cDNA kit (Thermo Scientific, Wilmington, DE, USA), then cDNA reaction volumes were diluted 10-fold with DEPC-treated ddH_2O. Real-time qRT-PCR was performed on two technical replicates of 20ul-reaction mixtures containing 200nM each of TSWV nucleocapsid (N) and thrips internal reference gene RP49 primers, iQ SYBER Green Supermix (Bio-Rad, Hercules, CA) and reactions were run on the iCycler iQ Thermal Cycler with a 96 x 0.2ml reaction module with iCycler iQ software (Bio-Rad). The 2-step amplification and melt protocol was run using the following cycling parameters: 95^{O}C for 3 mins, then 40 cycles of 95^{O}C for 1 min and 55^{O}C for 45s; then melt protocol of 55^{O}C for 1 min then 80 cycles of 10 seconds each with 0.5^{O}C increase in temperature at each cycle. The normalized abundance of TSWV N RNA to RP49 RNA was calculated for each developmental-stage time point using the equation: $E_{RP49}^{Ct(RP49)}/E_N^{Ct(N)}$ (Pfaffl, 2001); where E = PCR efficiency of a primer pair, and Ct = the fractional amplification cycle number at which florescence emitted during the reaction first exceeds background fluorescence.

To determine the efficiency of acquisition for each biological replicate, ten individuals were arbitrarily collected from both treatments at eh L1 21-hr time point for endpoint reverse transcriptase-PCR of TSWV N RNA using previously described methods (Badillo-Vargas et al., 2012). All insects sampled from the non-virus treatment (negative control) were determined to be PCR-negative for the virus.

Construction of phylogenetic dendrograms

Description of targeted genes was completed *in silico* to provide evidence for accurate selection of predicted transcripts. Target selection was based solely on computational annotation. Phylogenetic tree clusters were built to show similarities with other insect species: *Nilaparvata*

lugens (Brown planthopper), *Cimex lectularius* (Bed bug), *Graminella negrifrons* (Yellow-eyed leafhopper), *Pediculus humanus corporis* (Body louse), *Aphis glycines* (Soybean aphid), *Drosophila melanogaster* (Fruit fly), *Aedes aegypti* (Yellow fever mosquito), *Bemisia tabaci* (Silverleaf whitefly), *Bombyx mori* (Silkworm), *Apis mellifera* (Western honey bee), *Nasonia vitripennis* (Parasitoid wasp), *Acyrthosiphon pisum* (Pea aphid) with out-groups *Penaeus monodon* (Giant tiger prawn) and *Homo sapiens* (Human). An LG tree model type was selected using a best model finder in MEGA7 (Kumar et al., 2016). The LG model is common for amino acid replacement matices (Le and Gascuel, 2008). Trees were built with a bootstrap test (1000 replicates) (FELSENSTEIN, 1985). Branches with less than 50% agreement in bootstrap replciates were collapsed. All positions containing gaps and missing data were eliminated, and evolutionary analyses were conducted in MEGA7 (Kumar et al., 2016).

Synthesis of dsRNA molecules

Two key proteins operating in the RNAi pathway were chosen for the synthesis of dsRNA molecules (*i.e.* Dicer-2 and AGO2). Transcripts were identified using the i5k National Agricultural Library BLAST database tool for the *F. occidentalis* genome. Western flower thrips MAKER models (FOCC) were determined through protein sequence similarity with other organisms. Sequences putatively identified as Dicer-2 and AGO2 were used to design, *in silico*, long regions of sequence for dsRNA synthesis (Figure 3.5) (Appendix D). Primer design and selection of dsRNA target regions was completed using Snapdragon – dsRNA design (Hu et al., 2017). Primers were then synthesized (Integrated DNA Technologies, Inc., Coralville, Iowa) and working stocks were prepared for DNA synthesis with FailSafe high fidelity polymerase (Epicentre, Madison, WI). As a negative control, GFP was chosen for dsRNA synthesis as previously described (Badillo-Vargas et al., 2015). Amplicon size was validated on

electrophoresis gel and DNA was extracted for PCR cleanup with GeneJET Gel Extraction and DNA Cleanup Micro Kit (Thermo Scientific, Wilmington, DE, USA). A second PCR was run with T7 strand specific directional priming using the initial amplicon. Synthesized single strand DNA (ssDNA) was cleaned with the kit previously mentioned. The ssDNA was then used for standard protocol RNA synthesis T7 RiboMAX^{TM} Express system (Promega, Madison, WI, USA). The single strand RNA (ssRNA) was mixed in equal parts for each target to produce dsRNA and allowed to precipitate overnight a -20 ^{O}C. The final dsRNA product was spun down and collected for a dilution with 20ul of RNAse-free DNAse-free water.

Microinjection of female thrips with dsRNA molecules

A time-course experiment was conducted to explore changes in expression early (one day), middle (3 day), and late (6 day) expression of RNAi targeted genes. Three-day-old female thrips were collected from two separate treatments (*i.e.* non-exposed and TSWV-exposed) and injected with one of four treatments: H_2O, dsRNA-GFP, dsRNA-Dicer-2, and dsRNA-AGO2. A total of 36 individual females were injected within each factor (no-TSWV, TSWV) of each injection treatment using the methods of Badillo-Vargas et al. (2015). The Nanoinjector II (Drummond Scientific, Broomall, PA) was used on female thrips immobilized on double-sided tape adhering to microscope slides for micro-injection of 12nL at 3nL/s of either H2O or dsRNA (80ng per insect). The needle was used to pierce through the stretchable membrane between the second and third tergites of the abdomen (Badillo-Vargas et al., 2015). Individual injected females were then placed on green bean pods in clear plastic medicine cups and secured with lids with openings covered with thrips-proof mesh for ample gas exchange and ventilation. The cups were held in an incubator set at a 12h-photoperiod at 24^{O}C. Insects were sampled 24, 72 hpi, and

144 hours post injection (hpi) and flash-frozen in micro-centrifuge tubes and stored at -80^{O}C until further processed.

Quantitative qRT-PCR determination of normalized abundance for TSWV-N RNA and expression of transcript targets (*i.e.* DCR2 and AGO2) post microinjection with dsRNA

Total RNA was isolated from individual thrips using Chelex 100 (Bio-rad, Hercules, California) as previously described (Boonham et al., 2002). Complementary DNA (cDNA) was synthesized from RNA by loading the max amount of volume to the Verso^{TM} cDNA kit (Thermo Scientific, Wilmington, DE, USA) reaction (11ul). TSWV virus abundance was detected using previously described methods for normalized real-time qRT-PCR of TSWV nucleocapsid (N) RNA compared to *F. occidentalis* actin as an internal reference (Badillo-Vargas et al., 2012, Rotenberg et al., 2009b). Primers for qRT-PCR were constructed using Beacon7 software to detect and amplify transcript RNA (mRNA) amplicons outside of the regions targeted through RNAi by previously synthesized and injected dsRNA (Table 3.1). Measurement of transcript abundance was normalized through comparison to the same reference gene described above (Badillo-Vargas et al., 2015).

Statistical analysis of transcript abundance, larval offspring counts, percent survival, and viral RNA abundance.

To compare virus titers spanning development, normalized abundance data were analyzed statistically using SAS v.9.3 (SAS Institute, Cary, NC). The SAS procedure GLIMMIX was used to determine the best fit of data and residuals to perform Type III tests of fixed effects (F-tests), and LSMEANS and p-values were computed post hoc to determine the statistical

difference ($P < 0.05$) between pairwise developmental stage-time points. GLIMMIX analysis determined that the best fit of the normalized abundance data and accompanying residuals was lognormal distribution (link function –identity). GLIMMIX analyses were also used to determine best fit for normalized abundance values of target transcripts (*i.e.* DCR2 and AGO2) and production of offspring (Appendix C). Gamma was found to be the best-fit distribution for normalized abundance values of transcript expression and used for statistical tests with a cut-off for significance of $P < 0.05$. A poisson distribution was used for statistical test on number of offspring produced with a cut-off for significance of $P < 0.0001$ (Appendix C).

To determine the effect of dsRNA treatment on number of surviving insects at each observation day, non-parametric tests of independence between treatment (*i.e.* H_2O, GFP dsRNA, DCR2 dsRNA, AGO2 dsRNA) and life status (dead or alive) were performed using Fisher's Exact tests in in SAS v9.3 (SAS Institute, Cary, NC) (Appendix C). First, the test of independence was performed on 2 x 4 contingency tables (dead/alive vs treatment) for each day, excluding day 1 due to damage/death caused by microinjection-needle failure in a number of water-treated insects. If the null hypothesis of no-independence was rejected for any given day, Fisher Exact tests of independence were performed on 2 x 2 contingency tables to make pairwise comparisons between treatments.

Comparisons of TSWV-N abundance between treatments were completed using a standard analysis of variance (general linear model) (Minitab v.14, State College, PA, USA). The response variable (TSWV-N normalized abundance) was normalized (log2) and pairwise treatments comparisons completed using Tukey's simultaneous tests (adjusted p-values) (Minitab v.14, State College, PA, USA).

Figures and Tables

Table 3.1 Primer sequences used for dsRNA synthesis and real-time quantitative PCR**.**

Gene	Primer use	Sequence	Product length	Primer efficiency
GFP	dsRNA synthesis	T7F:GGATCCTAATACGACTCACTATAGGGGTGACCACCCTGACCTAC	305 bp	N/A
		F:GTGACCACCCTGACCTAC		
		T7R:GGATCCTAATACGACTCACTATAGGGTTGATGCCGTTCTTCTGC		
		R:TTGATGCCGTTCTTCTGC		
Dicer-2	dsRNA synthesis	T7F:GGATCCTAATACGACTCACTATAGGAGTGGATGAGAGTGCTGCCT	580 bp	N/A
		F:AGTGGATGAGAGTGCTGCCT		
		T7R:GGATCCTAATACGACTCACTATAGGAGGTTACGGCCACAATCAAG		
		R:AGGTTACGGCCACAATCAAG		
AGO2	dsRNA synthesis	T7F:GGATCCTAATACGACTCACTATAGGTGATGTGGCACACAAAGGTT	430 bp	N/A
		F:TGATGTGGCACACAAAGGTT		
		T7R:GGATCCTAATACGACTCACTATAGGAACCATTTTTGCAGTTTGGC		
		R:AACCATTTTTGCAGTTTGGC		
Dicer-2	qPCR	F:CTGCCGAATACCACCTTA	107 bp	1.98
		R:GTAAACCCTTCACAACATCTT		
AGO2	qPCR	F:AGATCCAACCGTTAAGATT	83 bp	1.98
		R:CCTCCATTACAAGTCTCAT		

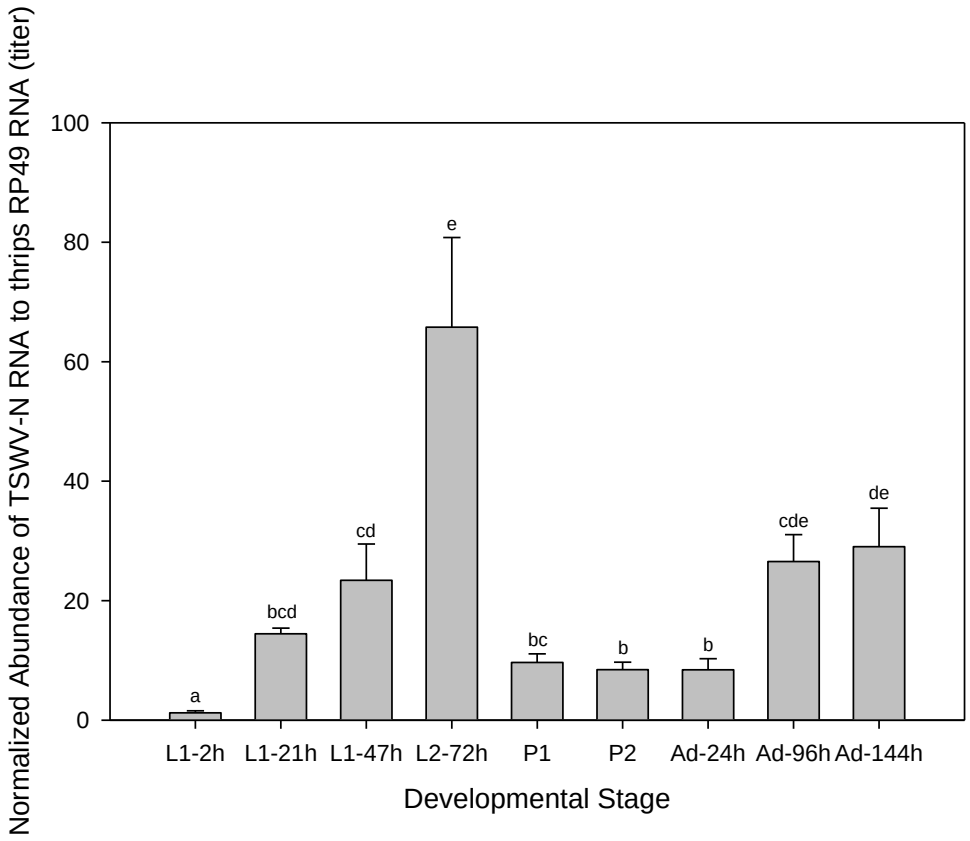

Figure 3.1 Two cycles of tomato spotted wilt virus accumulation during thrips development. L1 = first instar larvae allowed a 3-hr acquisition access period on TSWV-infected tissue, then reared on healthy green bean pods for 21 hours prior to sampling; P1 = pre-pupal stage; Ad-24 = adults sampled 24 hours after eclosure. Real-time qRT-PCR of nucleocapsid (N) RNA was used to estimate virus titer. The normalized abundance of TSWV N relative to an internal standard was calculated using the equation: $((E_{RP49})^{(CtRP49)}/(E_{TSWV\text{-}N})^{(CtTSWV\text{-}N)})$ (Pfaffl, 2001); where E = PCR efficiency of a primer pair, and Ct = the amplification cycle number at which fluorescence emitted during the reactions first exceeds background fluorescence and is inversely related to the initial template concentration in the PCR reaction. Each bar represents four biological replications $\pm$ standard error. Bars headed by different letters indicate statistical differences between pairwise means ($P < 0.05$).

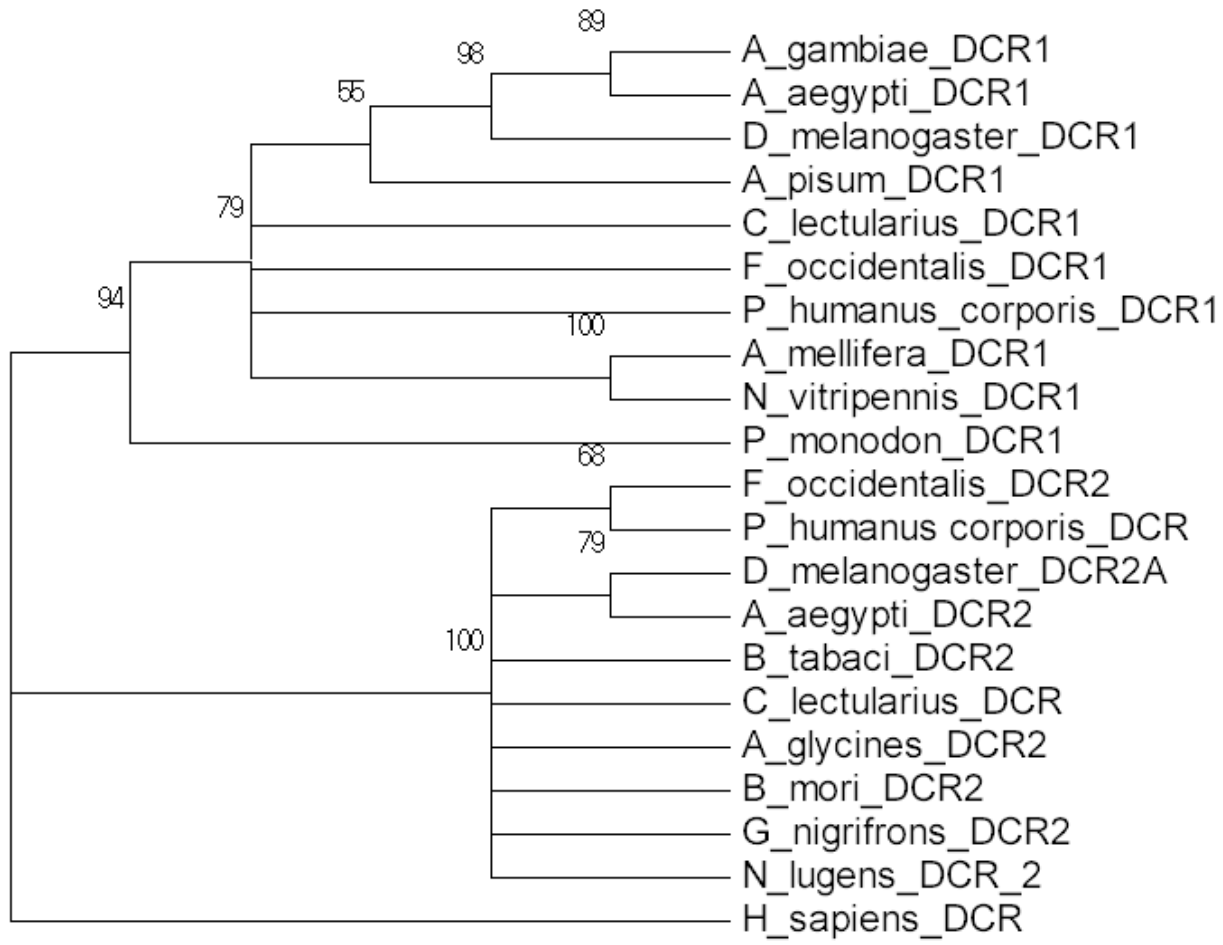

Figure 3.2 *F. occidentalis* Dicer-2 groups with other Dicer-2 sequences.

The evolutionary history was inferred using the Maximum Likelihood method. The percentage of replicate trees in which the associated taxa clustered together in the bootstrap test (1000 replicates) (FELSENSTEIN, 1985) is shown next to the branches. Branches reproduced in less than 50% of bootstrap replicates were collapsed. The analysis involved 21 amino acid sequences. All positions containing gaps and missing data were eliminated. There were a total of 336 positions in the final dataset. Evolutionary analyses were conducted in MEGA7 (Kumar et al., 2016).

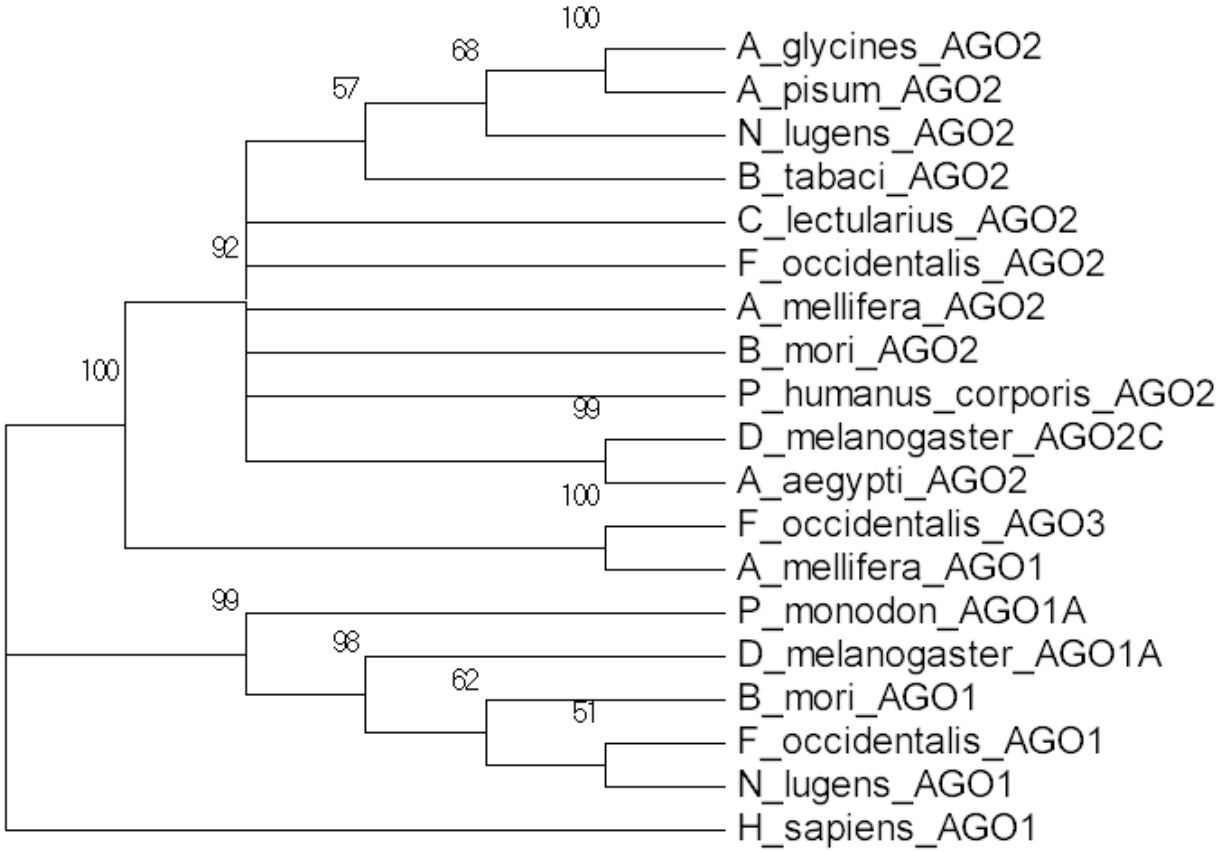

Figure 3.3 *F. occidentalis* AGO2 is divergent from other AGO2 sequences.

The evolutionary history was inferred using the Maximum Likelihood method. The percentage of replicate trees in which the associated taxa clustered together in the bootstrap test (1000 replicates) (FELSENSTEIN, 1985) is shown next to the branches. Branches reproduced in less than 50% of bootstrap replicates were collapsed. The analysis involved 19 amino acid sequences. All positions containing gaps and missing data were eliminated. There were a total of 602 positions in the final dataset. Evolutionary analyses were conducted in MEGA7 (Kumar et al., 2016).

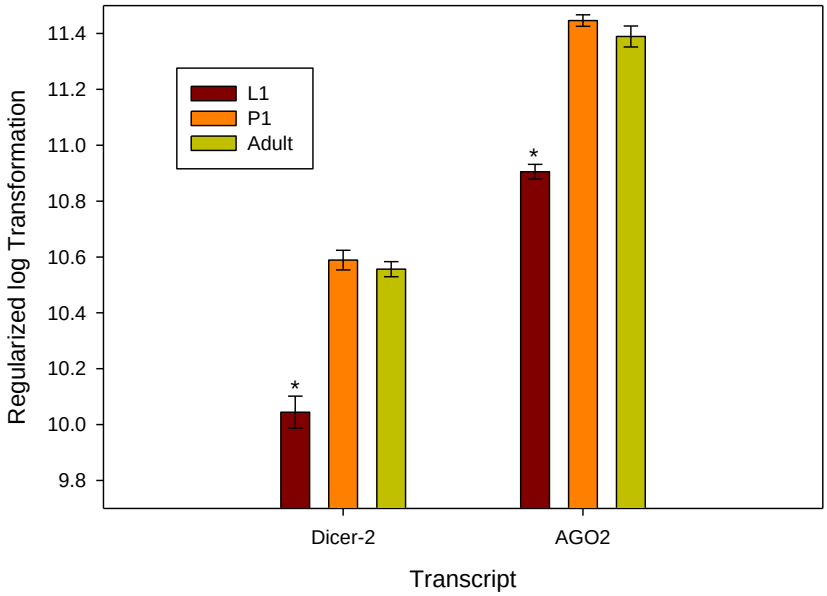

Figure 3.4 Basal level expression of Dicer-2 and AGO2 in three development stages of *Frankliniella occidentalis*.

Data was collected from my Illumina HiSeq RNAseq analysis of western flower thrips global gene expression (Chapter 2, non-exposed healthy thrips). A total of 75 to 100 individuals were grouped for L1 = young first instar larva 24 to 41 hours old; P1 = Pre-pupal stage; Adult = Adult stage, 24 hours after eclosure. Genome-reference-mapped read counts were generated as described in Appendix A, and normalized by regularized log transformation (log_2-scale) using DESEQ2 (Love et al., 2014a). Each bar represents the mean of four biological replicates $\pm$standard error with asterisk labeling significant differences across developmental stage comparisons (adjusted $P < 0.01$).

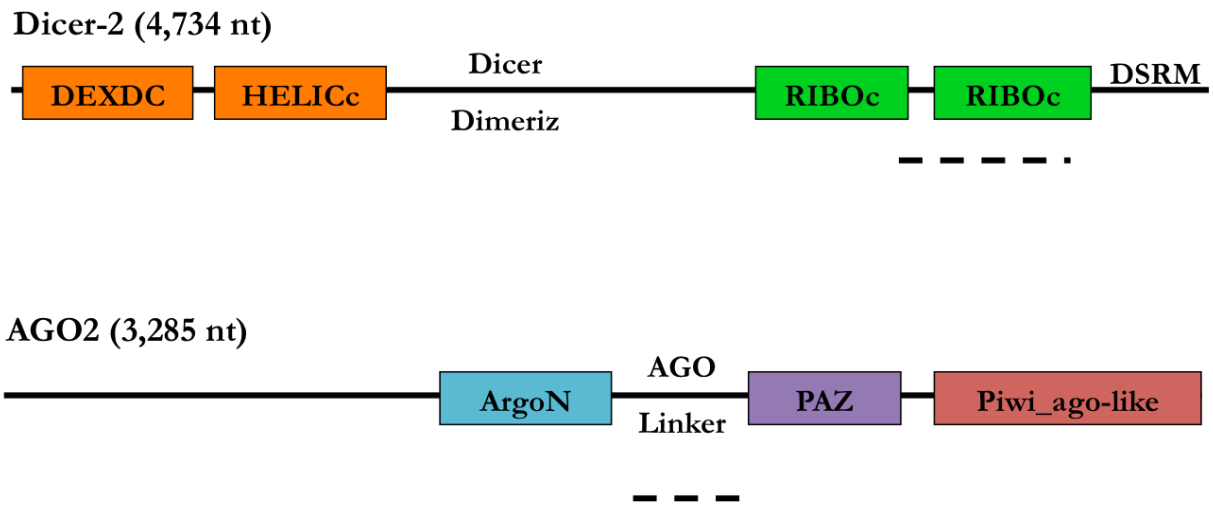

Figure 3.5 RNAi target regions within each transcript.

The dotted line represents the region targeted with synthesized dsRNA (Appendix D). Each box and label represent conserved functional domains of the transcript product. The Dicer-2 domains: DEAD-like helicase (DEDXDC), Helicase (HELICc), Dicer dimerization domain (Dicer Dimeriz), Ribonuclease III (RIBOc), Double stranded RNA-binding domain (DSRM). The AGO2 domains: N-terminal argonaute (ArgoN), Argonaute linker (AGO Linker), Piwi Argonaut Zwille (PAZ), Piwi Argonaut-like (Piwi_ago-like).

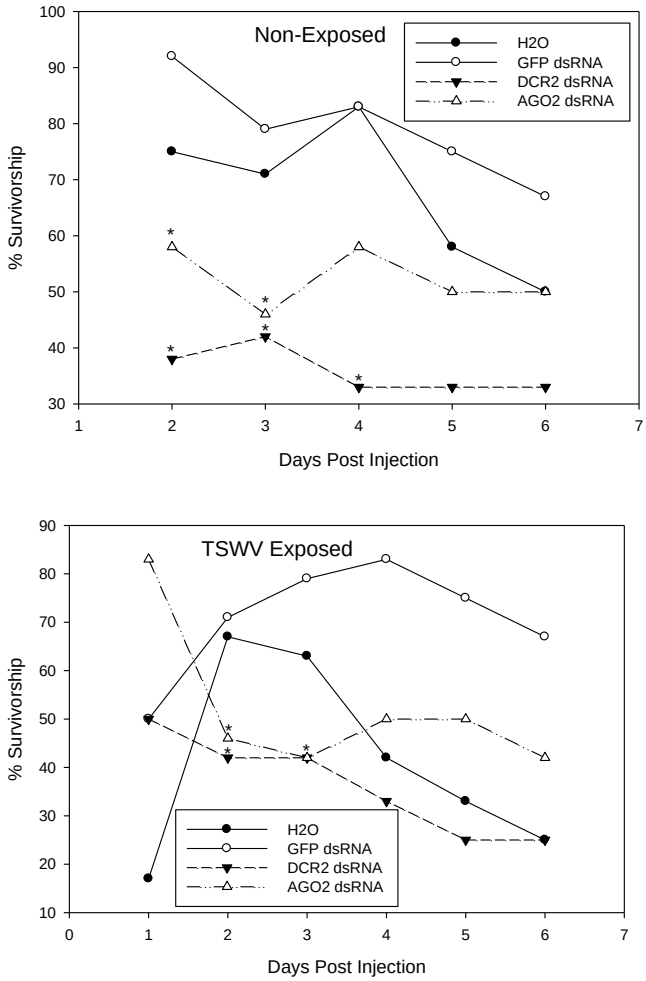

Figure 3.6 Percent survivorship decreases when insects are injected with Dicer-2 or AGO2 dsRNA.

The key indicates which treatments were used for all individual thrips counted. Percent survivorship was calculated by: (total number of alive thrips)/(total number of injected thrips)*100 for each day of observation. Non-exposed (no acquisition of TSWV allowed) thrips are represented in the top panel and TSWV-exposed thrips are represented in the bottom panel with asterisks (*) indicating significant differences ($P < 0.05$) between the dsRNA-DCR2 or -AGO2 treatment and GFP dsRNA control on day indicated. Day one was not included in statistical tests due to a faulty microinjection needle killing many insects as seen depicted in the bottom panel (TSWV-exposed).

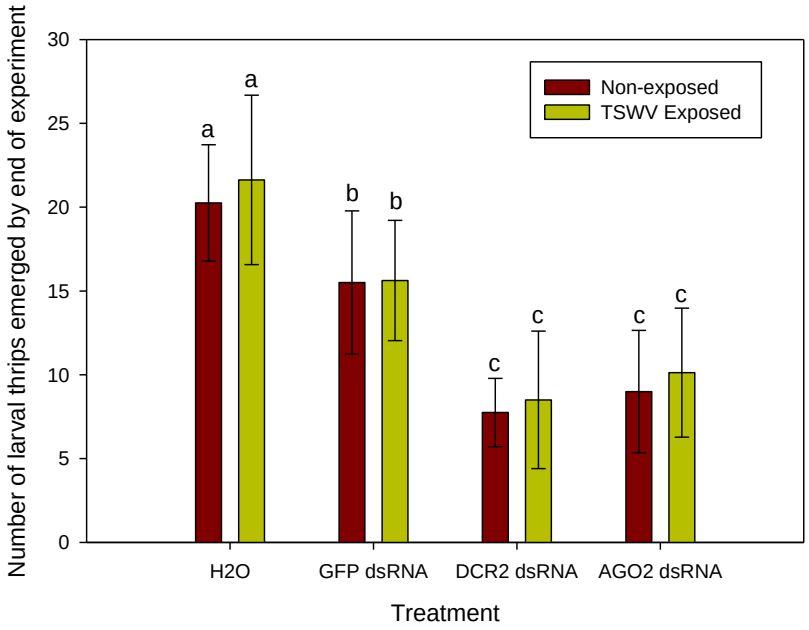

Figure 3.7 Larval counts determined two days after final insect sampling time point (6dpi). Larval offspring counted across eight cups with average plotted and error bars representing the standard error of the mean. Letters indicate significant differences between treatments ($P < 0.05$).

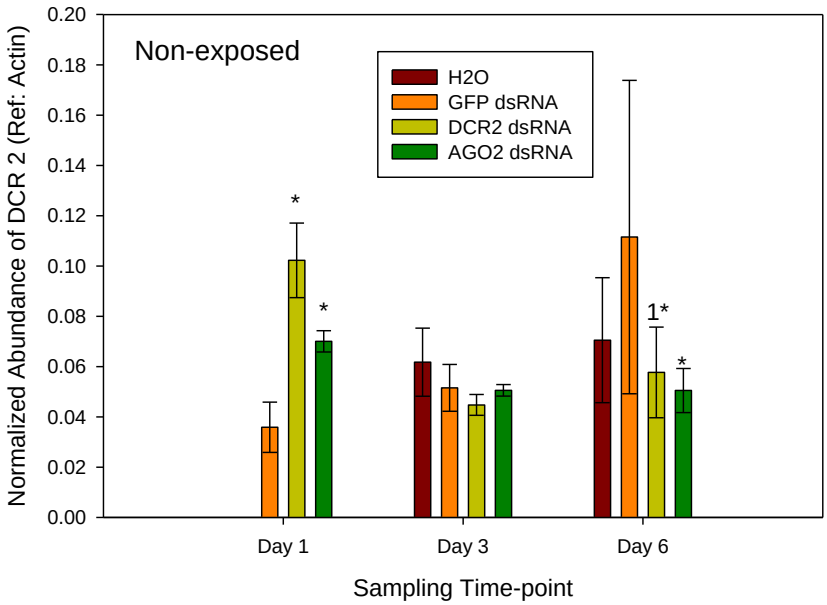

Figure 3.8 Expression of Dicer-2 (DCR2) after treatment with dsRNA in non-exposed adult thrips.

Each bar represents the normalized abundance of DCR2 transcript calculated as previously described with reference to actin as internal reference. The error bars represent standard error of three individual insects for each time-point and each treatment. Asterisk identifies significant differences between dsRNA-DCR2 or – AGO2 treatment and dsRNA-GFP within day, and number indicates significant difference between that treatment and the day number indicated ($P < 0.05$). Missing data at day 1 for H2O treatment was loss from death by injection with poorly cut needle.

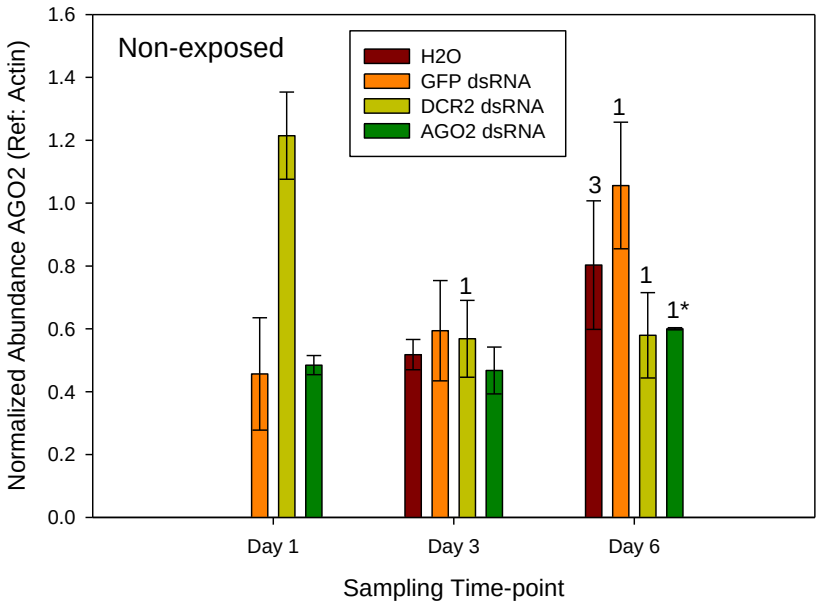

Figure 3.9 Expression of Argonaute-2 (AGO2) after treatment with dsRNA in non-exposed adult thrips.

Each bar represents the normalized abundance of AGO2 transcript calculated as previously described with reference to actin as internal reference. The error bars represent standard error of three individual insects for each time-point and each treatment. Asterisk identifies significant differences between dsRNA-DCR2 or – AGO2 treatment and dsRNA-GFP within day, and number indicates significant difference between that treatment and the day number indicated ($P < 0.05$). Missing data at day 1 for H2O treatment was loss from death by injection with poorly cut needle.

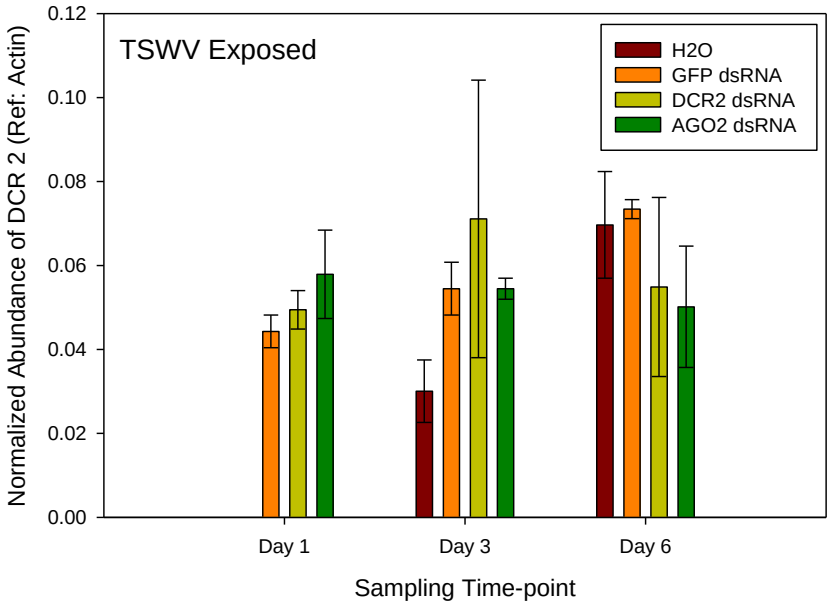

Figure 3.10 Expression of Dicer-2 (DCR2) after treatment with dsRNA in TSWV-exposed adult thrips.

Each bar represents the normalized abundance of DCR2 transcript calculated as previously described with reference to actin as internal reference. The error bars represent standard error of three individual insects for each time-point and each treatment. Asterisk identifies significant differences between dsRNA-DCR2 or – AGO2 treatment and dsRNA-GFP within day, and number indicates significant difference between that treatment and the day number indicated ($P < 0.05$). Missing data at day 1 for H2O treatment was loss from death by injection with poorly cut needle.

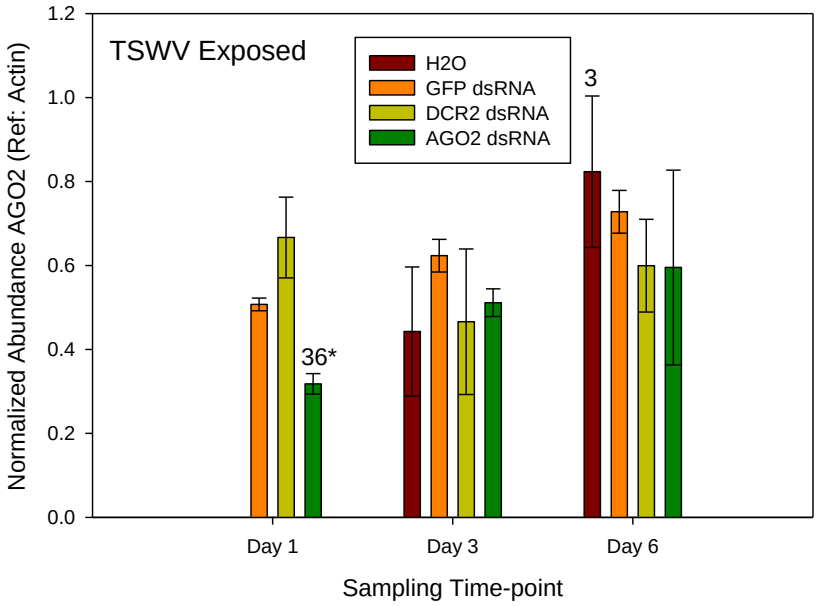

Figure 3.11 Expression of Argonaute-2 (AGO2) after treatment with dsRNA in TSWV-exposed adult thrips.

Each bar represents the normalized abundance of AGO2 transcript calculated as previously described with reference to actin as internal reference. The error bars represent standard error of three individual insects for each time-point and each treatment. Asterisk identifies significant differences between dsRNA-DCR2 or – AGO2 treatment and dsRNA-GFP within day, and number indicates significant difference between that treatment and the day number indicated ($P < 0.05$). Missing data at day 1 for H2O treatment was loss from death by injection with poorly cut needle.

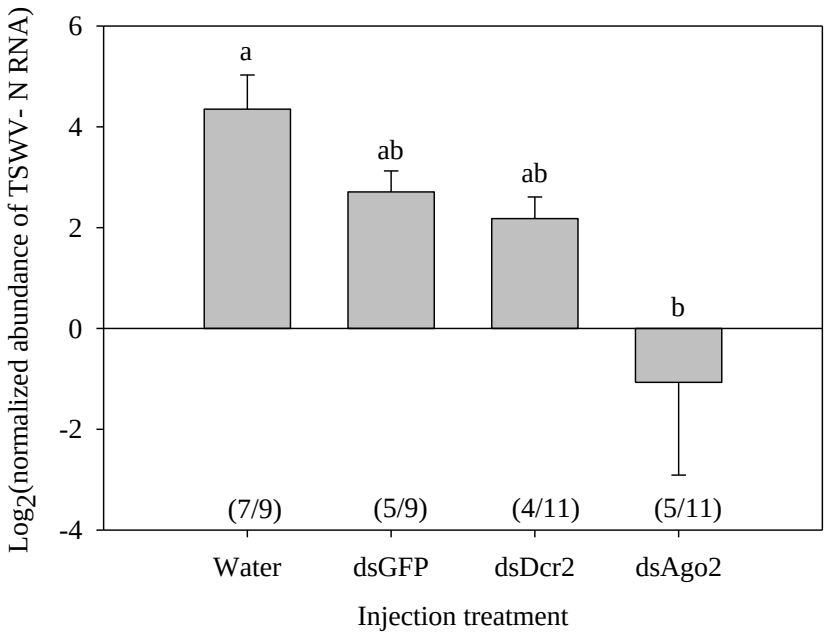

Figure 3.12 Effect of dsRNA treatment of virus titer in adult thrips.

Values in parentheses () indicate number of infected adults / number of adults sampled and analyzed. Bars represent means ± stderr of infected individuals from all sampling time points.

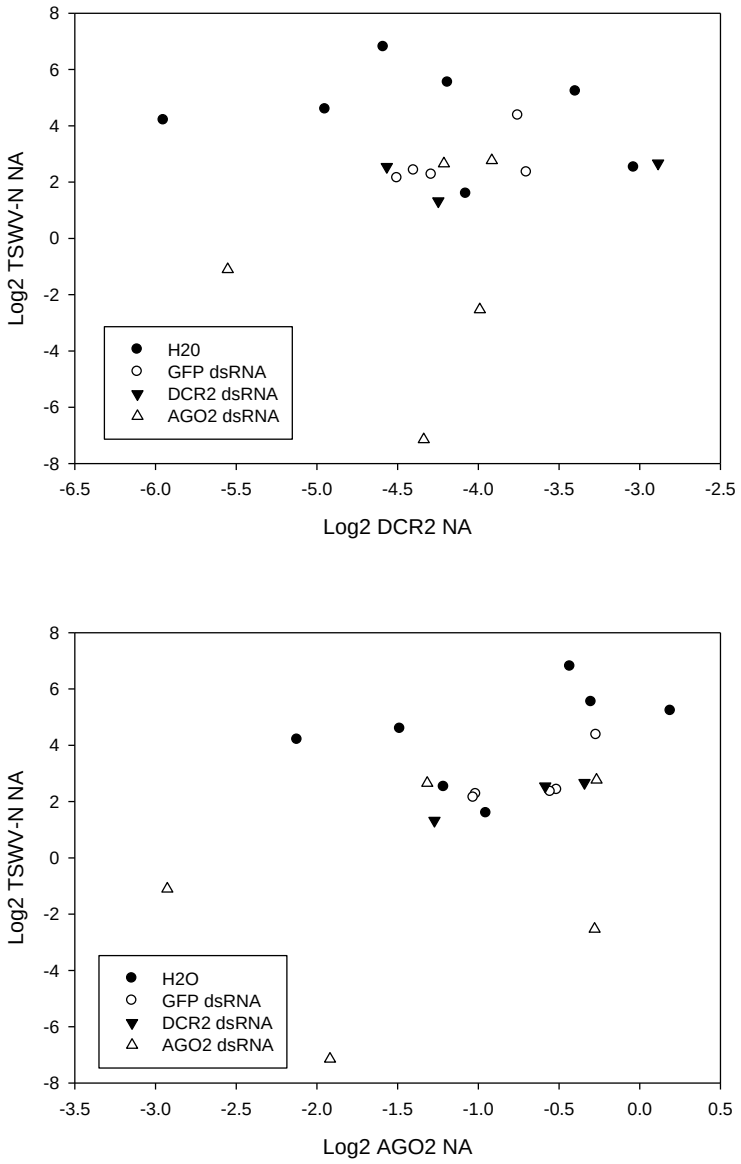

Figure 3.13 Exploration of possible association between viral RNA abundance and endogenous gene transcript abundance of DCR2 (top panel) and AGO2 (bottom panel) in TSWV-infected thrips.

Each data-point represents all infected thrips for all sampling time-points combined. The normalized abundance (NA) of TSWV N RNA, DCR2 RNA, and AGO2 RNA relative to an internal standard RNA (actin) was calculated as described in the methods.

Chapter 4 - Construction and testing of transgenic *Arabidopsis thaliana* expressing dsRNA hairpins to target *Frankliniella occidentalis* V-ATPase-B transcripts for RNAi-based silencing during feeding

Abstract

Frankliniella occidentalis is a polyphagous insect that feeds on fruit, vegetable, and ornamental crops. The adult life stage is winged and mobile allowing it to spread rapidly through field plots causing plant damage by both feeding and transmission of viruses. There are very few effective control strategies for this insect vector. Western flower thrips quickly develop resistance to pesticides and they avoid chemical control through hiding in small crevices in the plant structure. Novel control for the insect pest is highly sought after by vegetable and fruit growers, and RNA-interference-based insect control strategies are in the early stages of development. The specific objectives of my study were to 1) design and build hairpin expression vectors for transformation of plants, 2) transform *A. thaliana* with thrips specific targets and measure expression of dsRNA hairpins, 3) develop a feeding assay to deliver dsRNA hairpins orally to thrips and measure expression of the endogenous gene target and 4) determine if feeding on plant tissue transgenically-expressed dsRNA alters thrips survival and development measure insect development changes. Using previous knowledge of thrips RNAi targeting, thrips V-ATPase-B was chosen as an RNAi target for transformation vector construction. Both V-ATPase-B (thrips specific target) and GFP (negative control) constructs were built separately and transformed into *A. thaliana* for in plant expression of dsRNA hairpins. Expression of hairpin

dsRNA *in planta* was measured using the GUS linker and thrips were allowed to feed on transgenic plants. Transcript expression dynamics were measured in individual thrips for the target gene mRNA abundance after thrips were allowed to feed on plants expressing dsRNA hairpins. Feeding on either the dsRNA-V-ATPase-B transgenic line or the dsRNA-GFP transgenic line had a significant effect on expression of the thrips gene target compared to the wild type control plant. In addition, there was no significant silencing of V-ATPase-B expression in thrips feeding on transgenic plants expressing dsRNA-V-ATPase-B compared to those feeding on transgenics expressing dsRNA-GFP. It was apparent that the dsRNA-GFP transgenic line used in this study did not serve adequately as a negative dsRNA control. Analysis of oral-delivery of synthetic dsRNA –durability and gut-uptake in thrips is necessary for future development of successful plant-delivered RNAi-based strategies for controlling thrips pest species.

Introduction

The western flower thrips, *Frankliniella occidentalis*, are pests that feed on fruits, vegetables and ornamental crops causing both feeding damage and transmission of plant infecting viruses. They feed on a variety of plants that are economically important: tomato, peanut, potato, pepper, corn, and wheat. They exhibit a high level of locomotor activity, high fecundity, short generation time, and preference for concealed spaces (Morse and Hoddle, 2006). Thrips develop from egg to adult within 14 days under standard conditions (23 ^{O}C at 16h:8h light:day) (Moritz et al., 2004) starting with a newly hatched first instar larvae (L1) that feeds and molts to a second instar larva (L2). The insect then drops from the plant canopy to the soil and develops through two pupal stages (P1 and P2) before eclosure into adulthood (Lewis,

1973). The adult stage is winged and mobile allowing the insect to spread greater distances to feed on other plants, transmit phytoviruses and, if female, oviposit eggs for the generation of more thrips larva.

Current control strategies for this insect vector are few with insecticides not acting as an effective control strategy due to the insect's thigmotactic behavior of hiding within crevices on plant surfaces and ability to develop resistance to chemical controls (Dreistadt et al., 2007, Jensen, 1998, Morse and Hoddle, 2006). Thrips eggs are oviposited within the plant tissue and are protected from non-systemic foliar pesticides, while the pre-pupa (P1) and pupae (P2) are also protected because they drop to the soil during pupation. Effective systemic pesticides such as the organophosphate insecticide acephate, can only be used on ornamental nonfood crops. While insecticide resistance in field populations is prevalent with varied levels resistance reported throughout thrips populations in china (Wang et al., 2016b). Control of this insect pest through novel targeting tools will provide gene and species specific control.

Insects and other eukaryotes are known to have a mechanism for posttranscriptional gene regulation called the short interfering RNA (siRNA) pathway (Meister and Tuschl, 2004). The siRNA pathway is induced during the presence of double stranded RNA (dsRNA). The pattern recognition receptor, Dicer-2, recognizes dsRNA and cleaves the dsRNA into small RNA duplexes of approximately 21 nucleotides in length. These small RNA duplexes assemble into the RNA-induce Silencing Complex (RISC), a protein complex comprised of three or more enzymes. The central player in the RISC complex, Argonaute 2 (AGO2), is an RNA binding endonuclease that uses one strand of the small RNA duplex to act as guide for locating RNA sequences that are complementary to the guide strand. Once a complimentary sequence anneals

to the guide strand, AGO2 slices the RNA into small noncoding fragments, rendering the transcript ineffectual.

The holoenzyme V-ATPase is important for acidification of intracellular organelles and is comprised of 13 subunits. Subunits of V-ATPase, such as subunits A and E, have been targeted through RNAi with observable phenotypes (Baum et al., 2007, Huvenne and Smagghe, 2010). The holoenzyme pumps protons across plasma membranes of numerous cells types and it is prevalent within the insect gut (Wieczorek et al., 2009). A *Drosophila melanogaster* line with a knock-out mutation in V-ATPase-B is lethal to insect larval. Increase mortality is also described for *D. melanogaster*, *M. sexta*, *T. castaneum*, *N. lugens*, and *A. pism* when V-ATPase-E dsRNAs specific to each species were delivered through synthetic diets (Li et al., 2011, Whyard et al., 2009). Creating an expression vector targeting v-ATPase components and introducing it into plants for expression of dsRNA was shown to prevent development of larvae and produce mortality, providing control against western corn rootworm (Baum et al., 2007). Body weight of larvae Colorado potato beetle was significantly decreased by day six when they fed on bacteria-expressed dsRNA for separate treatments of V-ATPase-E and V-ATPase-B subunits (Zhu et al., 2011). These same subunits silenced in *P. maidis* also resulted increased mortality and reduced fecundity when insects fed on artificial diets or were injected with dsRNA (Yao et al., 2013).

Western flower thrips are known to have a functional RNAi system in which transcripts can be knocked down (*e.g.* 20 to 30% reduction in transcript level) through microinjection. Synthesized V-ATPase-B dsRNA was injected into adult female thrips and significant reduction in the relative abundance of V-ATPase-B was observed at both two and three days post injection. Reduction of V-ATPase-B transcript abundance resulted in increased mortality and reduced

fertility (number of viable offspring produced) (Badillo-Vargas et al., 2015). Injection of dsRNA provides a direct delivery tool for investigating gene function, but is not suitable for large scale insect control. Synthetic diets for western flower thrips have not been well developed, and feeding of sucrose alone appears to arrest larval development (Badillo-Vargas, unpublished data), precluding oral-delivery of dsRNAs to thrips. Construction of plants expressing dsRNA constructs for V-ATPase-B has provided another alternative for insect control development and exploration through feeding.

Results

Transgene expression in *Arabidopsis* plant leaves

As a prerequisite for my feeding experiment, it was essential to confirm that leaves of different ages from the transgenic plants expressed the transgene. The dsRNA linker (GUS) was amplified from transgenic leaf tissue from multiple leaves collected across two separate plants for each transgenic event at the T3 generation (*i.e.* GFP and V-ATPase-B), while no amplification from the wild-type plant was detected (Figure 4.1). The Cq values were within the dynamic range of the thermocycler (18.49 to 28.29 Cq), while the median normalized abundance of GUS for the V-ATPase-B plants was more dynamic across the two plants. The standard deviation spanning every leaf for the second GFP plant (2G2.6.2) plant was less when compared to the first plant (0.6 compared to 2.75). This was also true for the standard error of the mean (0.12 compared to 0.34). The second V-ATPase-B (2V3.11.6) plant had very similar standard deviation across the whole plant when compared to the first plant (0.45 compared to 0.47) and standard error of the mean (0.07 compared to 0.07). It appears that the variation of dsRNA

construct production within plant is less in the V-ATPase-B transgenic, but variation across plants is higher (Figure 4.1).

Basal expression of V-ATPase-B in *Frankliniella occidentalis*

Expression of V-ATPase-B spanning thrips development provided an important measurement for variation within each insect stage. The dynamic profiles of gene expression for this target gene necessitated synchronization of development, while also supporting the requirement of collection for an early time point (*i.e.* two days after exposure to transgenic plant tissue). RNA-Seq data from healthy thrips feed on green beans were used for measurements of the target gene. Differences in expression of V-ATPase-B were observed at three discrete thrips development stages with expression of V-ATPase-B 1.55 log2FoldChange higher ($padj < 0.01$) during the L1 stage when compared to the P1 and adult stage (Figure 4.2). The P1 stage had the lowest expression of V-ATPase-B when compared to both the L1 (see previous) and adult stage (-0.85 log2FoldChange, $padj < 0.01$).

Documentation of transgene incorporation (DNA) and expression in T1 to T3 parents

Transformed seeds were planted and leaf tissue was sampled for both genomic DNA isolation and RNA isolation for detection of genomic transformation and expression of the hairpin structure. Detection at the DNA level and RNA level was completed using primers specific for each target and positive plants were detected through use of the forward and reverse GUS primer and gene specific reverse primers (example in Figure 4.6). Each plant positive at

both the DNA and RNA level was selected for seed production and passed to the next generation (Table 4.2).

Expression of endogenous thrips V-ATPase-B during feeding on transgenic plants

Thrips V-ATPase-B expression was significantly different between the two completed biological replicates with the first biological replicate indicating a down-regulation of V-ATPase-B in thrips fed on transgenic plant tissue expressing the short hairpin for V-ATPase-B. This significant difference could not be replicated with second biological replicate providing that the overall thrips expression of V-ATPase-B was less when compared to the first biological replicate (Figure 4.3). In an attempt to isolate differences sooner in development, a day one sampling time-point was also sampled and measured. V-ATPase-B expression in thrips did not appear to vary significantly early in the feeding time-course, but a trend of down-regulation of V-ATPase-B for both transgenic plant treatments was observed in similarity to the day two expression data (Figure 4.4).

Development of thrips feeding on transgenic plants

Insect development stage was identified during destructive sampling for gene expression analysis. Development of thrips on transgenic plants appeared to be delayed when comparing the treatment in both biological replications. The GFP and V-ATPase-B transgenic plant treatments tended to have fewer larval stages early in the time-course when compared to the wild-type control. The GFP and V-ATPase-B treatments had an average percent of insects, 58.93 and 72.22 respectively, in the larval stage while the wild-type control still had 94.44% in the larval stage at day 4 (Figure 4.5). This was again true on day eight when wild-type control had 11.11% still in

the larval stage (Figure 4.5). The apparent increase in development was lost during the P1 and P2 stage where the transgenic treatments were delayed in development to adulthood (Figure 4.5).

Discussion

Plant protection from arthropod vectors and the viruses they transmit is a major priority for multiple economically important crops worldwide. The utility of a transgenics-based approach is virtually unexplored as a means of controlling thrips populations when compared to other major crop pests. The use of sequence specific targeting through RNAi for insect control is an enticing control strategy due to the species specificity and targeted controlled knock-down (Huvenne and Smagghe, 2010, Whyard et al., 2009). Each insect of interest for targeting with dsRNA technology must have the RNAi pathway tested and described for viability of control. *F. occidentalis* was shown to display a knock-down phenotype of V-ATPase-B through microinjection with 80ng of dsRNA (Badillo-Vargas et al., 2015). The next step in establishing a control RNAi control strategy for F. occidentalis was the creation of transgenic plants with dsRNA constructs for *F. occidentalis* specific V-ATPase-B mRNA sequences, and this was achieved through a standardized floral dip method with *A. thaliana* plants.

Under the described study conditions, experimental parameters, and selected controls (shp-GFP), silencing of V-ATPase-B in thrips developing to plants transgenically-expressing dsRNA of V-ATPase-B was not robust, evident by the different outcomes between the two biological replications. (Figure 4.3). It is clear that the expression of V-ATPase-B in thrips is dynamic during development (Figure 4.1) making detection of its expression highly variable in thrips populations that are not synchronized. Multiple controls were established to synchronize development with both brushing of green beans and experimentation within a climate-controlled

incubator. Even with the controls listed, it is possible that insect development variability confounded the measurements of expression between treatments. Ultimately the results indicate that targeted knock-down is not a major outcome of feeding on dsRNA producing *A. thaliana* tissue. Further exploration of dsRNA acquisition from feeding and uptake into the epithelial gut cells is needed to further describe how thrips are interacting with this novel control strategy. Exploration of successful dsRNA molecule acquisition and uptake is needed.

Western flower thrips feed in a piercing-sucking manner by piercing leaf cells with the mandible (Hunter and Ullman, 1989). During feeding, the insect punctures the leaf epidermis and withdraws cytoplasm from mesophyll cells (Whitfield et al., 2005b), which is a feeding style that supports acquisition and uptake of dsRNA expressed in the cytoplasm of a plant cell. What is currently unknown is how much dsRNA thrips might uptake from this type of feeding behavior and in what state dsRNA exists as it reaches the thrips gut. Thrips are small insects that tend to feed on a particular area of a plant while also have the tendency to be highly mobile. Feeding in short dynamic bursts might not provide a dsRNA level suitable for knock-down. Quantifying the amount of dsRNA obtained during thrips feeding would provide description for comparison with a previous dsRNA injection experiment (Badillo-Vargas et al., 2015). Previous studies have also identified the presence of transcripts for general digestive enzymes (*e.g.* nucleotidase) produced in the salivary glands of thrips (Stafford-Banks et al., 2014). Enzymes produced in the saliva and/or gut might actively degrade dsRNA molecules before reaching the gut epithelial cells for uptake.

Expression of V-ATPase-B in thrips appeared to change due to the treatment of transgenic versus non-transgenic. In general the expression of V-ATPas-B was lower in both the GFP and V-ATPase-B feeding treatment (Figure 4.3). GFP dsRNA, routinely used as an RNAi

control, has been shown to perturb expression of other insect genes (Nunes et al., 2013). Using dsGFP as a control for thrips previously also provided confounding results and, although not statistically significant, appeared to negatively impact survival and fecundity (Badillo-Vargas et al., 2015). It is also possible that a plant expressing a dsRNA through a 35S promoter might have an elevated stress response and act to increase plant defense pathways. An elevated stress response within the transgenic plants might have stimulated a difference in thrips feeding on the host plant. V-ATPase-B expression in thrips could be lower due to a secondary response in the thrips derived from plant stress. Thrips development was also dynamic when comparing the transgenic treatment to wild-type. Presence of larval thrips was reduced early during day four and day six when thrips were allowed to feed on transgenic plants (Figure 4.5). Thrips feeding on transgenic plants also showed an arrested pupal development (Figure 4.5). The above development types are indicative of differences arising from plant stress, and measuring plant defense gene expression within the transgenic plants might provide insight into how the plant is responding to the transgene.

Targeting V-ATPase-B in thrips might not produce a phenotype that is observable or detectable when thrips acquire dsRNA through feeding. When insects were injected with dsRNA, knock-down was within the range of 20 to 30% (Badillo-Vargas et al., 2015). Knock-down derived from feeding might not be detectable with qPCR and a phenotype may not be obvious. Another transcript target specific and necessary for a thrips development is likely to provide mortality phenotype and/or obvious delay in thrips development. With the advent of transcriptomics focused on *F. occidentalis* development, other targets can be designed for a specific phenotype and they can be derived from expression data (Appendix A).

Materials and Methods

F. occidentalis colony maintenance

Franklinella occidentalis (Pergande) originally obtained from Kamilo Iki Valley, Oahu, Hawaii, was maintained on green bean pods (*Phaseolus vulgaris*) in 16-oz clear plastic deli cups with lids adapted for air transfer using thrips-proof mesh. The colony was maintained at room temperature and as described previously (Ullman et al., 1992c).

Arabidopsis thaliana plant maintenance

For collecting seed spanning plant generations, planting soil (Metromix 360) was saturated with water in one inch planting pots. *Arabidopsis thaliana* seeds were sown on top of the soil and placed in a growth chamber at 22 ^{O}C with a 16h:8h light:dark phase at approximately 250um light intensity and seed was collected for each generation and labeled to identify the parent plant. Plants used for experimentation were placed in plastic food containers with drainage holes cut into the bottom for drainage and kept at 4^{O}C for seven days in the dark to synchronize germination (Thaler et al., 2001). The plants were then placed in a growth chamber with conditions listed above. Plants were transplanted into individual pots/containers at the eight-leaf stage and fertilized three to four days later using Carl Pool 20-20-20. Leaf tissue was collected from these plants for subsequent feeding assays.

Transgene design

Two sequences were selected for the construction of hairpin expression (i.e. GFP 305bp and thrips specific V-ATPase-B 500bp). The 5' region of the construct starts with the 35S promoter region for RNA synthesis within the plant. Each arm is inverted with respect to the other on a single strand with a GUS linker between the inversions. The generated RNA will be a single strand read from 5' to 3' and the complmentarity produced provides the folding into a hairpin structure.

Cloning V-ATPase-B target sequence into the donor vector (pENTR/D-TOPO)

A group of 75-100 insects were collected into a 1.7 ml microfuge tube using a fine paintbrush and flash-frozen in liquid nitrogen and stored at -80 ^{O}C as previously described (Schneweis et al., 2017). Total RNA was extracted and isolated from the group sample using TRIzol reagent (Invitrogen, Carlsbad, CA, USA) with methods described for thrips RNA collection (Badillo-Vargas et al., 2012). Total RNA yield was measured using the Nanodrop spectrophotometer (Agilent, Inc, Santa Clara, CA, USA)) ranging from 340 to 361 ng μl^{-1} (Schneweis et al., 2017). Complementary DNA (cDNA) was synthesized from 1 μg of total RNA with Verso^{TM} cDNA kit (Thermo Scientific, Wilmington, DE, USA) as described previously (Badillo-Vargas et al., 2012, Rotenberg et al., 2009b). Blunt end DNA fragments with a 5-prime CACC overhang on the reverse complement strand were produced with high fidelity FailSafe^{TM} PCR (Epicentre, Madison, WI, USA). The V-ATPase-B target was identified and targeted from previous sequence information (Badillo-Vargas et al., 2015). The control GFP target fragment was amplified from a previously built vector (Yao et al., 2013). DNA fragments were inserted into the pENTR/D-TOPO vector using a directional TOPO cloning reaction specified by the kit (Invitrogen, Carlsbad, CA, USA) and the completed vector was used for transformation of

chemically competent *E. coli* One Shot cells (Thermo Scientific, Wilmington, DE, USA). Cells were then plated on LB media with 50 μg/mL Kanamycin for selection. The length of in insert was determined by whole cell PCR and the sequence inserted was verified through DNA sequencing (GENEWIZ, South Plainfield, NJ, USA).

Subcloning target inserts from pENTR/D-TOPO into the destination vector (pANDA35HK) for agrobacterium transformation

Colonies of *E. coli* positive for the targeted insert (*e.g.* GFP control, V-ATPase-B) were grown overnight in selective broth and plasmid was purified using standard miniprep protocol (Qiagen, Germantown, MD, USA). The insert in the pENTR/D-TOPO vector was then recombined into pANDA35HK using a Gateway LR reaction (Invitrogen, Carlsbad, CA, USA) in both a forward and reverse complement orientation around a GUS linker(Miki and Shimamoto, 2004). After the LR reaction, DH10B *E. coli* cells were transformed using electroporation (Thermo Scientific, Wilmington, DE, USA) and plated for selection of the pANDA35HK vector with newly added inserts. Whole cell PCR was used to distinguish successful transformation for each target using M13 forward and reverse primers and only the reverse primer from the target insert. Plasmid DNA was subsequently sent for sequencing validation (GENEWIZ, South Plainfield, NJ, USA).

Transformation of agrobacterium with pANDA35HK::hp-vATPAse-B and pANDA35HK::GFP

A single colony of Agrobacterium LBA4404 was used to inoculate 5mL of LB in a 15mL snap cap falcon tube with 15 μg/mL Rifampicin. The transformation of the LBA4404 strain was

adapted from a protocol developed by Andrew Bent (University of Wisconsin Madison). The strain was inoculated into 50mL of LB medium with 0.5-1.0mL of the saturated culture and grown to a mid-log of OD600 between 0.5 and 1.0. The cultures were then chilled on ice and the supernatant was discarded. A total of 0.1mL of the bacterial suspension was placed into 1.5mL micro-centrifuge tubes and 1 μg of plasmid DNA with the target of interest was added to each tube. The tubes were then flash-frozen in liquid nitrogen and thawed for five minutes at 37^{O}C before incubation for two hours on a shaker at 30 ^{O}C. The plasmid/agro mixture was spun for 5 minutes at 4,000 RPM and the supernatant was removed before suspension of the cells in 100 μL of LB. The transformed agro was then plated on selective LB plates for subsequent whole cell PCR as described above. Each positive colony was back-transformed into *E. coli* and plasmid was extracted for conformation sequencing.

Transformation of *A. thaliana* using a floral dip method

A. thaliana were grown to the flowering stage and transformed using a floral dip method (Narusaka et al., 2010). Plants maintained at previously described conditions were collected when flowers were first identified. The flowers were dipped into agrobacterium containing each specific target (*i.e.* GFP and vATPase-B). Plants were then placed in plastic trash bags within the growth chamber to maintain humidity. The bags were removed 24 hours later. Newly formed flower buds were inoculated later during a secondary inoculation phase with the same method. Seeds were collected for the whole plant and stored in a 4 ^{O}C walk in cooler. The transformed seeds were then planted as described above and leaf tissue was sampled for both genomic DNA isolation and RNA isolation for detection of genomic transformation and expression of the hairpin structure. Jonathan Oliver and Joshua Ames made continuous checks for each generation of *A. thaliana* until the third generation. Expression of the hairpin constructs was then measured

using quantitative real time PCR, primers targeting the GUS linker within the hairpin structure, and an internal reference CAC (*i.e.* clathrin adaptor complex) derived from previous expression data for the Brassica species *B. juncea* (Chandna et al., 2012). The CAC primer set had 1.956 efficiency and amplified 112bp fragment from the *A. thaliana* plant tissue. Upon further inspection, the primer set has a two base-pair change in the reverse primer when compared to the *A. thaliana* gene on NCBI, but the primers from the published research were retained because of the measured efficiency (Chandna et al., 2012). The third generation plants (T3) were further tested for both construct within each transgenic plant to determine successful transgenic events for the targets. The final plants used for experimentation were GFP (G2.6.2) and V-ATPase-B (V3.11.6).

Selection of homozygous third generation transgenic plants

Homozygosity for each transgenic event was selected to provide stable expression of the short hairpin RNA. Transgenic *A. thaliana* plants were selected through antibiotic resistance to hygromycin B and PCR amplification at both the genomic DNA level and transcriptomic RNA leve performed in-lab by Jonathan Oliver and Joshua Ames. Plants were germinated and screened for the antibiotic marker on ½ Murashige and Skoog media containing 50µg/ml Kanamycin. The plants that showed successful growth were grown to produce leaves and tested for construct presence within the plant genome through DNA isolation with the DNAeasy Plant Mini Kit (Qiagen, Germantown, MD, USA) and PCR (Promega, Madison, WI, USA) with insert specific primers for the GUS linker. Expression of the GUS linker was also confirmed through RNA isolation with the RNAeasy Plant Mini Kit (Qiagen, Germantown, MD, USA), Turbo DNAse (Thermo Scientific, Waltham, MA, USA), cDNA synthesis (Thermo Scientific, Waltham, MA, USA), and PCR (Promega, Madison, WI, USA) (Figure 4.6 and Table 4.2).

Identification of a stably expressed internal reference gene during insect development

Rounded counts generated from a *F. occidentalis de novo* transcriptome assembly (Appendix B) were used to identify a target gene that was stably expressed throughout all 24 samples. The matrix representing the rounded counts was normalized using regularized log transformation (rlog) within the DESeq2 R package. The rlog function used a Tikhonov/ridge regularization to transform the data to a log2 scale while minimizing the differences between samples (DESeq2 version 1.2.10 R Documentation). The normalization of the dataset was then used to identify the coefficient of variation (CV) for each contig across all samples (i.e. four biological replications, three stages, and two treatments). The CV was then used to range the contigs in order from lowest variation to highest variation (Zemp et al., 2014). Thirty-six potential targets were identified and five were chosen for QRT-PCR primer design and subsequent efficiency testing. The primers were then used for measurement of quantification cycle (Cq) variance across thrips development stage and virus treatment. Within the five tested, a primer set targeting the contig comp27200_c0_seq13 (*i.e* Ablim) displayed the lowest Cq range and lowest Cq standard deviation. The primer set for comp27200_c0_seq13 was then used as an internal reference for V-ATPase-B expression experiments with QRT-PCR.

Thrips feeding assay on transgenic *A. thaliana* during insect development

Green beans were brushed to synchronize thrips emergence from eggs and a 17-hour insect emergence period was allowed. The zero to 17-hour old L1s were placed on leaf tissue approximately 25 to 30 days after transplanting. Groups of three individual thrips were placed on each leaf. A total of five plants per treatment (i.e. non-transgenic wild type, G2.6.2, and V3.11.6)

were used for leaf collection with each treatment replicated three times for each sampling time-point. Time-points for destructive sampling ranged from one, two, four, six, and eight days after insects were placed on leaf tissue treatments within a 14ml falcon tube. Tubes with both insect and leaf were randomized completely and kept within an incubator (12h:12h light:dark, at 24 OC). Samples were destructively collected at each time point by placing individual thrips in micro-centrifuge tubes and documenting insect development stage before flash freezing with liquid nitrogen. Individual thrips were then used for RNA extraction and endogenous expression of V-ATPase-B was measured using Ablim as an internal reference with previously described methods (Schneweis et al., 2017).

Figures and Tables

Table 4.1 Primer sequences used for cloning and real-time quantative PCR.

Gene	Primer use	Sequence	Product length	Primer efficiency
GFP	Cloning	F:CACCGTGACCACCCTGACCTAC R:TTGATGCCGTTCTTCTGC	309 bp	NA
V-ATPase-B	Cloning	F:CACCGGACCTTTGGTGATTTTGGA R:AACACAGATTTGCCTGGGAC	504 bp	NA
Ablim	qPCR	F:GATAGAGAGGGAAGATTT R:TCATCAGATATTGGAACT	102 bp	2.0
V-ATPase-B	qPCR	F:CAGATTCCTATCCTTACTATGC R:TGTGAAGTTGTCGGTCTA	106 bp	1.98
GUS linker	qPCR	F:TATTACGGATGGTATGTC R: GTATTCGGTGATGATAATC	114 bp	1.88
M13	Sequencing	F(-20):GTAAAACGACGGCCAG R:CAGGAAACAGCTATGAC	NA	NA

Table 4.2 Pedigree of third generation transgenic *Arabidopsis thaliana* plants selected for the feeding assay.

Genotype	Generation	Line name	Hairpin	Line	Kan Growth	PCR	RT-PCR
Col-0	T0	G2	shpGFP	2	Positive	Positive	N/A
Col-1	T0	V3	shpV-ATPase-B	3	Positive	Positive	N/A
Col-2	T1	G2.6	shpGFP	2	Positive	Positive	Positive
Col-3	T1	V3.11	shpV-ATPase-B	3	Positive	Positive	Positive
Col-4	T2	G2.6.2	shpGFP	2	Positive	Positive	Positive
Col-5	T2	V3.11.6	shpV-ATPase-B	3	Positive	Positive	Positive

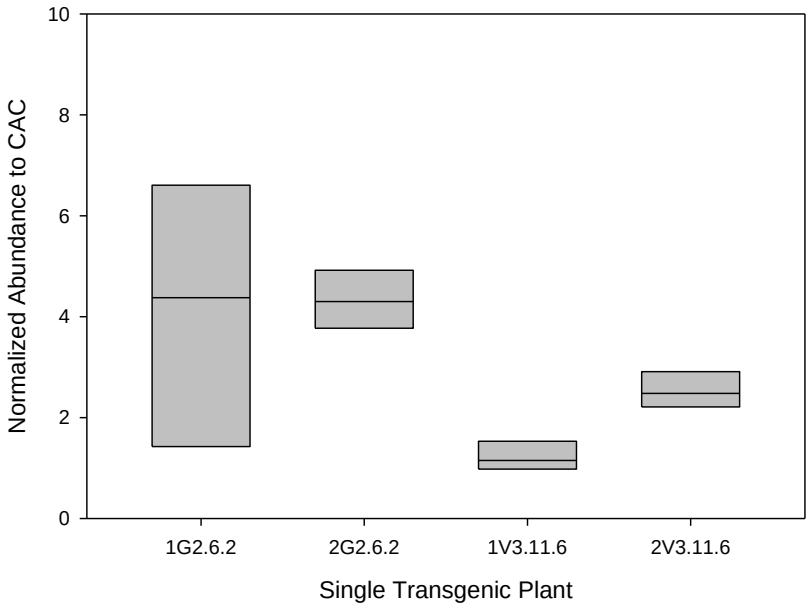

Figure 4.1 Expression of the shpRNA GUS linker in transgenic *A. thaliana* plant leaf tissue. Expression of the shpRNA GUS linker was measure in 5 to 8 different leaves spanning the whole plant. The abundance was normalized using the internal reference transcript target: clathrin adaptor complex (CAC). Two separate plants were sampled for each transgenic event (*i.e.* numbers 1 and 2). G2.6.2 and V3.11.6 represent the third generation of the shpGFP and shpV-ATPas-B line, respectively. SigmaPlot v.10.0 standard method was used to calculate the box boundaries (25^{th} and 75^{th} percentile) and the median represented as a solid line.

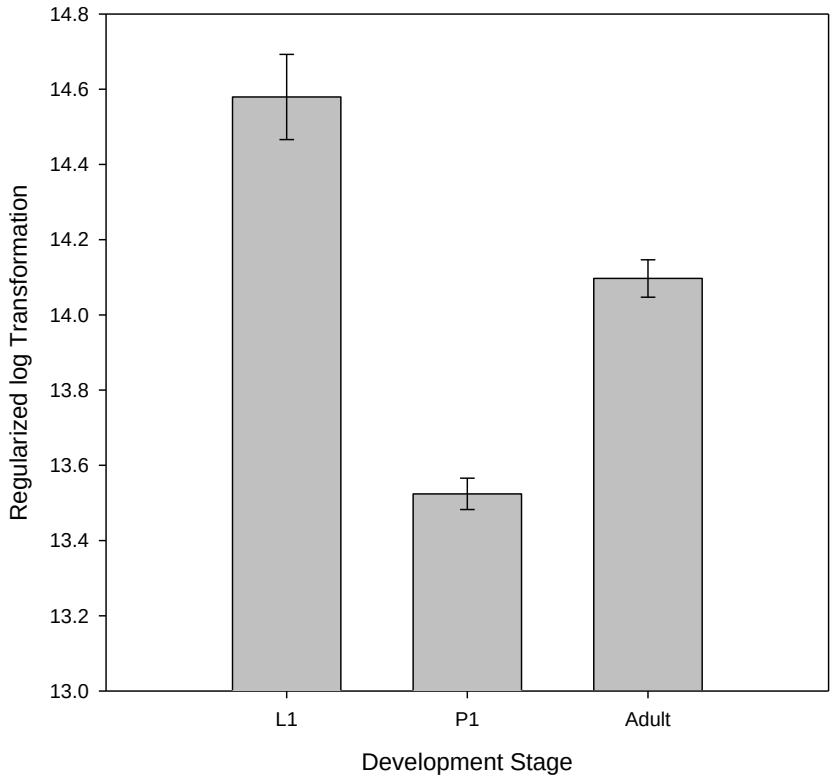

Figure 4.2 V-ATPase-B transcript expression in three development stages of *F. occidentalis*. Data was collected from Illumina HiSeq RNAseq analysis of western flower thrips global gene expression. L1 = the first instar larva 24-41 hours old; P1 = Pre-pupal stage; Adult = Adult stage 24 hours after eclosure. Counts were generated as described in Appendix A and they were transformed using a log2 scale (*i.e.* Regularized log Transformation). Four biological replicates were average with error bars representing the standard error of the mean.

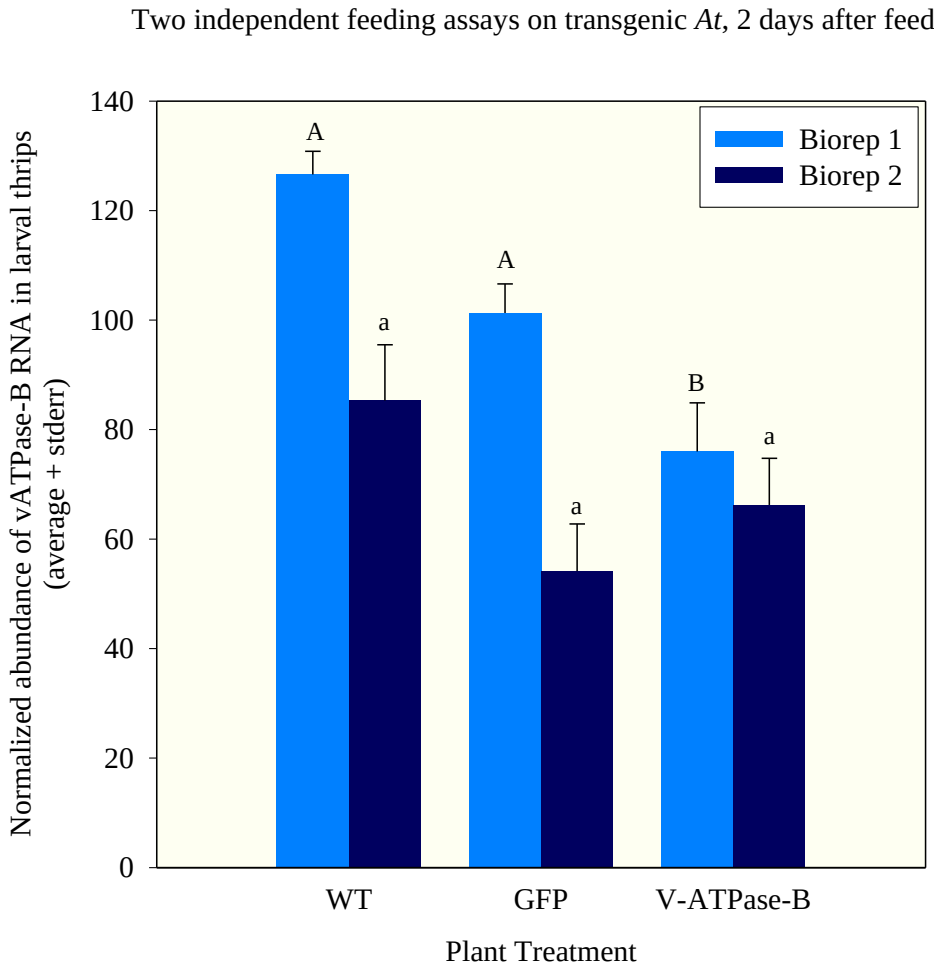

Figure 4.3 Biological Replicate 1: *Frankliniella occidentalis* V-ATPase-B expression at Day 2 of larval feeding on transgenic T2 plants expressing dsRNA hairpins.

Treatments included non-transgenic (W, wildtype), shpGFP-expressing (G), and shpV-ATPase-B-expressing (V) *Arabidopsis thaliana*. V-ATPase-B RNA was normalized to the thrips reference gene Actin Binding LIM Protein (Ablim). Each bar represents the mean of three experimental replicates + standard error. Bars headed with different letters indicate statistical differences between means (adjusted $P < 0.05$)

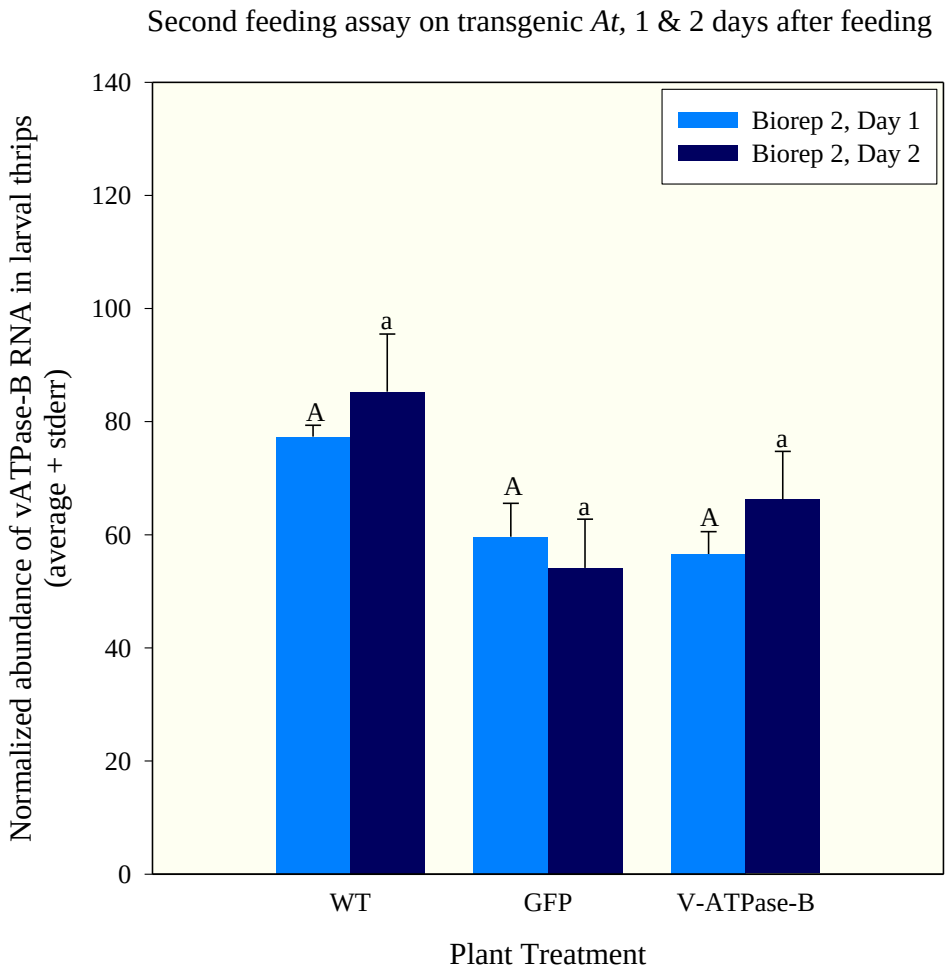

Figure 4.4 Biological Replicate 2: *Frankliniella occidentalis* V-ATPase-B expression at Day 1 and 2 of larval feeding on transgenic T2 plants expressing dsRNA hairpins. Treatments included non-transgenic (W, wildtype), shpGFP-expressing (G), and shpV-ATPase-B-expressing (V) *Arabidopsis thaliana*. V-ATPase-B RNA was normalized to the thrips reference gene Actin Binding LIM Protein (Ablim). Each bar represents the mean of three experimental replicates + standard error. Bars headed with different letters indicate statistical differences between means (adjusted $P < 0.05$)

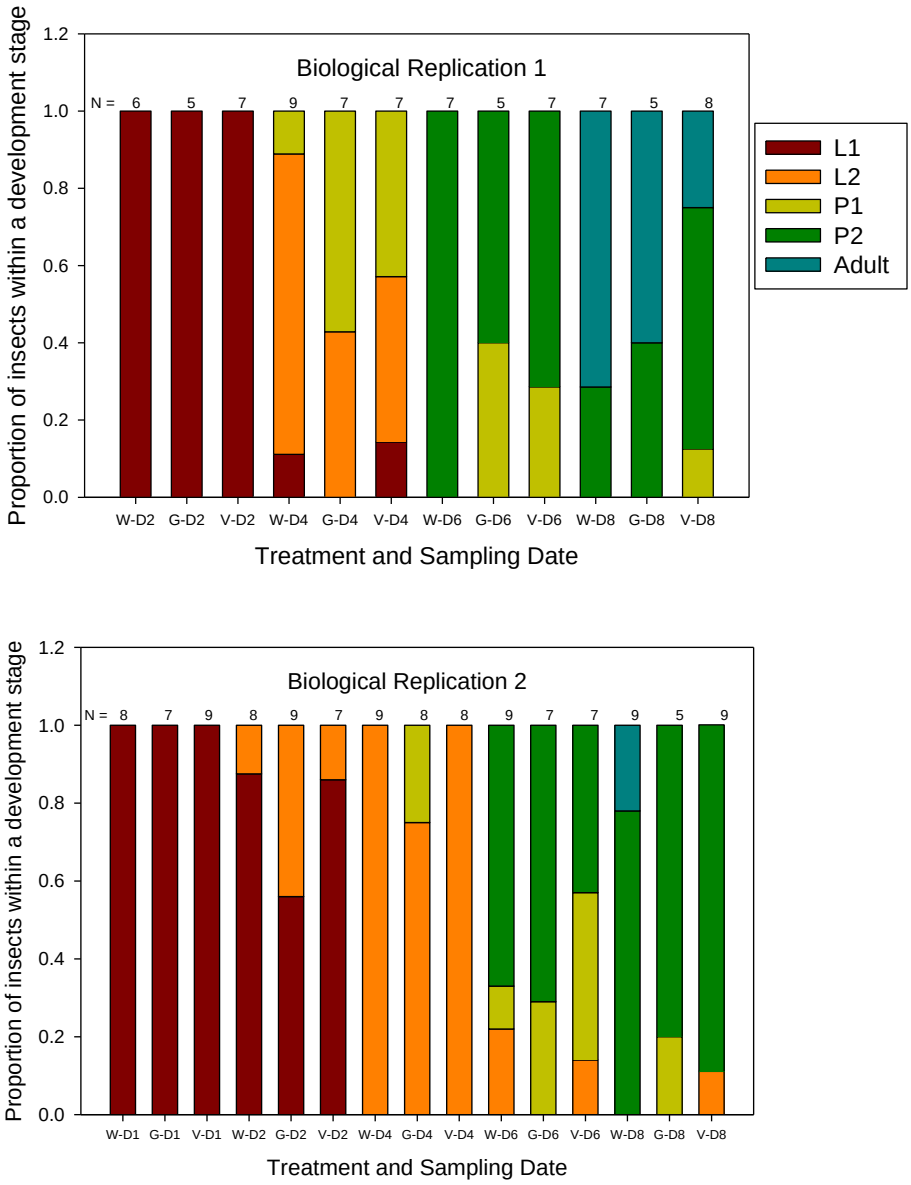

Figure 4.5 Composition of thrips developmental stages during feeding on T2 transgenics of Arabidopsis expressing short hairpin RNAs.

Treatments included non-transgenic (W, wildtype), shpGFP-expressing (G), and shpV-ATPase-B-expressing (V) *Arabidopsis thaliana*. The number of insects within a developmental stage were enumerated at each designated time point (D = day, number = day post exposure to the treatment) and expressed as the number of insects in one stage/total number of insects. The total number of insects represented in each bar is indicated in parenthesis ().

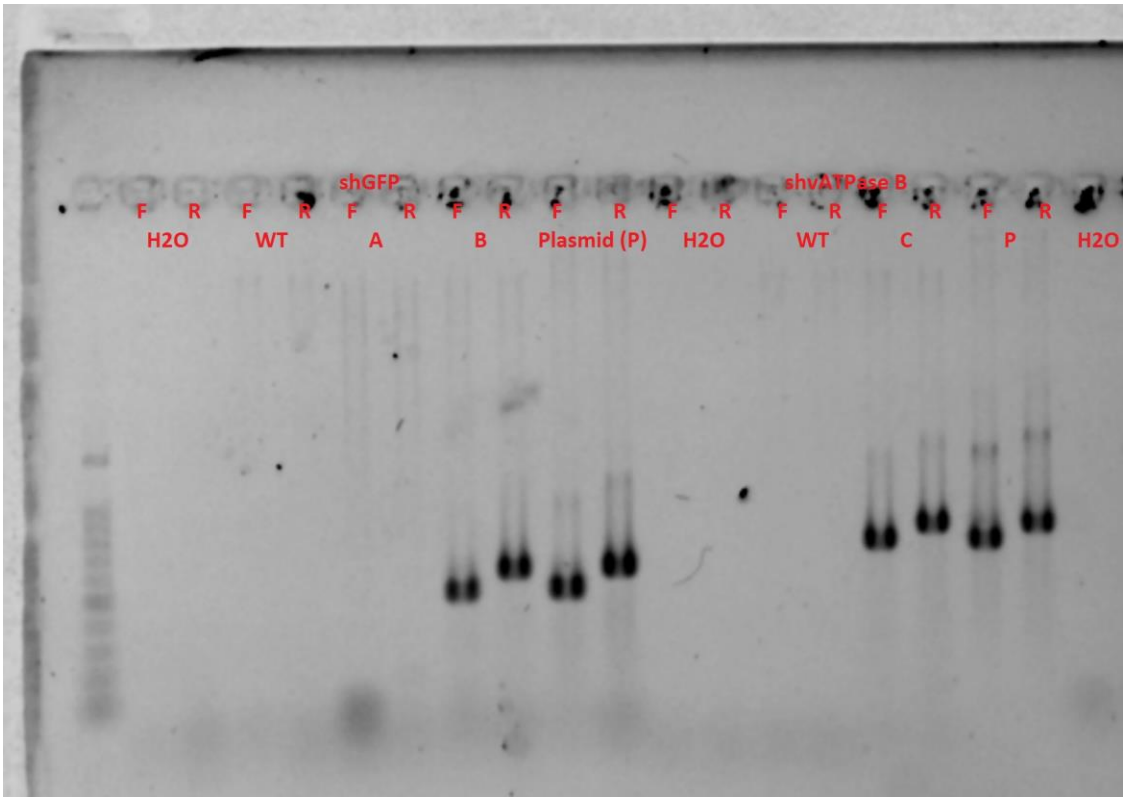

Figure 4.6 Plants representing the T1 generation display expression of the gene specific hairpin construct.

The uppermost labeling indicates the target for detection with short hairpin GFP (shGFP) and short hairpin V-ATPase-B (shvATPaseB). The letter at each well indicates the use of a forward target specific primer (F) and reverse GUS primer or reverse target specific primer (R) and reverse GUS primer. Identifiers below each forward (F) and reverse (R) describe the sample used for PCR from left to right: negative water control (H2O), wild-type (WT), plant A shGFP, plant B shGFP, shGFP plasmid positive control (Plasmid (P)), negative water control (H2O), wild-type (WT), plant C shvATPaseB, plant P shvATPaseB, negative water control (H2O).

Chapter 5 - Concluding Remarks

The research documented in this dissertation encompassed basic western flower thrips biology, mechanism study of the RNAi pathway in thrips, and the design of novel thrips pest control strategies. Through a transcriptomics approach, this work expands the basic knowledge underpinning the complex and dynamic relationship between thrips vectors and the plant viruses they transmit. It is now apparent that western flower thrips response to TSWV infection is development stage dependent in that each stage response uniquely and with different levels of expression. This new knowledge along with other reports of stage dependent infection sites (Montero-Astúa et al., 2016, Nagata et al., 1999) indicates that dismantling the virus-vector interaction should be leveraged differently depending on the targeted development stage. With new knowledge of responding transcripts, novel gene targets for virus-vector control can be built. Using whole body expression data as the groundwork for future studies, others can now explore tissue specific transcript expression responses in the midgut and salivary glands for further description of site-specific responses. Construction of this dataset also provides the resources needed for comparisons to other thrips species and their responses to orthtospoviruses.

Developing an understanding of direct interactions between *F. occidentalis* molecules and TSWV is challenging due to small insect size and variation of titer levels post acquisition. It appears that silencing Dicer-2 and Argonaut-2 had a deleterious effect on thrips irrespective of condition (+/- TSWV). Further investigation is needed to determine the cause of mortality. Preliminary support for a feedback between Dicer-2 and Argonaut-2 was also described when AGO2 acted to reduce Dicer-2 abundance. Biological replication is needed to further define this mechanism. Finally, abundance of TSWV was reduced when insects were challenged with AGO2 dsRNA. This is counter to what other systems describe (RNAi literature) and it needs to

be replicated. Low numbers of infected insects and overall low titers in dsRNA treated samples precluded drawing conclusions about the association between TSWV accumulation and RNAi gene expression. Higher numbers of injection to increase power will provide greater detail for future studies.

The first construction of dsRNA expressing transgenic plants expressing thrips-specific sequences was documented in this dissertation. Targeting of a transcript known to cause mortality in other insect systems (*i.e.* V-ATPase-B) provided the first glimpse into the up-coming challenges of thrips control using RNAi. Transgenic plants can be made to express thrips specific dsRNA at hight levels, but uptake during insect feeding needs to be further defined. An analysis of dsRNA direct uptake through oral-delivery is necessary for future development of plant-delivered RNAi-based strategies for controlling thrips. Using fluorescence, dsRNA could possibly be imaged during feeding to observe aquisition of the molecule into the gut lumen and then subsequent uptake into gut epithelial cells. Measurements of dsRNA quantity acquired will also help to describe amount ingested. Further fine scale analysis can also be completed using RNAseq to both quantify and sequence small RNAs derived from thrips feeding on dsRNA expressing plants.

References

Adkins, S., Choi, T., Israel, B., Bandla, M., Richmond, K., Schultz, K., Sherwood, J., German, T., 1996. Baculovirus expression and processing of tomato spotted wilt tospovirus glycoproteins. Phytopathology. 86, 849-855.

Albuquerque-Cunha, J.M., Gonzalez, M.S., Garcia, E.S., Mello, C.B., Azambuja, P., Almeida, J.C.A., de Souza, W., Nogueira, N.F.S., 2009. Cytochemical characterization of microvillar and perimicrovillar membranes in the posterior midgut epithelium of Rhodnius prolixus. Arthropod Struct.Dev. 38, 31-44.

Aliyari, R., Wu, Q., Li, H., Wang, X., Li, F., Green, L.D., Han, C.S., Li, W., Ding, S., 2008. Mechanism of Induction and Suppression of Antiviral Immunity Directed by Virus-Derived Small RNAs in Drosophila. Cell Host Microbe. 4, 387-397.

Anders, S., Huber, W., 2010. Differential expression analysis for sequence count data. Genome Biol. 11, R106.

Anders, S., Pyl, P.T., Huber, W., 2015. HTSeq-a Python framework to work with high-throughput sequencing data. Bioinformatics. 31, 166-169.

Attrill, H., Falls, K., Goodman, J.L., Millburn, G.H., Antonazzo, G., Rey, A.J., Marygold, S.J., FlyBase Consortium, 2016. FlyBase: establishing a Gene Group resource for Drosophila melanogaster. Nucleic Acids Res. 44, D786-D792.

Badillo-Vargas, I.E., Rotenberg, D., Schneweis, D.J., Hiromasa, Y., Tomich, J.M., Whitfield, A.E., 2012. Proteomic Analysis of Frankliniella occidentalis and Differentially Expressed Proteins in Response to Tomato Spotted Wilt Virus Infection. J.Virol. 86, 8793-8809.

Badillo-Vargas, I.E., Rotenberg, D., Schneweis, B.A., Whitfield, A.E., 2015. RNA interference tools for the western flower thrips, Frankliniella occidentalis. J.Insect Physiol. 76, 36-46.

Bandla, M., Campbell, L., Ullman, D., Sherwood, J., 1998. Interaction of tomato spotted wilt tospovirus (TSWV) glycoproteins with a thrips midgut protein, a potential cellular receptor for TSWV. Phytopathology. 88, 98-104.

Baum, J.A., Bogaert, T., Clinton, W., Heck, G.R., Feldmann, P., Ilagan, O., Johnson, S., Plaetinck, G., Munyikwa, T., Pleau, M., Vaughn, T., Roberts, J., 2007. Control of coleopteran insect pests through RNA interference. Nat.Biotechnol. 25, 1322-1326.

Beaty, B., Bishop, D., 1988. Bunyavirus-Vector Interactions. Virus Res. 10, 289-302.

Belliure, B., Janssen, A., Sabelis, M.W., 2008. Herbivore benefits from vectoring plant virus through reduction of period of vulnerability to predation. Oecologia. 156, 797-806.

Beresford, P., BasinskiGray, J., Chiu, J., Chadwick, J., Aston, W., 1997. Characterization of hemolytic and cytotoxic gallysins: A relationship with arylphorins. Dev.Comp.Immunol. 21, 253-266.

Bielza, P., 2008. Insecticide resistance management strategies against the western flower thrips, Frankliniella occidentalis. Pest Manag.Sci. 64, 1131-1138.

Black, L.L., Hobbs, H.A., Kammerlohr, D.S., 1996. Resistance of Capsicum chinense lines to tomato spotted wilt virus isolates from Louisiana, USA, and inheritance of resistance., 393-401.

Black, L., Hobbs, H., Gatti, J., 1991. Tomato Spotted Wilt Virus-Resistance in Capsicum-Chinense Pi 152225 and 159236. Plant Dis. 75, 863-863.

Black, L., Brakke, M., Vatter, A., 1963. Purification and Electron Microscopy of Tomato Spotted-Wilt Virus. Virology. 20, 120-&.

Boggiano, J.C., Vanderzalm, P.J., Fehon, R.G., 2011. Tao-1 Phosphorylates Hippo/MST Kinases to Regulate the Hippo-Salvador-Warts Tumor Suppressor Pathway. Dev.Cell. 21, 888-895.

Boiteux, L., Giordano, L., 1993. Genetic-Basis of Resistance Against 2 Tospovirus Species in Tomato (Lycopersicon-Esculentum). Euphytica. 71, 151-154.

Boiteux, L., Nagata, T., 1993. Susceptibility of Capsicum-Chinense Pi-159236 to Tomato Spotted Wilt Virus Isolates in Brazil. Plant Dis. 77, 210-210.

Boonham, N., Smith, P., Walsh, K., Tame, J., Morris, J., Spence, N., Bennison, J., Barker, I., 2002. The detection of Tomato spotted wilt virus (TSWV) in individual thrips using real time fluorescent RT-PCR (TaqMan). J.Virol.Methods. 101, 37-48.

Brackney, D.E., 2017. Implications of autophagy on arbovirus infection of mosquitoes. 22, 1-6.

Brault, V., Tanguy, S., Reinbold, C., Le Trionnaire, G., Arneodo, J., Jaubert-Possamai, S., Guernec, G., Tagu, D., 2010. Transcriptomic analysis of intestinal genes following acquisition of pea enation mosaic virus by the pea aphid Acyrthosiphon pisum. J.Gen.Virol. 91, 802-808.

Bridges, M., Jones, A., Bones, A., Hodgson, C., Cole, R., Bartlet, E., Wallsgrove, R., Karapapa, V., Watts, N., Rossiter, J., 2002. Spatial organization of the glucosinolate-myrosinase system in brassica specialist aphids is similar to that of the host plant. Proc.R.Soc.B-Biol.Sci. 269, 187-191.

Brittlebank, C.C., 1919. Tomato diseases. J. Agric. 17, 231-235.

Bucher, E., Sijen, T., de Haan, P., Goldbach, R., Prins, M., 2003. Negative-strand tospoviruses and tenuiviruses carry a gene for a suppressor of gene silencing at analogous genomic positions. J.Virol. 77, 1329-1336.

Burmester, T., 1999. Evolution and function of the insect hexamerins. Eur.J.Entomol. 96, 213-225.

Campbell, B., Dreyer, D., 1985. Host-Plant Resistance of Sorghum - Differential Hydrolysis of Sorghum Pectic Substances by Polysaccharases of Greenburg Biotypes (Schizaphis-Graminum, Homoptera, Aphididae). Arch.Insect Biochem.Physiol. 2, 203-215.

Campbell, C.L., Keene, K.M., Brackney, D.E., Olson, K.E., Blair, C.D., Wilusz, J., Foy, B.D., 2008. Aedes aegypti uses RNA interference in defense against Sindbis virus infection. BMC Microbiol. 8, 47.

Cantarel, B.L., Korf, I., Robb, S.M.C., Parra, G., Ross, E., Moore, B., Holt, C., Alvarado, A.S., Yandell, M., 2008. MAKER: An easy-to-use annotation pipeline designed for emerging model organism genomes. Genome Res. 18, 188-196.

Canton, J., Neculai, D., Grinstein, S., 2013. Scavenger receptors in homeostasis and immunity. Nat.Rev.Immunol. 13, 621-634.

Cassone, B.J., Michel, A.P., Stewart, L.R., Bansal, R., Mian, M.A.R., Redinbaugh, M.G., 2014a. Reduction in Fecundity and Shifts in Cellular Processes by a Native Virus on an Invasive Insect. Genome Biol.Evol. 6, 873-885.

Cassone, B.J., Wijeratne, S., Michel, A.P., Stewart, L.R., Chen, Y., Yan, P., Redinbaugh, M.G., 2014b. Virus-independent and common transcriptome responses of leafhopper vectors feeding on maize infected with semi-persistently and persistent propagatively transmitted viruses. BMC Genomics. 15, 133.

Chandna, R., Augustine, R., Bisht, N.C., 2012. Evaluation of Candidate Reference Genes for Gene Expression Normalization in Brassica juncea Using Real Time Quantitative RT-PCR. PLoS One. 7, e36918.

Chapman, R.F., 2013. The insects: structure and function., 5 ed. Cambridge University Press, Cambridge, UK.

Chen, D., Li, M., Wu, S., Lin, Y., Tsai, S., Lai, P., Lin, Y., Kuo, J., Meng, T., Chen, G., 2012a. The Bro1-domain-containing protein Myopic/HDPTP coordinates with Rab4 to regulate cell adhesion and migration. J.Cell.Sci. 125, 4841-4852.

Chen, Y., Cassone, B.J., Bai, X., Redinbaugh, M.G., Michel, A.P., 2012b. Transcriptome of the Plant Virus Vector Graminella nigrifrons, and the Molecular Interactions of Maize fine streak rhabdovirus Transmission. PLoS One. 7, e40613.

Cifuentes, D., Chynoweth, R., Guillen, J., De La Rua, P., Bielza, P., 2012. Novel Cytochrome P450 Genes, CYP6EB1 and CYP6EC1, Are Over-Expressed in Acrinathrin-Resistant Frankliniella occidentalis (Thysanoptera: Thripidae). J.Econ.Entomol. 105, 1006-1018.

Ciuffo, M., Finetti-Sialer, M., Gallitelli, D., Turina, M., 2005. First report in Italy of a resistance-breaking strain of Tomato spotted wilt virus infecting tomato cultivars carrying the Sw5 resistance gene. Plant Pathol. 54, 564-564.

Conesa, A., Gotz, S., Garcia-Gomez, J., Terol, J., Talon, M., Robles, M., 2005. Blast2GO: a universal tool for annotation, visualization and analysis in functional genomics research. Bioinformatics. 21, 3674-3676.

Cristofoletti, P., Ribeiro, A., Deraison, C., Rahbe, Y., Terra, W., 2003. Midgut adaptation and digestive enzyme distribution in a phloem feeding insect, the pea aphid Acyrthosiphon pisum. J.Insect Physiol. 49, 11-24.

Dawson, G., Griffiths, D., Pickett, J., Wadhams, L., Woodcock, C., 1987. Plant-Derived Synergists of Alarm Pheromone from Turnip Aphid, Lipaphis (Hyadaphis) Erysimi (Homoptera, Aphididae). J.Chem.Ecol. 13, 1663-1671.

DeHaan, P., Kormelink, R., Resende, R., Vanpoelwijk, F., Peters, D., Goldbach, R., 1991. Tomato Spotted Wilt Virus-L Rna Encodes a Putative Rna-Polymerase. J.Gen.Virol. 72, 2207-2216.

DeHann, P., Wagemakers, L., Peters, D., Goldbach, R., 1989. Molecular-Cloning and Terminal Sequence Determination of the S Rna and M Rna of Tomato Spotted Wilt Virus. J.Gen.Virol. 70, 3469-3473.

Dinkel, H., Van Roey, K., Michael, S., Kumar, M., Uyar, B., Altenberg, B., Milchevskaya, V., Schneider, M., Kuehn, H., Behrendt, A., Dahl, S.L., Damerell, V., Diebel, S., Kalman, S., Klein, S., Knudsen, A.C., Maeder, C., Merrill, S., Staudt, A., Thiel, V., Welti, L., Davey, N.E., Diella, F., Gibson, T.J., 2016. ELM 2016-data update and new functionality of the eukaryotic linear motif resource. Nucleic Acids Res. 44, D294-D300.

Dohner, K., Sodeik, B., 2005. The role of the cytoskeleton during viral infection. Curr.Top.Microbiol.Immunol. 285, 67-108.

Dreistadt, S.H., Phillips, P.A., O'Donnell, C.A., 2007. Thrips Integrated Pest Management for Home Gardeners and Landscape Professionals. Pest Notes University of California Agriculture and Natural Resources.

Duijsings, D., Kormelink, R., Goldbach, R., 2001. In vivo analysis of the TSWV cap-snatching mechanism: single base complementarity and primer length requirements. EMBO J. 20, 2545-2552.

Elliott, R.M., 1990. Molecular-Biology of the Bunyaviridae. J.Gen.Virol. 71, 501-522.

Enari, M., Sakahira, H., Yokoyama, H., Okawa, K., Iwamatsu, A., Nagata, S., 1998. A caspase-activated DNase that degrades DNA during apoptosis, and its inhibitor ICAD. Nature. 391, 43-50.

FELSENSTEIN, J., 1985. Confidence-Limits on Phylogenies - an Approach using the Bootstrap. Evolution. 39, 783-791.

Feng, Y., Krueger, E., Liu, S., Dorman, K., Bonning, B., Miller, A., 2017. Discovery of known and novel viral genomes in soybean aphid by deep sequencing. Phytobiomes. 1, 36-45.

Fletcher, S.J., Shrestha, A., Peters, J.R., Carroll, B.J., Srinivasan, R., Pappu, H.R., Mitter, N., 2016. The Tomato Spotted Wilt Virus Genome Is Processed Differentially in its Plant Host Arachis hypogaea and its Thrips Vector Frankliniella fusca. Front.Plant Sci. 7, 1349.

Francki, R.I.B., Fauquet, C., Knudson, D., Brown, F.:., 1991. Classification and nomenclature of viruses. Arch.Virol. 5.

Galiana-Arnoux, D., Dostert, C., Schneemann, A., Hoffmann, J.A., Imler, J., 2006. Essential function in vivo for Dicer-2 in host defense against RNA viruses in drosophila. Nat.Immunol. 7, 590-597.

Gammon, D.B., Mello, C.C., 2015. RNA interference-mediated antiviral defense in insects. Curr.Opin.Insect Sci. 8, 111-120.

Garcia, S., Billecocq, A., Crance, J., Prins, M., Garin, D., Bouloy, M., 2006. Viral suppressors of RNA interference impair RNA silencing induced by a Semliki Forest virus replicon in tick cells. J.Gen.Virol. 87, 1985-1989.

Gaum, W., Giliomee, J., Pringle, K., 1994. Life-History and Life-Tables of Western Flower Thrips, Frankliniella-Occidentalis (Thysanoptera, Thripidae), on English Cucumbers. Bull.Entomol.Res. 84, 219-224.

Gielen, J., DeHaan, P., Kool, A., Peters, D., Vangrinsven, M., Goldbach, R., 1991. Engineered Resistance to Tomato Spotted Wilt Virus, a Negative-Strand Rna Virus. Bio-Technology. 9, 1363-1367.

Gonzalez-Scarano, F., Nathanson, N., 1996. *Bunyaviridae*, in: Fields, B.N., Kinpe, D.M., Howley, P.M. (Eds.), . Lippincott-Raven, Philadelphia, pp. 1474-1504.

Grabherr, M.G., Haas, B.J., Yassour, M., Levin, J.Z., Thompson, D.A., Amit, I., Adiconis, X., Fan, L., Raychowdhury, R., Zeng, Q., Chen, Z., Mauceli, E., Hacohen, N., Gnirke, A., Rhind, N., di Palma, F., Birren, B.W., Nusbaum, C., Lindblad-Toh, K., Friedman, N., Regev, A., 2011. Full-length transcriptome assembly from RNA-Seq data without a reference genome. Nat.Biotechnol. 29, 644-U130.

Gutierrez-Cabrera, A.E., Alejandre-Aguilar, R., Hernandez-Martinez, S., Espinoza, B., 2014. Development and glycoprotein composition of the perimicrovillar membrane in Triatoma (Meccus) pallidipennis (Hemiptera: Reduviidae). Arthropod Struct.Dev. 43, 571-578.

Hannon, G., 2002. RNA interference. Nature. 418, 244-251.

Hansen, E., Funderburk, J., Reitz, S., Ramachandran, S., Eger, J., McAuslane, H., 2003. Within-plant distribution of Frankliniella species (Thysanoptera : Thripidae) and Orius insidiosus (Heteroptera : Anthocoridae) in field pepper. Environ.Entomol. 32, 1035-1044.

Harmel, N., Letocart, E., Cherqui, A., Giordanengo, P., Mazzucchelli, G., Guillonneau, F., De Pauw, E., Haubruge, E., Francis, F., 2008. Identification of aphid salivary proteins: a proteomic investigation of Myzus persicae. Insect Mol.Biol. 17, 165-174.

Heming, B., 1973. Metamorphosis of Pretarsus in Frankliniella-Fusca (Hinds) (Thripidae) and Haplothrips-Verbasci (Osborn) (Phlaeothripidae) (Thysanoptera). Can.J.Zool.-Rev.Can.Zool. 51, 1211-&.

Hoffmann, K., Qiu, W., Moyer, J., 2001. Overcoming host- and pathogen-mediated resistance in tomato and tobacco maps to the M RNA of Tomato spotted wilt virus. Mol.Plant-Microbe Interact. 14, 242-249.

Hopkins, R.J., van Dam, N.M., van Loon, J.J.A., 2009. Role of Glucosinolates in Insect-Plant Relationships and Multitrophic Interactions. Annu.Rev.Entomol. 54, 57-83.

Hover, S., King, B., Hall, B., Loundras, E., Taqi, H., Daly, J., Dallas, M., Peers, C., Schnettler, E., McKimmie, C., Kohl, A., Barr, J.N., Mankouri, J., 2016. Modulation of Potassium Channels Inhibits Bunyavirus Infection. J.Biol.Chem. 291, 3411-3422.

Hu, Y., Comjean, A., Roesel, C., Vinayagam, A., Flockhart, I., Zirin, J., Perkins, L., Perrimon, N., Mohr, S.E., 2017. FlyRNAi.org-the database of the Drosophila RNAi screening center and transgenic RNAi project: 2017 update. Nucleic Acids Res. 45, D672-D678.

Hunter, W., Ullman, D., 1992. Anatomy and Ultrastructure of the Piercing-Sucking Mouthparts and Paraglossal Sensilla of Frankliniella-Occidentalis (Pergande) (Thysanoptera, Thripidae). Int.J.Insect Morphol.Embryol. 21, 17-35.

Hunter, W., Ullman, D., 1989. Analysis of Mouthpart Movements during Feeding of Frankliniella-Occidentalis (Pergande) and Frankliniella-Schultzei Trybom (Thysanoptera, Thripidae). Int.J.Insect Morphol.Embryol. 18, 161-171.

Huvenne, H., Smagghe, G., 2010. Mechanisms of dsRNA uptake in insects and potential of RNAi for pest control: A review. J.Insect Physiol. 56, 227-235.

Inoue, T., Sakurai, T., Murai, T., Maeda, T., 2002. Accumulation and transmission of TSWV at larval and adult stages in six thrips species: distinct patterns between Frankliniella and Thrips, 59-65.

Jensen, S., 1998. Acetylcholinesterase activity associated with methiocarb resistance in a strain of western flower thrips, Frankliniella occidentalis (Pergande). Pestic.Biochem.Physiol. 61, 191-200.

Kanost, M.R., Jiang, H., 2015. Clip-domain serine proteases as immune factors in insect hemolymph. Curr.Opin.Insect Sci. 11, 47-55.

Kato, N., Mueller, C.R., Fuchs, J.F., McElroy, K., Wessely, V., Higgs, S., Christensen, B.M., 2008. Evaluation of the Function of a Type I Peritrophic Matrix as a Physical Barrier for Midgut Epithelium Invasion by Mosquito-Borne Pathogens in Aedes aegypti. Vector-Borne Zoonotic Dis. 8, 701-712.

Keene, K., Foy, B., Sanchez-Vargas, I., Beaty, B., Blair, C., Olson, K., 2004. RNA interference acts as a natural antiviral response to O'nyong-nyong virus (Alphavirus; Togaviridae) infection of Anopheles gambiae. Proc.Natl.Acad.Sci.U.S.A. 101, 17240-17245.

Kellmann, J., Liebisch, P., Schmitz, K., Piechulla, B., 2001. Visual representation by atomic force microscopy (AFM) of tomato spotted wilt virus ribonucleoproteins. Biol.Chem. 382, 1559-1562.

Kemp, C., Imler, J., 2009. Antiviral immunity in drosophila. Curr.Opin.Immunol. 21, 3-9.

Kikkert, M., Meurs, C., van de Wetering, F., Dorfmuller, S., Peters, D., Kormelink, R., Goldbach, R., 1998. Binding of tomato spotted wilt virus to a 94-kDa thrips protein. Phytopathology. 88, 63-69.

Kikkert, M., Van Lent, J., Storms, M., Bodegom, P., Kormelink, R., Goldbach, R., 1999. Tomato spotted wilt virus particle morphogenesis in plant cells. J.Virol. 73, 2288-2297.

Kikkert, M., Verschoor, A., Kormelink, R., Rottier, P., Goldbach, R., 2001. Tomato spotted wilt virus glycoproteins exhibit trafficking and localization signals that are functional in mammalian cells. J.Virol. 75, 1004-1012.

KISS, I., BENCZE, G., FODOR, A., SZABAD, J., FRISTROM, J., 1976. Prepupal Larval Mosaics in Drosophila-Melanogaster. Nature. 262, 136-138.

Kormelink, R., Storms, M., Vanlent, J., Peters, D., Goldbach, R., 1994. Expression and Subcellular Location of the Nsm Protein of Tomato Spotted Wilt Virus (Tswv), a Putative Viral Movement Protein. Virology. 200, 56-65.

Kumar, S., Stecher, G., Tamura, K., 2016. MEGA7: Molecular Evolutionary Genetics Analysis Version 7.0 for Bigger Datasets. Mol.Biol.Evol. 33, 1870-1874.

Lan, H., Chen, H., Liu, Y., Jiang, C., Mao, Q., Jia, D., Chen, Q., Wei, T., 2016. Small Interfering RNA Pathway Modulates Initial Viral Infection in Midgut Epithelium of Insect after Ingestion of Virus. J.Virol. 90, 917-929.

Law, M., Moyer, J., 1990. A Tomato Spotted Wilt-Like Virus with a Serologically Distinct N-Protein. J.Gen.Virol. 71, 933-938.

Le, S.Q., Gascuel, O., 2008. An improved general amino acid replacement matrix. Mol.Biol.Evol. 25, 1307-1320.

Levy, S.M., Falleiros, A.M.F., Moscardi, F., Gregorio, E.A., 2011. The role of peritrophic membrane in the resistance of Anticarsia gemmatalis larvae (Lepidoptera: Noctuidae) during the infection by its nucleopolyhedrovirus (AgMNPV). Arthropod Struct.Dev. 40, 429-434.

Lewandowski, D., Adkins, S., 2005. The tubule-forming NSm protein from Tomato spotted wilt virus complements cell-to-cell and long-distance movement of Tobacco mosaic virus hybrids. Virology. 342, 26-37.

Lewis, T., 1973. Thrips, their biology, ecology and economic importance. Academic Press Inc.

Li, J., Chen, Q., Lin, Y., Jiang, T., Wu, G., Hua, H., 2011. RNA interference in Nilaparvata lugens (Homoptera: Delphacidae) based on dsRNA ingestion. Pest Manag.Sci. 67, 852-859.

Li, W., Lewandowski, D.J., Hilf, M.E., Adkins, S., 2009. Identification of domains of the Tomato spotted wilt virus NSm protein involved in tubule formation, movement and symptomatology. Virology. 390, 110-121.

Linford, M.B., 1932. Transmission of the Pineapple yellow-spot virus by Thrips tabaci. Phytopathology. 22, 301-324.

Liu, W., Gray, S., Huo, Y., Li, L., Wei, T., Wang, X., 2015. Proteomic Analysis of Interaction between a Plant Virus and Its Vector Insect Reveals New Functions of Hemipteran Cuticular Protein. Mol.Cell.Proteomics. 14, 2229-2242.

Lopez-Soler, N., Cervera, A., Moores, G.D., Martinez-Pardo, R., Dolores Garcera, M., 2008. Esterase isoenzymes and insecticide resistance in Frankliniella occidentalis populations from the south-east region of Spain. Pest Manag.Sci. 64, 1258-1266.

Love, M., Anders, S., Huber, W., 2014a. Differential analysis of count data - the DESeq2 package. Vignette, 1.

Love, M., Huber, W., Anders, S., 2014b. Moderated estimation of fold change and dispersion for RNA-Seq data with DESeq2. bioRxiv, August 26, 2014.

Luan, J., Li, J., Varela, N., Wang, Y., Li, F., Bao, Y., Zhang, C., Liu, S., Wang, X., 2011. Global Analysis of the Transcriptional Response of Whitefly to Tomato Yellow Leaf Curl China Virus Reveals the Relationship of Coevolved Adaptations. J.Virol. 85, 3330-3340.

Maddrell, S.H.P., Gardiner, B.O.C., 1980. The permeability of the cuticular lining of the insect alimentary canal. J.Exp.Biol. 85, 227-237.

Manohar, D., Gullipalli, D., Dutta-Gupta, A., 2010. Ecdysteroid-mediated expression of hexamerin (arylphorin) in the rice moth, Corcyra cephalonica. J.Insect Physiol. 56, 1224-1231.

Margaria, P., Ciuffo, M., Turina, M., 2004. Resistance breaking strain of Tomato spotted wilt virus (Tospovirus; Bunyaviridae) on resistant pepper cultivars in Almeria, Spain. Plant Pathol. 53, 795-795.

Margaria, P., Miozzi, L., Rosa, C., Axtell, M.J., Pappu, H.R., Turina, M., 2015. Small RNA profiles of wild-type and silencing suppressor-deficient tomato spotted wilt virus infected Nicotiana benthamiana. Virus Res. 208, 30-38.

Maris, P., Joosten, N., Goldbach, R., Peters, D., 2004. Tomato spotted wilt virus infection improves host suitability for its vector Frankliniella occidentalis. Phytopathology. 94, 706-711.

Martinez, N.J., Gregory, R.I., 2013. Argonaute2 expression is post-transcriptionally coupled to microRNA abundance. RNA-Publ.RNA Soc. 19, 605-612.

McTaggart, S.J., Hannah, T., Bridgett, S., Garbutt, J.S., Kaur, G., Boots, M., 2015. Novel insights into the insect trancriptome response to a natural DNA virus. BMC Genomics. 16, 310.

Meister, G., Tuschl, T., 2004. Mechanisms of gene silencing by double-stranded RNA. Nature. 431, 343-349.

Miki, D., Shimamoto, K., 2004. Simple RNAi vectors for stable and transient suppression of gene function in rice. Plant Cell Physiol. 45, 490-495.

Milne, R., 1970. An Electron Microscope Study of Tomato Spotted Wilt Virus in Sections of Infected Cells and in Negative Stain Preparations. J.Gen.Virol. 6, 267-&.

Milne, R., Francki, R., 1984. Should Tomato Spotted Wilt Virus be Considered as a Possible Member of the Family Bunyaviridae. Intervirology. 22, 72-76.

Minakuchi, C., Tanaka, M., Miura, K., Tanaka, T., 2011. Developmental profile and hormonal regulation of the transcription factors broad and Kruppel homolog 1 in hemimetabolous thrips. Insect Biochem.Mol.Biol. 41, 125-134.

Misof, B., Liu, S., Meusemann, K., Peters, R.S., Donath, A., Mayer, C., Frandsen, P.B., Ware, J., Flouri, T., Beutel, R.G., Niehuis, O., Petersen, M., Izquierdo-Carrasco, F., Wappler, T., Rust, J., Aberer, A.J., Aspoeck, U., Aspoeck, H., Bartel, D., Blanke, A., Berger, S., Boehm, A., Buckley, T.R., Calcott, B., Chen, J., Friedrich, F., Fukui, M., Fujita, M., Greve, C., Grobe, P., Gu, S., Huang, Y., Jermiin, L.S., Kawahara, A.Y., Krogmann, L., Kubiak, M., Lanfear, R., Letsch, H., Li, Y., Li, Z., Li, J., Lu, H., Machida, R., Mashimo, Y., Kapli, P., McKenna, D.D., Meng, G., Nakagaki, Y., Luis Navarrete-Heredia, J., Ott, M., Ou, Y., Pass, G., Podsiadlowski, L., Pohl, H., von Reumont, B.M., Schuette, K., Sekiya, K., Shimizu, S., Slipinski, A., Stamatakis, A., Song, W., Su, X., Szucsich, N.U., Tan, M., Tan, X., Tang, M., Tang, J., Timelthaler, G., Tomizuka, S., Trautwein, M., Tong, X., Uchifune, T., Walzl, M.G., Wiegmann, B.M., Wilbrandt, J., Wipfler, B., Wong, T.K.F., Wu, Q., Wu, G., Xie, Y., Yang, S., Yang, Q., Yeates, D.K., Yoshizawa, K., Zhang, Q., Zhang, R., Zhang, W., Zhang, Y., Zhao, J., Zhou, C., Zhou, L., Ziesmann, T., Zou, S., Li, Y., Xu, X., Zhang, Y., Yang, H., Wang, J., Wang, J., Kjer, K.M., Zhou, X., 2014. Phylogenomics resolves the timing and pattern of insect evolution. Science. 346, 763-767.

Montero-Astua, M., Rotenberg, D., Leach-Kieffaber, A., Schneweis, B.A., Park, S., Park, J.K., German, T.L., Whitfield, A.E., 2014. Disruption of Vector Transmission by a Plant-Expressed Viral Glycoprotein. Mol.Plant-Microbe Interact. 27, 296-304.

Montero-Astúa, M., Ullman, D.E., Whitfield, A.E., 2016. Salivary gland morphology, tissue tropism and the progression of tospovirus infection in Frankliniella occidentalis. Virology. 493, 39-51.

Moritz, G., 1997. Structure, growth and development, in: Lewis, T. (Ed.), Thrips as Crop Pests. CAB International, New York, pp. 15-63.

Moritz, G., 1995. Morphogenetic development of some species of the Order Thysanoptera (Insecta). Plenum Publishing Co. Ltd, London, USA.

Moritz, G., Kumm, S., Mound, L., 2004. Tospovirus transmission depends on thrips ontogeny. Virus Res. 100, 143-149.

Moritz, G., 1989. The ontogenesis of Thysanoptera (Insecta) with special reference to the Panchaetothripine *Hercinothrips femoralis* (OM Reuter 1891) (Thysanoptera, Thripidae, Panchaetothripinae) - III. Prepupa and Pupa. Zoologische Jahrbücher, Abteilung für Anatomie und Ontogenie der Tiere. 118, 15.

Morse, J., Hoddle, M., 2006. Invasion biology of thrips. Annu.Rev.Entomol. 51, 67-89.

Muller, K., 1926. Beiträge zur Biologie, Anatomie, Histologie und inner metamorphose de Thripslarven. Zeitschrif für wissenschaftliche Zoologie. 130, 252.

Nagata, T., Inoue-Nagata, A., Smid, H., Goldbach, R., Peters, D., 1999. Tissue tropism related to vector competence of Frankliniella occidentalis for tomato spotted wilt tospovirus. J.Gen.Virol. 80, 507-515.

Nagata, T., Inoue-Nagata, A., van Lent, J., Goldbach, R., Peters, D., 2002. Factors determining vector competence and specificity for transmission of Tomato spotted wilt virus. J.Gen.Virol. 83, 663-671.

Narusaka, M., Shiraishi, T., Iwabuchi, M., Narusaka, Y., 2010. The floral inoculating protocol: a simplified Arabidopsis thaliana transformation method modified from floral dipping. Plant Biotechnol. 27, 349-351.

Navas, V., Funderburk, J., Olson, S., Beshear, R., 1991. Damage to Tomato Fruit by the Western Flower Thrips (Thysanoptera, Thripidae). J.Entomol.Sci. 26, 436-442.

Nunes, F.M.F., Aleixo, A.C., Barchuk, A.R., Bomtorin, A.D., Grozinger, C.M., Simoes, Z.L.P., 2013. Non-Target Effects of Green Fluorescent Protein (GFP)-Derived Double-Stranded RNA (dsRNA-GFP) Used in Honey Bee RNA Interference (RNAi) Assays. 4, 90-103.

Oliveira, V.C., Bartasson, L., Batista de Castro, M.E., Correa, J.R., Ribeiro, B.M., Resende, R.O., 2011. A silencing suppressor protein (NSs) of a tospovirus enhances baculovirus replication in permissive and semipermissive insect cell lines. Virus Res. 155, 259-267.

Oliver, J.E., Whitfield, A.E., 2016. The genus *Tospovirus*: Emerging bunyaviruses that threaten food security. Annu.Rev.Virol. 3, in press.

Pappu, H.R., Jones, R.A.C., Jain, R.K., 2009. Global status of tospovirus epidemics in diverse cropping systems: Successes achieved and challenges ahead. Virus Res. 141, 219-236.

Persley, D., Thomas, J., Sharman, M., 2006. Tospoviruses - an Australian perspective. Australas.Plant Pathol. 35, 161-180.

Pfaffl, M., 2001. A new mathematical model for relative quantification in real-time RT-PCR. Nucleic Acids Res. 29, e45.

Phipps, D., Chadwick, J., Aston, W., 1994. Gallysin-1, an Antibacterial Protein Isolated from Hemolymph of Galleria-Mellonella. Dev.Comp.Immunol. 18, 13-23.

Pittman, H.A., 1927. Spotted wilt of Tomatoes. 1, 74-77.

Poernbacher, I., Baumgartner, R., Marada, S.K., Edwards, K., Stocker, H., 2012. Drosophila Pez Acts in Hippo Signaling to Restrict Intestinal Stem Cell Proliferation. Curr.Biol. 22, 389-396.

Prins, M., Kikkert, M., Ismayadi, C., deGraauw, W., deHaan, P., Goldbach, R., 1997. Characterization of RNA-mediated resistance to tomato spotted wilt virus in transgenic tobacco plants expressing NSM gene sequences. Plant Mol.Biol. 33, 235-243.

Qiu, W., Geske, S., Hickey, C., Moyer, J., 1998. Tomato spotted wilt Tospovirus genome reassortment and genome segment-specific adaptation. Virology. 244, 186-194.

Qiu, W., Moyer, J., 1999. Tomato spotted wilt tospovirus adapts to the TSWV N gene-derived resistance by genome reassortment. Phytopathology. 89, 575-582.

Ramanathan, H.N., Jonsson, C.B., 2008. New and Old World hantaviruses differentially utilize host cytoskeletal components during their life cycles. Virology. 374, 138-150.

Reitz, S.R., 2009. Biology and Ecology of the Western Flower Thrips (Thysanoptera: Thripidae): the Making of a Pest. Fla.Entomol. 92, 7-13.

Reitz, S.R., 2008. Comparative bionomics of Frankliniella occidentalis and Frankliniella tritici. Fla.Entomol. 91, 474-476.

Rensende, R., DeHaan, P., Deavila, A., Kitajima, E., Kormelink, R., Goldbach, R., Peters, D., 1991. Generation of Envelope and Defective Interfering Rna Mutants of Tomato Spotted Wilt Virus by Mechanical Passage. J.Gen.Virol. 72, 2375-2383.

Richmond, K., Chenault, K., Sherwood, J., German, T., 1998. Characterization of the nucleic acid binding properties of tomato spotted wilt virus nucleocapsid protein. Virology. 248, 6-11.

Richter, C., Oktaba, K., Steinmann, J., Mueller, J., Knoblich, J.A., 2011. The tumour suppressor L(3)mbt inhibits neuroepithelial proliferation and acts on insulator elements. Nat.Cell Biol. 13, 1029-U46.

Riddiford, L., 1994. Cellular and Molecular Actions of Juvenile-Hormone .1. General-Considerations and Premetamorphic Actions. Adv.Insect Physiol. 24, 213-274.

Riddiford, L., Hiruma, K., Zhou, X., Nelson, C., 2003. Insights into the molecular basis of the hormonal control of molting and metamorphosis from Manduca sexta and Drosophila melanogaster. Insect Biochem.Mol.Biol. 33, 1327-1338.

Riley, D.G., Joseph, S.V., Srinivasan, R., Diffie, S., 2011. Thrips vectors of Tospoviruses. 2, 1-10.

Robles, J.A., Qureshi, S.E., Stephen, S.J., Wilson, S.R., Burden, C.J., Taylor, J.M., 2012. Efficient experimental design and analysis strategies for the detection of differential expression using RNA-Sequencing. BMC Genomics. 13, 484.

Rodriguez-Andres, J., Rani, S., Varjak, M., Chase-Topping, M.E., Beck, M.H., Ferguson, M.C., Schnettler, E., Fragkoudis, R., Barry, G., Merits, A., Fazakerley, J.K., Strand, M.R., Kohl, A., 2012. Phenoloxidase Activity Acts as a Mosquito Innate Immune Response against Infection with Semliki Forest Virus. PLoS Pathog. 8, e1002977.

Rosello, S., Diez, M., Nuez, F., 1996. Viral diseases causing the greatest economic losses to the tomato crop .1. The Tomato spotted wilt virus - A review. Sci.Hortic. 67, 117-150.

Rotenberg, D., Whitfield, A.E., 2010. Analysis of expressed sequence tags for Frankliniella occidentalis, the western flower thrips. Insect Mol.Biol. 19, 537-551.

Rotenberg, D., Jacobson, A.L., Schneweis, D.J., Whitfield, A.E., 2015. Thrips transmission of tospoviruses. Curr.Opin.Virol. 15, 80-89.

Rotenberg, D., Krishna Kumar, N.K., Ullman, D.E., Montero-Astua, M., Willis, D.K., German, T.L., Whitfield, A.E., 2009a. Variation in Tomato spotted wilt virus Titer in Frankliniella occidentalis and Its Association with Frequency of Transmission. Phytopathology. 99, 404-410.

Rotenberg, D., Krishna Kumar, N.K., Ullman, D.E., Montero-Astua, M., Willis, D.K., German, T.L., Whitfield, A.E., 2009b. Variation in Tomato spotted wilt virus Titer in Frankliniella occidentalis and Its Association with Frequency of Transmission. Phytopathology. 99, 404-410.

Sabin, L.R., Zheng, Q., Thekkat, P., Yang, J., Hannon, G.J., Gregory, B.D., Tudor, M., Cherry, S., 2013. Dicer-2 Processes Diverse Viral RNA Species. PLoS One. 8, e55458.

SAITOU, N., NEI, M., 1987. The Neighbor-Joining Method - a New Method for Reconstructing Phylogenetic Trees. Mol.Biol.Evol. 4, 406-425.

Samuel, G., Bald, J.G., Pittman, H.A., 1930. Investigations on "spotted wilt" of tomatoes in Australia. Commonw. Counc. Sci. Ind. Res. Bull. 44, 8-9 11.

Sanchez-Vargas, I., Scott, J.C., Poole-Smith, B.K., Franz, A.W.E., Barbosa-Solomieu, V., Wilusz, J., Olson, K.E., Blair, C.D., 2009. Dengue Virus Type 2 Infections of Aedes aegypti Are Modulated by the Mosquito's RNA Interference Pathway. PLoS Pathog. 5, e1000299.

Saucedo, L.J., Edgar, B.A., 2007. Filling out the Hippo pathway. Nat.Rev.Mol.Cell Biol. 8, 613-621.

Schmieder, R., Edwards, R., 2011a. Quality control and preprocessing of metagenomic datasets. Bioinformatics. 27, 863-864.

Schmieder, R., Edwards, R., 2011b. Quality control and preprocessing of metagenomic datasets. Bioinformatics. 27, 863-864.

Schnettler, E., Hemmes, H., Huismann, R., Goldbach, R., Prins, M., Kormelink, R., 2010a. Diverging Affinity of Tospovirus RNA Silencing Suppressor Proteins, NSs, for Various RNA Duplex Molecules. J.Virol. 84, 11542-11554.

Schnettler, E., Hemmes, H., Huismann, R., Goldbach, R., Prins, M., Kormelink, R., 2010b. Diverging Affinity of Tospovirus RNA Silencing Suppressor Proteins, NSs, for Various RNA Duplex Molecules. J.Virol. 84, 11542-11554.

Schneweis, D.J., Whitfield, A.E., Rotenberg, D., 2017. Thrips developmental stage-specific transcriptome response to tomato spotted wilt virus during the virus infection cycle in Frankliniella occidentalis, the primary vector. Virology. 500, 226-237.

Shelly, S., Lukinova, N., Bambina, S., Berman, A., Cherry, S., 2009. Autophagy Is an Essential Component of Drosophila Immunity against Vesicular Stomatitis Virus. Immunity. 30, 588-598.

Silva, C., Ribeiro, A., Gulbenkian, S., Terra, W., 1995. Organization, Origin and Function of the Outer Microvillar (Perimicrovillar) Membranes of Dysdercus-Peruvianus (Hemiptera) Midgut Cells. J.Insect Physiol. 41, 1093-1103.

Silva, C., Silva, J., Vasconcelos, F., Petretski, M., DaMatta, R., Ribeiro, A., Terra, W., 2004. Occurrence of midgut perimicrovillar membranes in paraneopteran insect orders with comments on their function and evolutionary significance. Arthropod Struct.Dev. 33, 139-148.

Simon, M., Johansson, C., Lundkvist, A., Mirazimi, A., 2009. Microtubule-dependent and microtubule-independent steps in Crimean-Congo hemorrhagic fever virus replication cycle. Virology. 385, 313-322.

Spassova, M., Prins, T., Folkertsma, R., Klein-Lankhorst, R., Hille, J., Goldbach, R., Prins, M., 2001. The tomato gene Sw5 is a member of the coiled coil, nucleotide binding, leucine-rich repeat class of plant resistance genes and confers resistance to TSWV in tobacco. Mol.Breed. 7, 151-161.

Stafford, C.A., Walker, G.P., Ullman, D.E., 2011. Infection with a plant virus modifies vector feeding behavior. Proc.Natl.Acad.Sci.U.S.A. 108, 9350-9355.

Stafford-Banks, C.A., Rotenberg, D., Johnson, B.R., Whitfield, A.E., Ullman, D.E., 2014. Analysis of the Salivary Gland Transcriptome of Frankliniella occidentalis. PLoS One. 9, e94447.

Stevens, M., Scott, S., Gergerich, R., 1991. Inheritance of a Gene for Resistance to Tomato Spotted Wilt Virus (Tswv) from Lycopersicon-Peruvianum Mill. Euphytica. 59, 9-17.

Stobbs, L., Broadbent, A., Allen, W., Stirling, A., 1992. Transmission of Tomato Spotted Wilt Virus by the Western Flower Thrips to Weeds and Native Plants found in Southern Ontario. Plant Dis. 76, 23-29.

Storms, M., Kormelink, R., Peters, D., vanLent, J., Goldbach, R., 1995. The nonstructural NSm protein of tomato spotted wilt virus induces tubular structures in plant and insect cells. Virology. 214, 485-493.

Storms, M., van der Schoot, C., Prins, M., Kormelink, R., van Lent, J., Goldbach, R., 1998. A comparison of two methods of microinjection for assessing altered plasmodesmal gating in tissues expressing viral movement proteins. Plant J. 13, 131-140.

Takahashi, R., 1921. Metamorphosis of Thysanoptera. Zool. Mag. 35, 85.

Takeda, A., Sugiyama, K., Nagano, H., Mori, M., Kaido, M., Mise, K., Tsuda, S., Okuno, T., 2002a. Identification of a novel RNA silencing suppressor, NSs protein of Tomato spotted wilt virus. FEBS Lett. 532, 75-79.

Takeda, A., Sugiyama, K., Nagano, H., Mori, M., Kaido, M., Mise, K., Tsuda, S., Okuno, T., 2002b. Identification of a novel RNA silencing suppressor, NSs protein of Tomato spotted wilt virus. FEBS Lett. 532, 75-79.

Tang, T., Li, X., Yang, X., Yu, X., Wang, J., Liu, F., Huang, D., 2014. Transcriptional Response of Musca domestica Larvae to Bacterial Infection. PLoS One. 9, e104867.

Tao, W., Zhang, S., Turenchalk, G., Stewart, R., St John, M., Chen, W., Xu, T., 1999. Human homologue of the Drosophila melanogaster lats tumour suppressor modulates CDC2 activity. Nat.Genet. 21, 177-181.

Telfer, W., Kunkel, J., 1991. The Function and Evolution of Insect Storage Hexamers. Annu.Rev.Entomol. 36, 205-228.

Tentchev, D., Verdin, E., Marchal, C., Jacquet, M., Aguilar, J.M., Moury, B., 2011. Evolution and structure of Tomato spotted wilt virus populations: evidence of extensive reassortment and insights into emergence processes. J.Gen.Virol. 92, 961-973.

Thaler, J., Stout, M., Karban, R., Duffey, S., 2001. Jasmonate-mediated induced plant resistance affects a community of herbivores. Ecol.Entomol. 26, 312-324.

Trapnell, C., Roberts, A., Goff, L., Pertea, G., Kim, D., Kelley, D.R., Pimentel, H., Salzberg, S.L., Rinn, J.L., Pachter, L., 2012. Differential gene and transcript expression analysis of RNA-seq experiments with TopHat and Cufflinks. Nat.Protoc. 7, 562-578.

Tsuda, S., Fujisawa, I., Ohnishi, J., Hosokawa, D., Tomaru, K., 1996. Localization of tomato spotted wilt tospovirus in larvae and pupae of the insect vector Thrips setosus. Phytopathology. 86, 1199-1203.

Ullman, D.E., Cho, J.J., Mau, R.F.L., Hunter, W.B., Westcot, D.M., Custer, D.M., 1992a. Thrips-tomato spotted wilt virus interactions: morphological, behavioral and cellular components influencing thrips transmission, in: Cho, J.J., Custer, D.M. (Eds.), Advances in Disease Vector Research. Springer-Verlag New York, Inc., Heidelberg, NY, pp. 195.

Ullman, D., Cho, J., Mau, R., Westcot, D., Custer, D., 1992b. A Midgut Barrier to Tomato Spotted Wilt Virus Acquisition by Adult Western Flower Thrips. Phytopathology. 82, 1333-1342.

Ullman, D., Cho, J., Mau, R., Westcot, D., Custer, D., 1992c. A Midgut Barrier to Tomato Spotted Wilt Virus Acquisition by Adult Western Flower Thrips. Phytopathology. 82, 1333-1342.

Ullman, D., German, T., Sherwood, J., Westcot, D., Cantone, F., 1993. Tospovirus Replication in Insect Vector Cells - Immunocytochemical Evidence that the Nonstructural Protein Encoded by the S-Rna of Tomato Spotted Wilt Tospovirus is Present in Thrips Vector Cells. Phytopathology. 83, 456-463.

Ullman, D., Westcot, D., Chenault, K., Sherwood, J., German, T., Bandla, M., Cantone, F., Duer, H., 1995. Compartmentalization, Intracellular-Transport, and Autophagy of Tomato Spotted Wilt Tospovirus Proteins in Infected Thrips Cells. Phytopathology. 85, 644-654.

van de Wetering, F., Goldbach, R., Peters, D., 1996. Tomato spotted wilt tospovirus ingestion by first instar larvae of Frankliniella occidentalis is a prerequisite for transmission. Phytopathology. 86, 900-905.

van de Wetering, F., Hulshof, J., Posthuma, K., Harrewijn, P., Goldbach, R., Peters, D., 1998. Distinct feeding behavior between sexes of Frankliniella occidentalis results in higher scar production and lower tospovirus transmission by females. Entomol.Exp.Appl. 88, 9-15.

van Rij, R.P., Saleh, M., Berry, B., Foo, C., Houk, A., Antoniewski, C., Andino, R., 2006. The RNA silencing endonuclease Argonaute 2 mediates specific antiviral immunity in Drosophila melanogaster. Genes Dev. 20, 2985-2995.

Vankamme, A., Henstra, S., Ie, T., 1966. Morphology of Tomato Spotted Wilt Virus. Virology. 30, 574-&.

vanPoelwijk, F., Boye, K., Oosterling, R., Peters, D., Goldbach, R., 1993. Detection of the L-Protein of Tomato Spotted Wilt Virus. Virology. 197, 468-470.

Vogel, C., Marcotte, E.M., 2012. Insights into the regulation of protein abundance from proteomic and transcriptomic analyses. Nat.Rev.Genet. 13, 227-232.

Wang, L., Wang, X., Wei, X., Huang, H., Wu, J., Chen, X., Liu, S., Wang, X., 2016a. The autophagy pathway participates in resistance to tomato yellow leaf curl virus infection in whiteflies. Autophagy. 12, 1560-1574.

Wang, Z., Gong, Y., Jin, G., Li, B., Chen, J., Kang, Z., Zhu, L., Gao, Y., Reitz, S., Wei, S., 2016b. Field-evolved resistance to insecticides in the invasive western flower thrips Frankliniella occidentalis (Pergande) (Thysanoptera: Thripidae) in China. Pest Manag.Sci. 72, 1440-1444.

Wang, Z., Wilhelmsson, C., Hyrsl, P., Loof, T.G., Dobes, P., Klupp, M., Loseva, O., Moergelin, M., Ikle, J., Cripps, R.M., Herwald, H., Theopold, U., 2010. Pathogen Entrapment by Transglutaminase-A Conserved Early Innate Immune Mechanism. PLoS Pathog. 6, e1000763.

Watanabe, H., Tokuda, G., 2010. Cellulolytic Systems in Insects. Annu.Rev.Entomol. 55, 609-632.

Waterhouse, R.M., Kriventseva, E.V., Meister, S., Xi, Z., Alvarez, K.S., Bartholomay, L.C., Barillas-Mury, C., Bian, G., Blandin, S., Christensen, B.M., Dong, Y., Jiang, H., Kanost, M.R., Koutsos, A.C., Levashina, E.A., Li, J., Ligoxygakis, P., MacCallum, R.M., Mayhew, G.F., Mendes, A., Michel, K., Osta, M.A., Paskewitz, S., Shin, S.W., Vlachou, D., Wang, L., Wei, W., Zheng, L., Zou, Z., Severson, D.W., Raikhel, A.S., Kafatos, F.C., Dimopoulos, G., Zdobnov, E.M., Christophides, G.K., 2007. Evolutionary dynamics of immune-related genes and pathways in disease-vector mosquitoes. Science. 316, 1738-1743.

Whitfield, A., Ullman, D., German, T., 2005a. Tomato spotted wilt virus glycoprotein G(C) is cleaved at acidic pH. Virus Res. 110, 183-186.

Whitfield, A., Ullman, D., German, T., 2005b. Tospovirus-thrips interactions. Annu.Rev.Phytopathol. 43, 459-489.

Whitfield, A., Ullman, D., German, T., 2004. Expression and characterization of a soluble form of Tomato spotted wilt virus glycoprotein G(N). J.Virol. 78, 13197-13206.

Whyard, S., Singh, A.D., Wong, S., 2009. Ingested double-stranded RNAs can act as species-specific insecticides. Insect Biochem.Mol.Biol. 39, 824-832.

Wieczorek, H., Beyenbach, K.W., Huss, M., Vitavska, O., 2009. Vacuolar-type proton pumps in insect epithelia. J.Exp.Biol. 212, 1611-1619.

Wijkamp, I., Almarza, N., Goldbach, R., Peters, D., 1995. Distinct Levels of Specificity in Thrips Transmission of Tospoviruses. Phytopathology. 85, 1069-1074.

Wijkamp, I., Goldbach, R., Peters, D., 1996a. Propagation of tomato spotted wilt virus in Frankliniella occidentalis does neither result in pathological effects nor in transovarial passage of the virus. Entomol.Exp.Appl. 81, 285-292.

Wijkamp, I., Peters, D., 1993. Determination of the Median Latent Period of 2 Tospoviruses in Frankliniella-Occidentalis, using a Novel Leaf Disk Assay. Phytopathology. 83, 986-991.

Wijkamp, I., VandeWetering, F., Goldbach, R., Peters, D., 1996b. Transmission of tomato spotted wilt virus by Frankliniella occidentalis; Median acquisition and inoculation access period. Ann.Appl.Biol. 129, 303-313.

Wijkamp, I., Vanlent, J., Kormelink, R., Goldbach, R., Peters, D., 1993. Multiplication of Tomato Spotted Wilt Virus in its Insect Vector, Frankliniella-Occidentalis. J.Gen.Virol. 74, 341-349.

Willis, J.H., 2010. Structural cuticular proteins from arthropods: Annotation, nomenclature, and sequence characteristics in the genomics era. Insect Biochem.Mol.Biol. 40, 189-204.

Xu, Y., Zhou, W., Zhou, Y., Wu, J., Zhou, X., 2012. Transcriptome and Comparative Gene Expression Analysis of Sogatella furcifera (Horvath) in Response to Southern Rice Black-Streaked Dwarf Virus. PLoS One. 7, e36238.

Yao, J., Rotenberg, D., Afsharifar, A., Barandoc-Alviar, K., Whitfield, A.E., 2013. Development of RNAi Methods for Peregrinus maidis, the Corn Planthopper. PLoS One. 8, e70243.

Yu, J., Zheng, Y., Dong, J., Klusza, S., Deng, W., Pan, D., 2010. Kibra Functions as a Tumor Suppressor Protein that Regulates Hippo Signaling in Conjunction with Merlin and Expanded. Dev.Cell. 18, 288-299.

Zemp, N., Minder, A., Widmer, A., 2014. Identification of Internal Reference Genes for Gene Expression Normalization between the Two Sexes in Dioecious White Campion. PLoS One. 9, e92893.

Zhang, F., Guo, H., Zheng, H., Zhou, T., Zhou, Y., Wang, S., Fang, R., Qian, W., Chen, X., 2010. Massively parallel pyrosequencing-based transcriptome analyses of small brown planthopper (Laodelphax striatellus), a vector insect transmitting rice stripe virus (RSV). BMC Genomics. 11, 303.

Zhang, Z., Zhang, P., Li, W., Zhang, J., Huang, F., Yang, J., Bei, Y., Lu, Y., 2013. De novo transcriptome sequencing in Frankliniella occidentalis to identify genes involved in plant virus transmission and insecticide resistance. Genomics. 101, 296-305.

Zhou, X., Tarver, M.R., Bennett, G.W., Oi, F.M., Scharf, M.E., 2006. Two hexamerin genes from the termite Reticulitermes flavipes: Sequence, expression, and proposed functions in caste regulation. Gene. 376, 47-58.

Zhou, X., Riddiford, L., 2002. Broad specifies pupal development and mediates the 'status quo' action of juvenile hormone on the pupal-adult transformation in Drosophila and Manduca. Development. 129, 2259-2269.

Zhu, F., Xu, J., Palli, R., Ferguson, J., Palli, S.R., 2011. Ingested RNA interference for managing the populations of the Colorado potato beetle, Leptinotarsa decemlineata. Pest Manag.Sci. 67, 175-182.

Zhu, K.Y., Merzendorfer, H., Zhang, W., Zhang, J., Muthukrishnan, S., 2016. Biosynthesis, Turnover, and Functions of Chitin in Insects. Annu.Rev.Entomol. 61, 177-196.

Zuckerkandl, J., Pauling, L., 1965. Evolutionary divergence and convergence in proteins, in: Bryson, V., Vogal, H.J. (Eds.), Evolving Genes and Proteins. Academic Press, New York, pp. 97-166.

Appendix A - Developmentally-regulated whole-body expression profiles in *Frankliniella occidentalis*

Abstract

The insect order Thysanoptera is comprised exclusively of thrips, and *Frankliniella occidentalis* is one of the most well-characterized thrips species with regards to ecology, pest biology, and tospovirus-vector interactions. Thrips metamorphosis is intermediate between holo- and hemi-metabolism, and is often referred to as re-metabolism due to the dissolution and reconstruction of several imaginifugal structures during pupation. Thrips develop through a first (L1) and second (L2) instar larval stage to a pre-pupal (P1) and pupal (P2) stage, eclosing as winged males and females. A description of transcriptome dynamics during development provides definition of the molecular expression patterns during thrips metamorphosis. Using the i5k *F. occidentalis* genome as a reference, single-end reads generated from four biological replicates of Illumina RNA-Seq libraries of healthy pools of L1 (L), P1 (P), and adult (A) thrips were mapped (Bowtie2 and Tophat2) to produce one assembled transcriptome per developmental stage, and reads were enumerated for differential expression (DE) analyses (HTSeq). The number of DE transcripts ranged from 7,221 to 8,551 across the three stages, and transcript annotations included key proteins involved in insect molting, metamorphosis, and organ development with the pre-pupa indicated as the most unique expresser within each category.

Introduction

Frankliniella occidentalis (Pergrande), commonly known as the Western flower thrips, is a unique organism that develops through a lifecycle consisting of two actively feeding larval

stages (L1 and L2), a quiescent pre-pupal (P1) and pupal (P2) stage and an adult stage. Western flower thrips are a member of the insect order Thysanoptera (family Thripidae). They are herbivorous, polyphagous insect pests that feed on a broad range of plant species causing crop losses worldwide (Reitz, 2009). Thrips develop quickly from egg to adult within 14 days under standard conditions (23 ^{O}C at 16h:8h light:day) (Moritz et al., 2004), and development of thrips is intermediate between hemi- and holo-metabolism (Lewis, 1973) with the larval stages resembling a smaller version of the adult (hemi-), and the pupa developing through dissolution (holo-) of imaginifugal structures and reformation of internal anatomical structures (e.g. reproductive organs, sensory organs, and digestive tract) (Moritz, 1995). During the late L2 stage, the insect drops from the plant to the soil, does not eat, and develops through the pupal stages.

The continuous growth and development spanning each larval stage is a quick process in which cell proliferation must continually occur until the insect prepares to molt. The successful dissolution of organ structures and reformation also demands a controlled cell cycling pattern for successful molting. One pathway explored in other insects, Hippo, acts to restrain cell proliferation while also promote apoptosis in differentiating epithelial cells. It is comprised of growth-inhibitory proteins and one growth-promoting factor (Saucedo and Edgar, 2007). A total of fifteen genes have been identified in the Hippo/Warts tumor suppressor pathway for Drosophila providing a resource for detection of similar genes in other insects enabling studies of cell regulation. The expression levels of genes within this pathway have never been explored in Western flower thrips.

Insect molting is controlled by ecdysteroids and juvenile hormone (JH). JH is expressed during the larval insect stage to enable growth of the larva and development through the larval

stages and disable the act of molting. Prothoracicotropic hormone (PTTH) then initiates the timing of the molt to pupa and its release is controlled by both insect size and environmental factors (*e.g.* day length). Prior to molting in *Manduca sexta*, mRNAs for ecdysone receptor and transcription factor increase to higher levels to trigger the insect molt (Riddiford et al., 2003). Another gene, *broad*, also directs pupal development and is necessary for the induction of pupa-specific genes (Minakuchi et al., 2011, Zhou and Riddiford, 2002). The *broad* gene has been measured at the expression level in *F. occidentalis* during development through molting stages, and it was shown to increase at the larva-prepupa transition and decrease in the pupal stage (Minakuchi et al., 2011). Global identification of molting transcripts within thrips and detection of expression has not been accomplished, and description of these molecular expression patterns could depict development tactics for this unique insect order.

Exploration of global gene expression during *F. occidentalis* development is now possible with the development of the i5K genome. The draft genome was sequenced, assembled and computationally annotated by the Baylor College of Medicine, Human Genome Sequencing Center (BCM-HGSC, Houston, TX, USA), and the advent of this genome resource now provides the opportunity to explore gene expression changes occurring during each development stage of *F. occidentalis*. Experimental design from a previous experiment has provided a dataset comprised of a four biological replicate sampling of three thrips development stages (i.e. L1 (L), P1 (P), and Adult (A)) (Schneweis et al., 2017). This three stage development set provides the structure for exploring both the Hippo and molting pathway.

Results

Detection of transcript expression variation among three insect stages

Transcript expression dynamics were different across the first instar larva (L), the pre-pupa (P), and adult (A) development stages. All three stages, including four biological replicates for each stage sample, were separated by two principle components with the adult stage determined as most different along principle component one (PC1) when compare to the other two stages (*i.e.* L and P). Principle component two portrayed the difference between the L and P stage as ranging from -30 to 30 units (60 total units), but it was not as different as the adult stage with a total of 80+ units of distance between it and the other two stages (Figure A.1).

Differential transcript expression between stages

Pairwise comparisons were made between each of the three development stages using contrasts. A significant number of transcripts were differentially expressed (DE) with an adjusted p-value of less than 0.01. The largest number of DE transcripts was measured between the P and A (P-A) stage (8,551 padj < 0.01) with the L vs. P (L-P) (7,612 padj < 0.01) and the L vs. A (L-A) (7,221 padj < 0.01) following. When adding an additional restriction to the dataset (padj < 0.01 and log2Fold > 4), the P-A comparison retained the highest number of differences with a switch occurring where the L-A has a higher number of differences than the L-P (Table A.1). A log2Fold change greater than four is equal to a greater than two fold change. The reduction in number of DE transcripts observed with this restriction is indicative of the high number of small fold changes between stages. It also further supports observations in the PCA (Figure A.1).

The L-P fold changes range from -8.11 to 9.54 (Figure A.2) with a total of 392 transcripts up (76%) and 121 down (24%) in the larva when compared to pre-pupa (Figure A.3). With 76% of DE transcripts up regulated in the L stage, it appears that transcripts with larger than two fold-

change DE are down regulated in the P stage (Figure A.4). The P-A contrast had the highest fold changes and largest number of DE transcripts with a range from -11.24 to 9.96 (Figure A.2). The number of up and down transcripts was almost equal with 534 up and 529 down for pre-pupa compared to adult (Figure A.3). Similarly with the L-P comparison, larva had a greater number of up regulated transcripts (470, 62%) and less down regulated (281, 37%) (Figure A.3) when compared to the adult. The up expressed transcripts between both L-P and L-A (Figure A.4) indicate a potential grouping of genes important for early development and lifestyle.

The top DE transcripts between stages play roles in metabolism. Metabolic shifts between each stage appeared to be an important factor for description of differences. The top ten DE transcripts during the L-P comparison consisted of GO terms for transport, metabolic process, proteolysis, methylation, and peptidase activity (Table A.2). All of the top ten transcripts were up expressed in the larva stage indicating the presence of reduction in metabolism and transport during the non-feeding pre-pupa stage. More non-annotated (NA) transcripts were present when comparing the top ten for the P-A comparison along with a mix in up and down expressing transcripts (Table A.2). Finally the L-A comparison displayed transcripts as top changers for GO terms involved in the membrane, all of which were up regulated in the larva stage (Table A.2).

Transcripts involved in regulating organ size are dynamic between stages

The Hippo signaling pathway is a regulatory pathway for organ size. Thrips sequences were identified using *Drosophila* protein sequences as a search tool for similarity. The top hit for eleven genes active in the Hippo pathway were identified and expression data indicated variation spanning the different life stages (Table A.3). The pre-pupa stage is an important stage for the

remetabolie phase of insect development in which tissue differentiation, re-organization, and dissolution of some larval structures occurs (Muller, 1926) including gut epithelium (Moritz, 1989, Muller, 1926). Statistically significant expression level variation was detected within the pre-pupa stage across eight of the eleven (72%) transcripts involved in the hippo pathway (Table A.3). Transcripts similar to mop, Tao, wts, Zyx, l3mbt, sd, kibra, hpo, ed & fred, yki, and Pez were all up regulated in the pre-pupa stage when compared to the larva stage. This is indicative of a major stage specific dynamic shift during the pre-pupa stage, a stage when organ structures are changing and wings are developing. The Tao and l3mbt similar transcripts (i.e. tumor suppressor genes) are down regulated when compared to the adult stage with the rest of the significant changers up regulated in pre-pupa when compared to adult (Table A.3).

Expression of molting genes unique in pre-pupa

Thrips transcripts identified as similar to know molting regulating gens were identified in as top hits when compared to Drosophila. These genes showed large fold changes spanning different development stages with the pre-pupa being the most unique in expression (Table A.4). Out of 24 identified molting transcripts, the pre-pupa stage was significantly the highest expresser for 15 transcripts (63%). A total of six transcripts identified as similar to ecdysone receptors and ecdysone induce proteins were up regulated in the pre-pupa stage when compared to other stages with a 5.2 log2FoldChange up regulation of ecdysis triggering hormone (ETH) within pre-pupa between P-A (Table A.4). ETH was also highly expressed in larva when compared to adult (5.2 log2FoldChange).

Discussion

The main aim of this study was to detect, document, and measure transcriptomic shifts that arise from transitions between three key development time-points in the insect *F. occidentalis* growth. Very little is known about re-metabolism in Thysanoptera at the molecular level, and the importance of describing this intermediate between holo- and hemi-metabolism is necessary for understanding the insect order. We selected three insect development stages that encompass key changes in thrips morphology (Moritz, 1989, Muller, 1926). The first instar larva stage (L) is a motile insect stage that is continuously feeding in preparation for the pre-pupa stage (P). The transition into the pupa stage induces dissolution and reconstruction of imaginifugal structures (Moritz, 1995, Takahashi, 1921). The adult insect ecloses from the pupa (P2) stage and proceeds to expend energy on feeding and reproduction. The three development-stage time-points selected for this study produced contrasting whole transcriptome expression profiles. At the whole transcriptome level, adult insect transcriptomes were very different from the larva and pupa transcriptomes (Figure A.1). The adult stage had the largest gene expression variance when compared to the other two stages (i.e. larva and pupa).

Each stage was used as a baseline for measuring statistically different transcript expression in pairwise comparisons. Differences in transcript abundance were apparent with thousands of transcripts differentially expressed (Table A.1). Interestingly the pre-pupa stage had the highest number of DE transcripts when compared to the other two stages (padj <0.01). This continued to hold true when a fold change restriction was also placed on the dataset with the greatest number of DE transcripts in the pupa versus adult comparison (1,063) and an equally split number of up and down regulated transcripts. The significant fold changes of transcript expression within the pre-pupa stage appear to be descriptive of the remetabolie insect phase.

The re-metabolism insect phase operates in some similarity with the holo-metabolism with regards to a non-motile insect phase in which tissue re-organization occurs. The Hippo signaling pathway is indicative of organ development and it operates to control cell number through regulating proliferation and apoptosis in differentiating epithelial cells (Saucedo and Edgar, 2007). Using *Drosophila* as a translated protein gene model, top hits to multiple Hippo sequences were extracted from the *F. occidentalis* transcriptome dataset. Within the Hippo transcript subset, the pre-pupa stage was the most unique in expression variance. Mop, which plays a role in cell adhesion (Chen et al., 2012a), was up regulated when compared to the other two stages. The support of cell adhesion and up-regulation of Tao, restriction of cell proliferation in insect epithelial (Boggiano et al., 2011), and up-regulation of wts, a negative regulator of cellular cycle (Tao et al., 1999), is indicative of reduction in organ development. Pez was also up-regulated and functions through action as a negative upstream regulator of Yorkie and it was shown to restrict growth of the adult midgut epithelium (Poernbacher et al., 2012). Up-regulation of l(3)mbt, when compared to larva, is also descriptive of cell proliferation reduction. L3mbt, a tumor suppressor, will produce brain tumors from overproliferation of neuroepithelial cells when mutated (Richter et al., 2011). Kibra was also up-regulated and it is a tumor suppressor protein and is essential in the Hippo pathway (Table A.3). Loss of Kibra produces imaginal disc overgrowth and defective Hippo signaling (Yu et al., 2010). Likely a progenitor to tissue reconstruction, the large number of cell proliferation reducers up-regulated provides a whole body insect description of tissue size retention and reduction of growth. Reduction of cell proliferation, during the pre-pupa stage, when compared to the larva and adult stage is a molting step that could provide energy retention and conservation before the instigation of programed cell death for reconstruction in the pupa stage (P2).

Insect molting and metamorphosis is controlled through induction and reduction of both a molting hormone (ecdysone) and juvenile hormone (JH). The production of JH declines at the larval stage and ecdysone promotes molting in a cyclical fashion from larva to pupa and again pupa to adult (Riddiford, 1994). The broad gene is necessary for production of pupa-specific genes and it acts to promote metamorphosis from the larval stage to the pupa stage (KISS et al., 1976, Zhou and Riddiford, 2002). In a previous study, the broad transcript was expressed high at the lara-prepupa transition in *F. occidentalis* (Minakuchi et al., 2011). The broad transcript identified in this present study was 2.76 log2Fold higher in pre-pupa than in larva and 3.74 log2Fold higher in pupa than in adult. High expression of the broad gene and induced expression of ecdysone receptors/proteins during pre-pupa is an evident measurement of the molting process. Thrips display similar patterns to *Manduca sexta* of increased expression of ecdysone receptors prior to the pupation phase(Riddiford et al., 2003). In general the transcripts identified within the molting pathway were up-regulated in the pupa stage, and they were also uniquely expressed when compared to the other stages.

This study is the first to explore global transcriptome abundances spanning three different development stages of an insect in the order Thysanoptera. Dynamic shifts in both the molting signaling pathway and the Hippo signaling pathway describe a unique molecular process for development from larva to pupa to adult. The exploration of development within thrips has furthered the description of expression changes important for insect stage transitions. *F. occidentalis* is a major crop pest that cause plant damage and it also vectors plant viruses. This knew database of knowledge could help to develop new strategies for insect control by providing genetic targets for knock-down/out to inhibit insect growth and subsequently reduce insect spread.

Materials and Methods

F. occidentalis colony maintenance

Franklinella occidentalis (Pergande) originally obtained from Kamilo Iki Valley, Oahu, Hawaii, was maintained on green bean pods (*Phaseolus vulgaris*) in 16-oz clear plastic deli cups with lids adapted for air transfer using thrips-proof mesh. The colony was maintained at room temperature and as described previously (Ullman et al., 1992c).

Biological samples for detection of transcriptome changes between insect development stages

Four biological replications of an insect development time-course experiment were completed to determine gene expression in developing thrips. Thrips were allowed to emerge from green bean pods for 17 hours, they were collected, and then placed on healthy *Emilia sonchifolia* for three hours as a control for a previous study (Schneweis et al., 2017). Groups of thrips were sampled during the L1 stage (42 h after emergence from green beans), the P1 stage (approximately 90% were identified at this stage with the use of a stereoscope), and the adult stage comprised of females and males (24 h after eclosion). One cohort of 75-100 insects was collected from each development stage into a 1.7 ml microfuge tube using a fine paintbrush, then immediately flash-frozen in liquid nitrogen and stored at -80 ^{O}C. Total RNA was extracted from each sample using TRIzol reagent (Invitrogen, Carlsbad, CA) using methods previously described (Badillo-Vargas et al., 2012). RNA yields were determined using the Nanodrop spectrophotometer (Agilent, Inc, Santa Clara, CA, USA), and aliquots of each sample were stored at -80 ^{O}C for RNA sequencing.

RNA sequencing

Three developmental stage-time samples across four biological replicates (*i.e* 12 RNA samples total) were selected for sequencing based on key stages for thrips developmental biology. The L1 stage is an early first instar larva, prior to pupation, that feeds on plant tissue and is known to be an important stage for acquisition and subsequent infection of/by *Tomato spotted wilt virus* (Schneweis et al., 2017). The pre-pupa stage (P1) was chosen because it is a starting stage for the remetabolie phase of insect development in which tissue differentiation, re-organization, and dissolution of some larval structures occurs (Muller, 1926) including gut epithelium (Moritz, 1989, Muller, 1926). The adult stage occurs after eclosure from the P2 stage providing expression analysis post pupation when insect reproduction is occurring.

The twelve RNA samples were treated with a DNAse treatment, quantified, and checked for quality as previously described (Schneweis et al., 2017). Multiplex single-end sequencing of indexed RNA-Seq libraries using Illumina Hi-Seq 2000 was completed for the three insect stages from a previous sequencing event and the control samples were used for present stage comparisons (Schneweis et al., 2017).

Read-alignment and differential expression analysis

The i5K Frankliniella occidentalis genome was used as a reference for alignments of stage specific RNA-Seq reads (Schneweis et al., 2017). The HTseq pipeline (Anders et al., 2015) provided as a resource at the iPlant Collaborative Discovery Environment (currently CYVERSE, http://www.cyverse.org) was used to generate raw counts for reads aligned back to the reference genome. Gene models predicted by MAKER (Cantarel et al., 2008) provided the gene structures for count collection with the HTseq pipeline. The MAKER predictions were used across all

insect stage data to generate reads which allowed for the creation of a count matrix with rows representing the gene models and columns representing the counts from four biological replicates of three stage specific RNA-Seq datasets (*i.e.* a total of twelve).

The count matrix was imported into R Studio (v0.98.945) for differential expression analysis using DESeq2 (v1.4.5) (Love et al., 2014b). Pairwise comparisons between each of the three stages was completed with the youngest stage as the comparative factor level as follows: (Larva vs. Pre-pupa), (Pre-pupa vs. Adult), and (Larva vs. Adult). Default parameters were used for detection of differential expression as described in the DESeq2 vignette (Love et al., 2014a). Size factors were estimated using the median ratio method (Anders and Huber, 2010) and dispersions were estimated using the pipeline established within the DESeq2 package (Love et al., 2014a). A negative binomial GLM was fitted to the dataset and Wald test p-values were calculated for each comparison. Significant fold changes were selected (adjusted p-value = 0.01) and the MAKER model identifiers were collected for selection of gene sequence and annotations from an assembled transcriptome generated previously (Schneweis et al., 2017). Each stage transcriptome was used independently for a local blastX (v2.2.28) using a non-redundant database maintained on the Beocat computer cluster at Kansas State University. Each of the final datasets were restricted by transcript size ranging from 500bp to 7999bp length.

Identifying gene ontologies (GO) terms for differentially-expressed transcripts

Gene ontologies were mapped (E < 10-3) to differentially expressed transcript sequences using Blast2GO basic (https://www.blast2go.com) (Conesa et al., 2005). The software was run locally with Mac OS on the stage specific datasets ranging from 6,479 to 7,646 transcripts.

Identification of pathway transcripts for pathway expression analysis

Pathways were selected using the interactive fly database as a method for generating insect development databases (http://www.sdbonline.org/sites/fly/aimain/5zygotic.htm). Genes were identified from the pathway lists through links to FlyBase (Attrill et al., 2016) and translated protein sequences were selected for building sequence databases for tblastn sequence searches within DE databases created from differential expression analysis of thrips sequence data. The top *F. occidentalis* MAKER model hit was selected as a representative of the pathway gene, and expression data was pulled for the identified model. This regularized log (RLD) transformed data was collected for mapping transformed counts. The fold change expression data was then used for creating analysis of pathway expression between stage comparisons and identifying statistical significance.

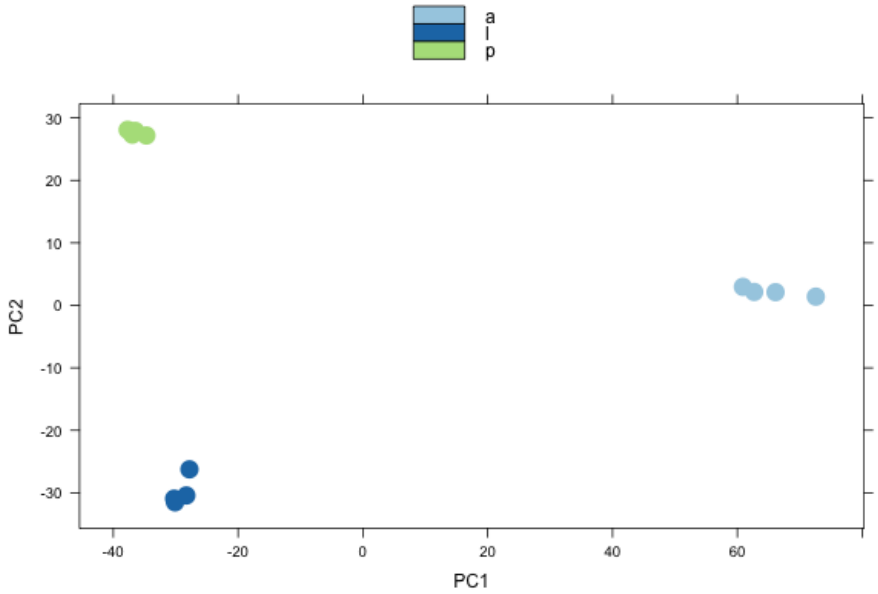

Figure A.1 Principle Component analysis (PCA) of development stages.
Raw counts were transformed with a regularized log transformation (log2 scale) to minimize differences between samples and normalize to library size. Three colors were used to distinguish the different samples. The larva stage is dark blue (l), the pre-pupa stage is sea green (p), and the adult stage is light blue (a). Samples were separated along two components to measure variance (i.e. PC1 and PC2).

Table A.1 Number of differentially expressed MAKER models.

Contrast	Number DE (padj < 0.01)	Number DE (padj < 0.01, log2FoldChange > 4)
L vs. P	7,612	513
P vs. A	8,551	1,063
L vs. A	7,221	750

Three contrasts were made for detection of Differential Expression (DE) between three separate insect stages. The comparisons were made in pairwise combinations of the three: larva (L) versus pre-pupa (P) versus adult (A). An adjusted p-value of less than 0.01 was used to identify significance and the data was further restricted to only include transcripts with log2FoldChanges greater than four (i.e. a fold change greater than two).

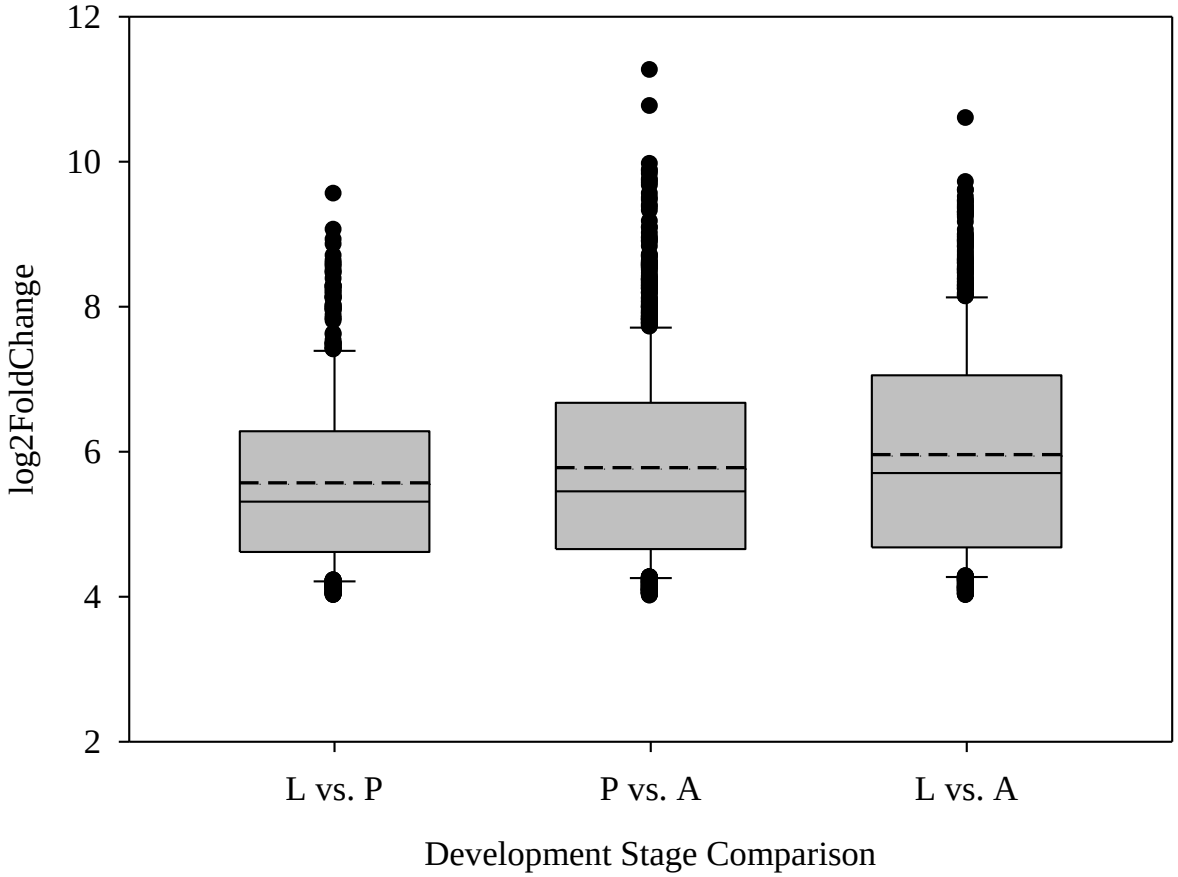

Figure A.2 Distribution of log2FoldChange values for differentially expressed transcripts between development stages.

The larva (L), pre-pupa (P), and adult (A) stages were comprised of four biological replicates. Each represented stage was used for pairwise comparisons and an adjusted p-value of less than 0.01 with a greater than four log2FoldChange was used to restrict the dataset. SigmaPlot v.10.0 standard method was used to calculate the box boundaries (25^{th} and 75^{th} percentile), the median and mean represented as a solid and dashed line, respectively, comprising the box. The error bars represent the 10^{th} and 90^{th} percentiles and the outliers are represented as solid dots.

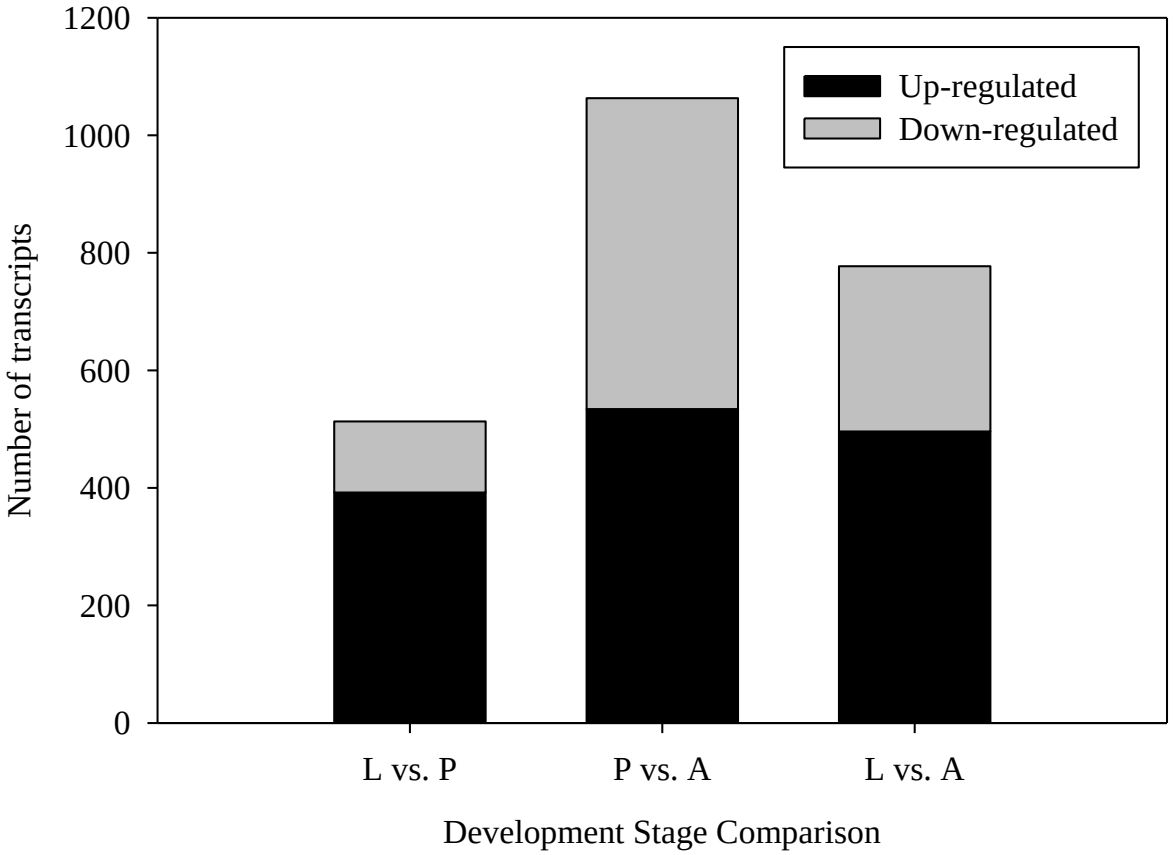

Figure A.3 Number and direction of change of differentially expressed transcripts.
The number and direction of change between each stage comparison was determined by using the first stage in the comparison as the reference point. The larva (L), pre-pupa (P), and adult (A) stage were used for pairwise comparisons, and the number of transcripts up and down is descriptive of the expression within the reference stage (e.g. 392 transcripts up and 121 down in the L stage when compared to P).

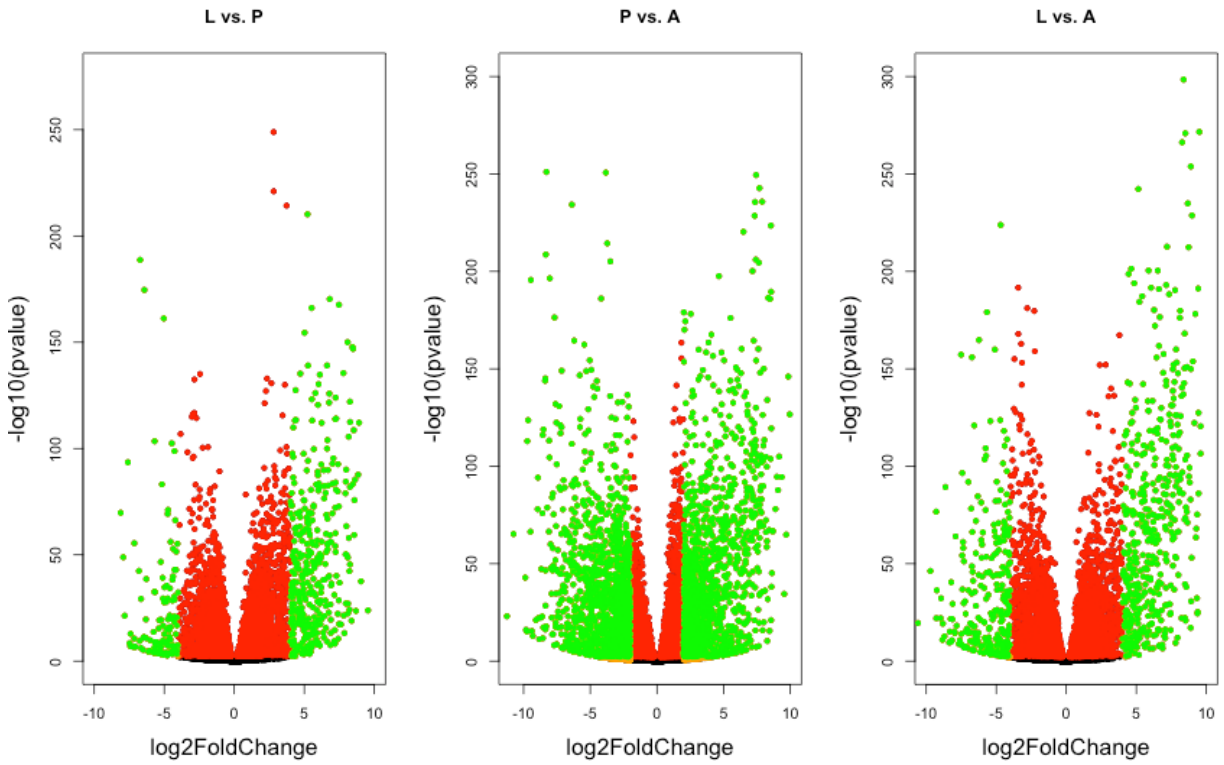

Figure A.4 Volcano plots of development stage pairwise comparisons.

Differential expression was detected across all MAKER models (transcripts) for each pairwise stage comparison: larva (L), pre-pupa (P), and adult (A). The log2FoldChange was plotted on the x-axis with the –log10(p-value) plotted on the y-axis. The dots are red if adjusted p-value is less than 0.01, orange if log2FoldChange is greater than 4, and green if both are true.

Table A.2 Top ten most dynamic transcript sequences in each of the three development stage comparisons

[a]Stage comp	[b]Transcript	log2FoldChange	Gene description (Blastx)	Similarity mean (%)	E-value (Top hit)	GO term
						P:organic substance metabolic
L vs. P	FOCC016717-RA	9.54	beta glucosidase 11	54.50%	2.35E-69	process
	FOCC009257-RA	9.05	potential cell surface flocculin	57.86%	3.49E-06	P:proteolysis
	FOCC009475-RA	8.91	---NA---			
	FOCC013503-RA	8.85	farnesoic acid O-methyltransferase	46.30%	1.44E-11	P:methylation
	FOCC009718-RA	8.62	cathepsin-L-like cysteine peptidase 02	74.10%	3.06E-165	P:proteolysis
	FOCC005657-RA	8.58	Apolipo D	55.10%	4.75E-23	P:transport
	FOCC012818-RA	8.56	piggyBac transposable element-derived 3-like	57.80%	1.84E-79	
	FOCC007547-RA	8.53	---NA---			
						F:peptidase
	FOCC007230-RA	8.48	Trypsinogen precursor of ANTRYP7	58.20%	2.49E-48	activity
			hypothetical protein			P:vaculor
	FOCC014766-RA	8.46	LOTGIDRAFT_232212	47.30%	3.43E-15	transport
						F:hydrolase
P vs. A	FOCC016005-RA	-11.25	isoform A	49.20%	9.88E-14	activity
	FOCC014322-RA	-10.75	---NA---			
						F:hydrolase
	FOCC014999-RA	-9.87	glycoside hydrolase family 45	69%	3.20E-55	activity
	FOCC008774-RA	9.85	---NA---			
	FOCC009477-RA	-9.72	---NA---			
						F:structural constituent of
	FOCC003831-RA	9.69	Larval cuticle protein A3A	91.80%	1.90E-25	cuticle
	FOCC005242-RA	9.54	---NA---			
						P:carbohydrate metabolic
	FOCC015215-RA	-9.48	lactase-phlorizin hydrolase	53.90%	1.10E-56	process
	FOCC011698-RA	-9.45	---NA---			
	FOCC007864-RA	-9.38	---NA---			
L vs. A	FOCC010261-RA	-10.59	---NA---			
	FOCC002425-RA	-9.70	---NA---			
	FOCC001736-RA	9.59	---NA---			
	FOCC001747-RA	9.59	---NA---			
						P:metabolic
	FOCC003013-RA	9.50	hemocyanin subunit type 1 precursor	57.60%	4.91E-167	process
	FOCC011984-RA	9.45	cuticular CPT2	80.60%	9.43E-19	F:ATP binding
	FOCC017290-RA	9.44	osiris 12	56.10%	8.23E-16	C:membrane

FOCC017476-RA	9.42	hypothetical protein EAI_13802	66.50%	3.81E-17	
		PREDICTED: hypothetical protein			
FOCC016858-RA	9.36	LOC100679021	54%	1.89E-24	C:membrane
FOCC003491-RA	9.35	osiris 19	61.70%	6.78E-29	C:membrane

[a] Pairwise Comparison made between each of the three insect development stages: Larva (L), Pre-pupa (P), and Adult (A). [b]FOCC is the identifier for transcripts assembled from MAKER-predicted gene models

Table A.3 Dynamics in expression for transcripts similar to Hippo signaling pathway

[a]MAKER model	L ([b]AVG-rld)	P ([b]AVG-rld)	A ([b]AVG-rld)	[c]Putative similarity	[d]Significantly different
FOCC006780-RA	9.61	10.36	9.97	mop	L-P-A
FOCC012386-RA	9.39	9.67	10.24	Tao	L-P-A
FOCC004131-RA	10.22	10.71	11.15	l(3)mbt	L-P-A
FOCC005645-RA	10.37	11.22	10.05	sd	L-P-A
FOCC011450-RA	9.06	9.26	9.36	Zyx	L
FOCC004468-RA	7.99	8.56	8.65	hpo	L
FOCC009228-RA	6.58	7.33	7.15	Pez	L
FOCC005881-RA	9.09	9.83	8.96	wts	P
FOCC007481-RA	8.4	9.27	8.38	kibra	P
FOCC017046-RA	7.74	9.01	7.14	ed & fred	P
FOCC004850-RA	7.24	8.59	7.66	yki	P

[a] FOCC is the identifier for transcripts assembled from MAKER-predicted gene models. [b] Average regularized log2 transformation of raw counts spanning four biological replicates for each development stage. [c] Transcript similarity determined by top hit in tblastn with *Drosophila* as query and *F. occidentalis* transcript MAKER models as subject. [d] Significant difference determined by DESeq2 analysis (*e.g* L-P-A indicating significant differences among all comparisons, L indicating significant differences between L and others).

Table A.4 Dynamics in expression for transcripts similar to molting signaling pathway

MAKER model	L (rld)	P (rld)	A (rld)	Putative similarity	Significantly different
FOCC009448-RA	8.73	10.69	8.12	broad	L-P-A
FOCC013148-RA	13.04	12.48	10.1	hr46	L-P-A
FOCC011115-RA	9.68	8.82	7.88	ETHR	L-P-A
FOCC003474-RA	4.56	9.42	6.83	Eip93F	L-P-A
FOCC011408-RA	12.23	13.09	11.17	ftz-f1	L-P-A
FOCC008047-RA	10.77	10.99	11.17	usp	L-P-A
FOCC012885-RA	12.86	13.06	13.19	Npc1a	L
FOCC011172-RA	11.03	11.78	10.91	crol	P
FOCC014045-RA	8.44	9.27	8.62	EcR	P
FOCC006043-RA	8	8.55	8.12	Gcn5	P
FOCC007203-RA	9.12	10.05	9.21	Hr78	P
FOCC009944-RA	9.67	10.67	9.42	rut	P
FOCC009751-RA	9.91	10.28	9.9	Set2	P
FOCC007123-RA	8.57	8.58	5.45	ETH	A
FOCC004890-RA	8.38	8.44	6.47	Eip74EF	A
FOCC012271-RA	11.94	12.19	10.78	Eip75B	A
FOCC010348-RA	8.77	9.06	7.39	Hr38	A
FOCC002538-RA	10.24	10.11	7.35	Hr4	A
FOCC013473-RA	9.99	10.26	10.15	ecd	Only L vs.P
FOCC005398-RA	7.16	8.19	7.83	Met	Only L vs.P
FOCC001712-RA	6.26	6.59	6.02	Eip63E	Only P vs. A
FOCC005835-RA	0.21	1.19	0.05	Kr-h1	Only P vs. A
FOCC007673-RA	9.73	9.95	9.67	Itp-r83A	Only P vs. A
FOCC005461-RA	-0.4	0.6	-0.56	Pka-C1	Only P vs. A

[a] FOCC is the identifier for transcripts assembled from MAKER-predicted gene models. [b] Average regularized log2 transformation of raw counts spanning four biological replicates for each development stage. [c] Transcript similarity determined by top hit in tblastn with *Drosophila* as query and *F. occidentalis* transcript MAKER models as subject. [d] Significant difference determined by DESeq2 analysis (*e.g* L-P-A indicating significant differences among all comparisons, Only L vs. P indicating significant differences only between those stages).

Appendix B - *De novo* transcriptome assembly of *Frankliniella occidentalis* RNA-seq reads

Results

Processing raw mRNAseq data and *de-novo* assembly for construction of the *Frankliniella occidentalis* transcriptome model

A transcriptome representing TSWV-infected and non-infected *Frankliniella occidentalis* was assembled de novo to serve as a reference for quantifying the effect of virus infection on global gene expression (*i. e.*, counts of reads per assembled contig) in the insect vector. Illumina sequencing of a total of 24 RNAseq libraries generated from three developmental stage-times (L1-21h, P1, Adult-24h) and two treatments (+/- virus) sampled from four independent biological replications of the TSWV accumulation experiment (Figure 1) resulted in a total of 878,175,618 raw 100bp reads yielding 68,441 Mb of sequence. On average over all libraries, 78.2% raw reads passed the initial filter with a mean Phred quality score of 33.86 .

The raw RNAseq dataset was subjected to Prinseq for further data cleaning resulting in a removal of 80% of the reads (Table 2), of which 63% were exact read repeats. Removal of read redundancy does not affect the assembly other than to effectively decrease computational time. The reduced dataset of 177,404,322 sequences, with a mean length of 98.76bp, had a mean GC content of 45.98 ± 12.90%, and it was this sequence library that was then used for assembly with the Trinity pipeline. The resultant assembly produced a total of 81,402 contigs which was further restricted by a low and high threshold size of 500 bp and 7999 bp, respectively, to produce at a

model transcriptome of 56,542 contigs. The final transcriptome model had a mean contig length of 2932.97bp, and an N50 of 4,177bp.

Discussion

Generating a transcriptome model for a virus vector and the order Thysanoptera

A previously built model using sanger sequencing and 454Roche technology represents a portion of the total transcriptome for *F. occidentalis* (Badillo-Vargas et al., 2012, Rotenberg and Whitfield, 2010). This new transcriptome model constructed for *F. occidentalis* provides novel information to the insect order Thysanoptera. The model constructed consists of 56,542 contigs that are inclusive of isoform and allelic differences. The assembly was a challenging process due to multiple development stages with two treatments and four biological replications under lab conditions. *De novo* assembly with Trinity uses computer algorithms that construct k-mers and then subsequently uses de-bruijn graphing for pathway construction to produce strings that become the basis of contigs (Grabherr et al., 2011). This process is established without the use of a reference. It is in complete agreement with the Latin expression "from the beginning". The raw sequences are used from the beginning to build a model, and the *De novo* process is based largely on the model that it is trying to represent. Multiple approaches were used to achieve a usable transcriptome for *F. occidentalis*. One of the largest fundamental changes was producing an algorithmic requirement for the presence of 2 k-mers before subsequent construction of components. This change enabled the production of fewer contigs that were relevant to the model. It provided a mechanism to manipulate a greedy program, Trinity, and make it act more conservatively. A similar number of "unigenes", with a total of 59,932 unigenes were found in

one other *F. occidentalis* transcriptome study (Zhang et al., 2013). This assembly has enabled the study of differential expression during virus infection, and it has enabled a new understanding of the dynamic and complex interaction between TSWV and *F. occidentalis*.

Materials and Methods

RNAseq Processing

The raw RNAseq data was cleaned and trimmed to remove low quality bases. Tag sequences were removed through the use of Illumina library indexing approach. Raw RNAseq data was subjected to Prinseq-lite, version 0.20.3, for trimming and cleaning pre-assembly (Schmieder and Edwards, 2011b). All large-scale data manipulation steps were performed using the Beocat computer cluster at Kansas State University. The minimum mean quality score allowed was a phred score of 23. Sequences were filtered out if they contained characters other than A, C, G, T, or N. All sequences with Ns were removed from the dataset. Exact duplicates were also removed before assembly so as to reduce computational time. A threshold score of 20 for Phred was used for trimming both the 5' and 3' ends of each sequence produced. The minimum length allowed to pass filter was 90bp and reads with strings of 15 Ts and/or 15 As were removed.

De-novo Assembly with Trinity and post processing

The Trinity assembly pipeline, release version 2013-02-25, was used for de-novo assembly of the cleaned and trimmed RNAseq reads (Grabherr et al., 2011). A minimum k-mer coverage of 2 was chosen during use of the pipeline so as to reduce the complexity of graphing and decrease the likelihood of fusion transcripts during construction of contiguous consensus

sequences (contigs). Defaults were used for all other options within the Trinity assembly pipeline. The assembly was allowed 10 gigabytes for Jellyfish memory. Post-assembly processing was done using Prinseq-lite with a minimum contig length requirement of 500bp, a maximum contig length of 7,999bp, and removal of low complexity sequences using the DUST algorithm with an lc threshold of 7.

Table B.1 Raw sequence yield and quality metrics for the biological samples contributing to reference transcriptome model

Biological Replication	Sample	Yield (Mbases)	Percent that Pass Filter	Raw Reads	Percent Perfect Index Reads	Mean Quality Score Pass Filter (Phred)
1	L1-24 Healthy	2,775	85.15	32,585,907	97.83	33.4
2	L1-24 Healthy	3,203	86.58	36,993,218	98.48	34.48
3	L1-24 Healthy	2,444	70.84	34,495,838	94.58	33.85
4	L1-24 Healthy	2,072	69.9	29,643,082	97.71	33.74
1	P1 Healthy	3,303	84.42	39,133,443	97.97	33.31
2	P1 Healthy	3,025	86.31	35,049,319	98.53	34.53
3	P1 Healthy	2,556	68.35	37,391,561	96.59	33.9
4	P1 Healthy	2,808	71.69	39,170,587	97.06	33.85
1	Ad-24 Healthy	3,506	85.62	40,944,452	96.14	33.14
2	Ad-24 Healthy	3,521	86.72	40,599,599	98.72	34.4
3	Ad-24 Healthy	2,707	68.4	39,582,789	96.1	33.47
4	Ad-24 Healthy	2,893	71.9	40,231,629	97.42	33.8
1	L1-24 TSWV	2,823	85.63	32,970,619	96.18	33.41
2	L1-24 TSWV	2,692	86.94	30,970,227	98.25	34.49
3	L1-24 TSWV	2,425	69.11	35,087,579	93.93	33.62
4	L1-24 TSWV	2,762	72.97	37,855,800	97.64	34.02
1	P1 TSWV	3,417	87.06	39,253,613	97.92	33.64
2	P1 TSWV	3,035	87.51	34,682,745	97.84	34.55
3	P1 TSWV	2,302	69.1	33,313,535	96.34	33.59
4	P1 TSWV	2,914	72.09	40,419,691	95.28	34.08
1	Ad-24 TSWV	2,122	86.17	24,622,116	95.02	33.56
2	Ad-24 TSWV	3,200	86.11	37,158,570	97.78	34.23
3	Ad-24 TSWV	3,246	67.88	47,812,867	95.56	33.56
4	Ad-24 TSWV	2,690	70.4	38,206,832	98.36	33.9

Table B.1 Raw sequence yield and quality metrics for the biological samples contributing to reference transcriptome model

Data Type	Number of Sequences	Percent of RAW Data
RAW	878,175,618	100%
Raw Sequences Removed By Prinseq	**Number of Sequences**	**Percent of RAW Data**
Sequences Trimmed	44,128,895	5.03%
Sequences Shorter than 90bp	167,552,611	19.08%
Sequences Low Mean Quality	436,713	0.05%
Sequences with Ns	42,057,034	4.79%
Exact Repeats	446,596,043	50.85%
Prinseq Cleaned Dataset	177,404,322	20.20%
Trinity Data Type	**Number of Contigs**	**Percent of Assembled Transcriptome**
Trinity Assembled Transcriptome	81,402	100.00%
Removed Contigs Shorter than 500bp	20,243	24.87%
Removed Contigs Longer than 7999bp	4,617	5.67%
Final Transcriptome Model	56,542	69.46%

The raw RNAseq dataset and its' total reduction is represented in the top categories highlighted in grey. The number of raw sequences removed and percent of raw data the remove sequences represent are displayed in the second row of categories. The final grey row depicts the assembled transcriptome and the reduction established by removal of small and large contigs.

Appendix C - RNAi Microinjections: Statistical tables for tests of significance

Table C.1 Statistical test of normalized abundance of Dicer-2 using gamma response with 49 degrees of freedom.

Type III Tests of Fixed Effects

Effect	Num DF	Den DF	F Value	Pr > F
trt	3	49	0.53	0.6658
condt	1	49	2.75	0.1034
day	2	49	3.17	0.0509
trt*condt	3	49	0.83	0.4813
trt*day	6	49	3.86	0.0031
condt*day	2	49	0.88	0.4209
trt*condt*day	5	49	2.49	0.0437

trt	condt	day	_trt	_condt	_day	Estimate	Standard Error	t Value	Pr > |t|	Adj P
ago2	h	1	ago2	h	3	0.01667	0.1789	0.09	0.9262	1
ago2	h	1	ago2	h	6	-0.116	0.1789	-0.65	0.5198	1
ago2	h	1	ago2	v	1	0.1661	0.16	1.04	0.3043	1
ago2	h	1	ago2	v	3	-0.027	0.1789	-0.15	0.8807	1
ago2	h	1	ago2	v	6	-0.111	0.1789	-0.62	0.5379	1
ago2	h	1	dcr2	h	1	-0.73	0.1789	-4.08	0.0002	0.0249
ago2	h	1	dcr2	h	3	-0.08367	0.1789	-0.47	0.6421	1
ago2	h	1	dcr2	h	6	-0.095	0.1789	-0.53	0.5978	1
ago2	h	1	dcr2	v	1	-0.1821	0.16	-1.14	0.2608	0.9999
ago2	h	1	dcr2	v	3	0.01833	0.1789	0.1	0.9188	1
ago2	h	1	dcr2	v	6	-0.115	0.1789	-0.64	0.5234	1
ago2	h	1	gfp	h	1	0.028	0.1789	0.16	0.8763	1
ago2	h	1	gfp	h	3	-0.1097	0.1789	-0.61	0.5427	1
ago2	h	1	gfp	h	6	-0.5713	0.1789	-3.19	0.0025	0.2206
ago2	h	1	gfp	v	1	-0.023	0.1789	-0.13	0.8982	1
ago2	h	1	gfp	v	3	-0.1393	0.1789	-0.78	0.4399	1
ago2	h	1	gfp	v	6	-0.244	0.1789	-1.36	0.1789	0.999
ago2	h	1	w	h	3	-0.03367	0.1789	-0.19	0.8515	1
ago2	h	1	w	h	6	-0.3187	0.1789	-1.78	0.0811	0.9735
ago2	h	1	w	v	1	0.09383	0.2	0.47	0.6411	1
ago2	h	1	w	v	3	0.04167	0.1789	0.23	0.8168	1
ago2	h	1	w	v	6	-0.339	0.1789	-1.89	0.064	0.9516

ago2	h	3	ago2	h	6	-0.1327	0.1789	-0.74	0.4619	1
ago2	h	3	ago2	v	1	0.1495	0.16	0.93	0.3549	1
ago2	h	3	ago2	v	3	-0.04367	0.1789	-0.24	0.8082	1
ago2	h	3	ago2	v	6	-0.1277	0.1789	-0.71	0.4789	1
ago2	h	3	dcr2	h	1	-0.7467	0.1789	-4.17	0.0001	0.0191
ago2	h	3	dcr2	h	3	-0.1003	0.1789	-0.56	0.5775	1
ago2	h	3	dcr2	h	6	-0.1117	0.1789	-0.62	0.5354	1
ago2	h	3	dcr2	v	1	-0.1987	0.16	-1.24	0.2202	0.9997
ago2	h	3	dcr2	v	3	0.001667	0.1789	0.01	0.9926	1
ago2	h	3	dcr2	v	6	-0.1317	0.1789	-0.74	0.4653	1
ago2	h	3	gfp	h	1	0.01133	0.1789	0.06	0.9498	1
ago2	h	3	gfp	h	3	-0.1263	0.1789	-0.71	0.4835	1
ago2	h	3	gfp	h	6	-0.588	0.1789	-3.29	0.0019	0.1818
ago2	h	3	gfp	v	1	-0.03967	0.1789	-0.22	0.8255	1
ago2	h	3	gfp	v	3	-0.156	0.1789	-0.87	0.3875	1
ago2	h	3	gfp	v	6	-0.2607	0.1789	-1.46	0.1515	0.9975
ago2	h	3	w	h	3	-0.05033	0.1789	-0.28	0.7796	1
ago2	h	3	w	h	6	-0.3353	0.1789	-1.87	0.0669	0.9562
ago2	h	3	w	v	1	0.07717	0.2	0.39	0.7013	1
ago2	h	3	w	v	3	0.025	0.1789	0.14	0.8894	1
ago2	h	3	w	v	6	-0.3557	0.1789	-1.99	0.0524	0.9257
ago2	h	6	ago2	v	1	0.2821	0.16	1.76	0.0841	0.9761
ago2	h	6	ago2	v	3	0.089	0.1789	0.5	0.6211	1
ago2	h	6	ago2	v	6	0.005	0.1789	0.03	0.9778	1
ago2	h	6	dcr2	h	1	-0.614	0.1789	-3.43	0.0012	0.1319
ago2	h	6	dcr2	h	3	0.03233	0.1789	0.18	0.8573	1
ago2	h	6	dcr2	h	6	0.021	0.1789	0.12	0.907	1
ago2	h	6	dcr2	v	1	-0.06607	0.16	-0.41	0.6815	1
ago2	h	6	dcr2	v	3	0.1343	0.1789	0.75	0.4564	1
ago2	h	6	dcr2	v	6	0.001	0.1789	0.01	0.9956	1
ago2	h	6	gfp	h	1	0.144	0.1789	0.8	0.4248	1
ago2	h	6	gfp	h	3	0.006333	0.1789	0.04	0.9719	1
ago2	h	6	gfp	h	6	-0.4553	0.1789	-2.54	0.0141	0.6207
ago2	h	6	gfp	v	1	0.093	0.1789	0.52	0.6055	1
ago2	h	6	gfp	v	3	-0.02333	0.1789	-0.13	0.8968	1
ago2	h	6	gfp	v	6	-0.128	0.1789	-0.72	0.4777	1
ago2	h	6	w	h	3	0.08233	0.1789	0.46	0.6474	1
ago2	h	6	w	h	6	-0.2027	0.1789	-1.13	0.2628	0.9999
ago2	h	6	w	v	1	0.2098	0.2	1.05	0.2993	1
ago2	h	6	w	v	3	0.1577	0.1789	0.88	0.3825	1
ago2	h	6	w	v	6	-0.223	0.1789	-1.25	0.2185	0.9997
ago2	v	1	ago2	v	3	-0.1931	0.16	-1.21	0.2333	0.9998
ago2	v	1	ago2	v	6	-0.2771	0.16	-1.73	0.0896	0.9802

ago2	v	1	dcr2	h	1	-0.8961	0.16	-5.6	<.0001	0.0002
ago2	v	1	dcr2	h	3	-0.2498	0.16	-1.56	0.125	0.9939
ago2	v	1	dcr2	h	6	-0.2611	0.16	-1.63	0.1091	0.9898
ago2	v	1	dcr2	v	1	-0.3482	0.1386	-2.51	0.0153	0.6434
ago2	v	1	dcr2	v	3	-0.1478	0.16	-0.92	0.3602	1
ago2	v	1	dcr2	v	6	-0.2811	0.16	-1.76	0.0852	0.977
ago2	v	1	gfp	h	1	-0.1381	0.16	-0.86	0.3922	1
ago2	v	1	gfp	h	3	-0.2758	0.16	-1.72	0.0911	0.9812
ago2	v	1	gfp	h	6	-0.7375	0.16	-4.61	<.0001	0.0052
ago2	v	1	gfp	v	1	-0.1891	0.16	-1.18	0.243	0.9999
ago2	v	1	gfp	v	3	-0.3055	0.16	-1.91	0.0621	0.9481
ago2	v	1	gfp	v	6	-0.4101	0.16	-2.56	0.0135	0.6081
ago2	v	1	w	h	3	-0.1998	0.16	-1.25	0.2178	0.9997
ago2	v	1	w	h	6	-0.4848	0.16	-3.03	0.0039	0.3023
ago2	v	1	w	v	1	-0.0723	0.1833	-0.39	0.695	1
ago2	v	1	w	v	3	-0.1245	0.16	-0.78	0.4404	1
ago2	v	1	w	v	6	-0.5051	0.16	-3.16	0.0027	0.2375
ago2	v	3	ago2	v	6	-0.084	0.1789	-0.47	0.6408	1
ago2	v	3	dcr2	h	1	-0.703	0.1789	-3.93	0.0003	0.0379
ago2	v	3	dcr2	h	3	-0.05667	0.1789	-0.32	0.7528	1
ago2	v	3	dcr2	h	6	-0.068	0.1789	-0.38	0.7055	1
ago2	v	3	dcr2	v	1	-0.1551	0.16	-0.97	0.3373	1
ago2	v	3	dcr2	v	3	0.04533	0.1789	0.25	0.801	1
ago2	v	3	dcr2	v	6	-0.088	0.1789	-0.49	0.625	1
ago2	v	3	gfp	h	1	0.055	0.1789	0.31	0.7598	1
ago2	v	3	gfp	h	3	-0.08267	0.1789	-0.46	0.6461	1
ago2	v	3	gfp	h	6	-0.5443	0.1789	-3.04	0.0038	0.2953
ago2	v	3	gfp	v	1	0.004	0.1789	0.02	0.9823	1
ago2	v	3	gfp	v	3	-0.1123	0.1789	-0.63	0.533	1
ago2	v	3	gfp	v	6	-0.217	0.1789	-1.21	0.231	0.9998
ago2	v	3	w	h	3	-0.00667	0.1789	-0.04	0.9704	1
ago2	v	3	w	h	6	-0.2917	0.1789	-1.63	0.1095	0.9899
ago2	v	3	w	v	1	0.1208	0.2	0.6	0.5486	1
ago2	v	3	w	v	3	0.06867	0.1789	0.38	0.7028	1
ago2	v	3	w	v	6	-0.312	0.1789	-1.74	0.0875	0.9787
ago2	v	6	dcr2	h	1	-0.619	0.1789	-3.46	0.0011	0.1237
ago2	v	6	dcr2	h	3	0.02733	0.1789	0.15	0.8792	1
ago2	v	6	dcr2	h	6	0.016	0.1789	0.09	0.9291	1
ago2	v	6	dcr2	v	1	-0.07107	0.16	-0.44	0.6589	1
ago2	v	6	dcr2	v	3	0.1293	0.1789	0.72	0.4732	1
ago2	v	6	dcr2	v	6	-0.004	0.1789	-0.02	0.9823	1
ago2	v	6	gfp	h	1	0.139	0.1789	0.78	0.441	1
ago2	v	6	gfp	h	3	0.001333	0.1789	0.01	0.9941	1

ago2	v	6	gfp	h	6	-0.4603	0.1789	-2.57	0.0132	0.6011
ago2	v	6	gfp	v	1	0.088	0.1789	0.49	0.625	1
ago2	v	6	gfp	v	3	-0.02833	0.1789	-0.16	0.8748	1
ago2	v	6	gfp	v	6	-0.133	0.1789	-0.74	0.4608	1
ago2	v	6	w	h	3	0.07733	0.1789	0.43	0.6675	1
ago2	v	6	w	h	6	-0.2077	0.1789	-1.16	0.2514	0.9999
ago2	v	6	w	v	1	0.2048	0.2	1.02	0.3109	1
ago2	v	6	w	v	3	0.1527	0.1789	0.85	0.3977	1
ago2	v	6	w	v	6	-0.228	0.1789	-1.27	0.2086	0.9996
dcr2	h	1	dcr2	h	3	0.6463	0.1789	3.61	0.0007	0.086
dcr2	h	1	dcr2	h	6	0.635	0.1789	3.55	0.0009	0.1002
dcr2	h	1	dcr2	v	1	0.5479	0.16	3.42	0.0013	0.1343
dcr2	h	1	dcr2	v	3	0.7483	0.1789	4.18	0.0001	0.0186
dcr2	h	1	dcr2	v	6	0.615	0.1789	3.44	0.0012	0.1303
dcr2	h	1	gfp	h	1	0.758	0.1789	4.24	<.0001	0.0159
dcr2	h	1	gfp	h	3	0.6203	0.1789	3.47	0.0011	0.1216
dcr2	h	1	gfp	h	6	0.1587	0.1789	0.89	0.3795	1
dcr2	h	1	gfp	v	1	0.707	0.1789	3.95	0.0002	0.0356
dcr2	h	1	gfp	v	3	0.5907	0.1789	3.3	0.0018	0.1761
dcr2	h	1	gfp	v	6	0.486	0.1789	2.72	0.0091	0.5003
dcr2	h	1	w	h	3	0.6963	0.1789	3.89	0.0003	0.0419
dcr2	h	1	w	h	6	0.4113	0.1789	2.3	0.0258	0.7824
dcr2	h	1	w	v	1	0.8238	0.2	4.12	0.0001	0.0224
dcr2	h	1	w	v	3	0.7717	0.1789	4.31	<.0001	0.0127
dcr2	h	1	w	v	6	0.391	0.1789	2.19	0.0337	0.8446
dcr2	h	3	dcr2	h	6	-0.01133	0.1789	-0.06	0.9498	1
dcr2	h	3	dcr2	v	1	-0.0984	0.16	-0.61	0.5415	1
dcr2	h	3	dcr2	v	3	0.102	0.1789	0.57	0.5712	1
dcr2	h	3	dcr2	v	6	-0.03133	0.1789	-0.18	0.8617	1
dcr2	h	3	gfp	h	1	0.1117	0.1789	0.62	0.5354	1
dcr2	h	3	gfp	h	3	-0.026	0.1789	-0.15	0.8851	1
dcr2	h	3	gfp	h	6	-0.4877	0.1789	-2.73	0.0089	0.4938
dcr2	h	3	gfp	v	1	0.06067	0.1789	0.34	0.736	1
dcr2	h	3	gfp	v	3	-0.05567	0.1789	-0.31	0.757	1
dcr2	h	3	gfp	v	6	-0.1603	0.1789	-0.9	0.3746	1
dcr2	h	3	w	h	3	0.05	0.1789	0.28	0.7811	1
dcr2	h	3	w	h	6	-0.235	0.1789	-1.31	0.1951	0.9994
dcr2	h	3	w	v	1	0.1775	0.2	0.89	0.3792	1
dcr2	h	3	w	v	3	0.1253	0.1789	0.7	0.4869	1
dcr2	h	3	w	v	6	-0.2553	0.1789	-1.43	0.1599	0.9981
dcr2	h	6	dcr2	v	1	-0.08707	0.16	-0.54	0.5889	1
dcr2	h	6	dcr2	v	3	0.1133	0.1789	0.63	0.5294	1
dcr2	h	6	dcr2	v	6	-0.02	0.1789	-0.11	0.9115	1

dcr2	h	6	gfp	h	1	0.123	0.1789	0.69	0.495	1
dcr2	h	6	gfp	h	3	-0.01467	0.1789	-0.08	0.935	1
dcr2	h	6	gfp	h	6	-0.4763	0.1789	-2.66	0.0105	0.538
dcr2	h	6	gfp	v	1	0.072	0.1789	0.4	0.6891	1
dcr2	h	6	gfp	v	3	-0.04433	0.1789	-0.25	0.8053	1
dcr2	h	6	gfp	v	6	-0.149	0.1789	-0.83	0.409	1
dcr2	h	6	w	h	3	0.06133	0.1789	0.34	0.7332	1
dcr2	h	6	w	h	6	-0.2237	0.1789	-1.25	0.2172	0.9997
dcr2	h	6	w	v	1	0.1888	0.2	0.94	0.3498	1
dcr2	h	6	w	v	3	0.1367	0.1789	0.76	0.4486	1
dcr2	h	6	w	v	6	-0.244	0.1789	-1.36	0.1789	0.999
dcr2	v	1	dcr2	v	3	0.2004	0.16	1.25	0.2164	0.9997
dcr2	v	1	dcr2	v	6	0.06707	0.16	0.42	0.677	1
dcr2	v	1	gfp	h	1	0.2101	0.16	1.31	0.1954	0.9994
dcr2	v	1	gfp	h	3	0.0724	0.16	0.45	0.653	1
dcr2	v	1	gfp	h	6	-0.3893	0.16	-2.43	0.0187	0.6979
dcr2	v	1	gfp	v	1	0.1591	0.16	0.99	0.3251	1
dcr2	v	1	gfp	v	3	0.04273	0.16	0.27	0.7906	1
dcr2	v	1	gfp	v	6	-0.06193	0.16	-0.39	0.7004	1
dcr2	v	1	w	h	3	0.1484	0.16	0.93	0.3583	1
dcr2	v	1	w	h	6	-0.1366	0.16	-0.85	0.3975	1
dcr2	v	1	w	v	1	0.2759	0.1833	1.5	0.1388	0.9962
dcr2	v	1	w	v	3	0.2237	0.16	1.4	0.1684	0.9985
dcr2	v	1	w	v	6	-0.1569	0.16	-0.98	0.3316	1
dcr2	v	3	dcr2	v	6	-0.1333	0.1789	-0.75	0.4597	1
dcr2	v	3	gfp	h	1	0.009667	0.1789	0.05	0.9571	1
dcr2	v	3	gfp	h	3	-0.128	0.1789	-0.72	0.4777	1
dcr2	v	3	gfp	h	6	-0.5897	0.1789	-3.3	0.0018	0.1782
dcr2	v	3	gfp	v	1	-0.04133	0.1789	-0.23	0.8183	1
dcr2	v	3	gfp	v	3	-0.1577	0.1789	-0.88	0.3825	1
dcr2	v	3	gfp	v	6	-0.2623	0.1789	-1.47	0.149	0.9972
dcr2	v	3	w	h	3	-0.052	0.1789	-0.29	0.7726	1
dcr2	v	3	w	h	6	-0.337	0.1789	-1.88	0.0656	0.9542
dcr2	v	3	w	v	1	0.0755	0.2	0.38	0.7075	1
dcr2	v	3	w	v	3	0.02333	0.1789	0.13	0.8968	1
dcr2	v	3	w	v	6	-0.3573	0.1789	-2	0.0514	0.9227
dcr2	v	6	gfp	h	1	0.143	0.1789	0.8	0.428	1
dcr2	v	6	gfp	h	3	0.005333	0.1789	0.03	0.9763	1
dcr2	v	6	gfp	h	6	-0.4563	0.1789	-2.55	0.0139	0.6168
dcr2	v	6	gfp	v	1	0.092	0.1789	0.51	0.6094	1
dcr2	v	6	gfp	v	3	-0.02433	0.1789	-0.14	0.8924	1
dcr2	v	6	gfp	v	6	-0.129	0.1789	-0.72	0.4743	1
dcr2	v	6	w	h	3	0.08133	0.1789	0.45	0.6514	1

dcr2	v	6	w	h	6	-0.2037	0.1789	-1.14	0.2605	0.9999
dcr2	v	6	w	v	1	0.2088	0.2	1.04	0.3016	1
dcr2	v	6	w	v	3	0.1567	0.1789	0.88	0.3855	1
dcr2	v	6	w	v	6	-0.224	0.1789	-1.25	0.2165	0.9997
gfp	h	1	gfp	h	3	-0.1377	0.1789	-0.77	0.4453	1
gfp	h	1	gfp	h	6	-0.5993	0.1789	-3.35	0.0016	0.1585
gfp	h	1	gfp	v	1	-0.051	0.1789	-0.29	0.7768	1
gfp	h	1	gfp	v	3	-0.1673	0.1789	-0.94	0.3542	1
gfp	h	1	gfp	v	6	-0.272	0.1789	-1.52	0.1349	0.9956
gfp	h	1	w	h	3	-0.06167	0.1789	-0.34	0.7318	1
gfp	h	1	w	h	6	-0.3467	0.1789	-1.94	0.0584	0.9406
gfp	h	1	w	v	1	0.06583	0.2	0.33	0.7435	1
gfp	h	1	w	v	3	0.01367	0.1789	0.08	0.9394	1
gfp	h	1	w	v	6	-0.367	0.1789	-2.05	0.0456	0.9037
gfp	h	3	gfp	h	6	-0.4617	0.1789	-2.58	0.0129	0.5958
gfp	h	3	gfp	v	1	0.08667	0.1789	0.48	0.6303	1
gfp	h	3	gfp	v	3	-0.02967	0.1789	-0.17	0.869	1
gfp	h	3	gfp	v	6	-0.1343	0.1789	-0.75	0.4564	1
gfp	h	3	w	h	3	0.076	0.1789	0.42	0.6729	1
gfp	h	3	w	h	6	-0.209	0.1789	-1.17	0.2484	0.9999
gfp	h	3	w	v	1	0.2035	0.2	1.02	0.314	1
gfp	h	3	w	v	3	0.1513	0.1789	0.85	0.4018	1
gfp	h	3	w	v	6	-0.2293	0.1789	-1.28	0.2059	0.9996
gfp	h	6	gfp	v	1	0.5483	0.1789	3.06	0.0035	0.2833
gfp	h	6	gfp	v	3	0.432	0.1789	2.41	0.0195	0.7099
gfp	h	6	gfp	v	6	0.3273	0.1789	1.83	0.0734	0.9653
gfp	h	6	w	h	3	0.5377	0.1789	3.01	0.0042	0.3159
gfp	h	6	w	h	6	0.2527	0.1789	1.41	0.1642	0.9983
gfp	h	6	w	v	1	0.6652	0.2	3.33	0.0017	0.1673
gfp	h	6	w	v	3	0.613	0.1789	3.43	0.0012	0.1336
gfp	h	6	w	v	6	0.2323	0.1789	1.3	0.2002	0.9995
gfp	v	1	gfp	v	3	-0.1163	0.1789	-0.65	0.5186	1
gfp	v	1	gfp	v	6	-0.221	0.1789	-1.24	0.2226	0.9998
gfp	v	1	w	h	3	-0.01067	0.1789	-0.06	0.9527	1
gfp	v	1	w	h	6	-0.2957	0.1789	-1.65	0.1048	0.9882
gfp	v	1	w	v	1	0.1168	0.2	0.58	0.5619	1
gfp	v	1	w	v	3	0.06467	0.1789	0.36	0.7193	1
gfp	v	1	w	v	6	-0.316	0.1789	-1.77	0.0836	0.9757
gfp	v	3	gfp	v	6	-0.1047	0.1789	-0.59	0.5612	1
gfp	v	3	w	h	3	0.1057	0.1789	0.59	0.5575	1
gfp	v	3	w	h	6	-0.1793	0.1789	-1	0.3211	1
gfp	v	3	w	v	1	0.2332	0.2	1.17	0.2494	0.9999
gfp	v	3	w	v	3	0.181	0.1789	1.01	0.3167	1

gfp	v	3	w	v	6	-0.1997	0.1789	-1.12	0.2699	0.9999
gfp	v	6	w	h	3	0.2103	0.1789	1.18	0.2454	0.9999
gfp	v	6	w	h	6	-0.07467	0.1789	-0.42	0.6783	1
gfp	v	6	w	v	1	0.3378	0.2	1.69	0.0976	0.9849
gfp	v	6	w	v	3	0.2857	0.1789	1.6	0.1168	0.9921
gfp	v	6	w	v	6	-0.095	0.1789	-0.53	0.5978	1
w	h	3	w	h	6	-0.285	0.1789	-1.59	0.1176	0.9923
w	h	3	w	v	1	0.1275	0.2	0.64	0.5268	1
w	h	3	w	v	3	0.07533	0.1789	0.42	0.6756	1
w	h	3	w	v	6	-0.3053	0.1789	-1.71	0.0942	0.9831
w	h	6	w	v	1	0.4125	0.2	2.06	0.0445	0.8995
w	h	6	w	v	3	0.3603	0.1789	2.01	0.0495	0.9171
w	h	6	w	v	6	-0.02033	0.1789	-0.11	0.91	1
w	v	1	w	v	3	-0.05217	0.2	-0.26	0.7953	1
w	v	1	w	v	6	-0.4328	0.2	-2.16	0.0354	0.8552
w	v	3	w	v	6	-0.3807	0.1789	-2.13	0.0384	0.8721

Table C.2 Statistical test of normalized abundance of AGO2 using gamma response with 49 degrees of freedom.

Type III Tests of Fixed Effects

Effect	Num DF	Den DF	F Value	Pr > F
trt	3	49	3.29	0.0283
condt	1	49	3.35	0.0732
day	2	49	6.75	0.0026
trt*condt	3	49	0.29	0.8353
trt*day	6	49	4.28	0.0015
condt*day	2	49	0.93	0.4028
trt*condt*day	5	49	1.2	0.3253

trt	condt	day	_trt	_condt	_day	Estimate	Standard Error	t Value	Pr > |t|	Adj P
ago2	h	1	ago2	h	3	0.03502	0.2595	0.13	0.8932	1
ago2	h	1	ago2	h	6	-0.2147	0.2595	-0.83	0.412	1
ago2	h	1	ago2	v	1	0.4201	0.2321	1.81	0.0764	0.9688
ago2	h	1	ago2	v	3	-0.05425	0.2595	-0.21	0.8353	1
ago2	h	1	ago2	v	6	-0.2063	0.2595	-0.8	0.4304	1
ago2	h	1	dcr2	h	1	-0.9192	0.2595	-3.54	0.0009	0.102
ago2	h	1	dcr2	h	3	-0.1593	0.2595	-0.61	0.542	1
ago2	h	1	dcr2	h	6	-0.1791	0.2595	-0.69	0.4933	1
ago2	h	1	dcr2	v	1	-0.3191	0.2321	-1.37	0.1754	0.9988
ago2	h	1	dcr2	v	3	0.03859	0.2595	0.15	0.8824	1
ago2	h	1	dcr2	v	6	-0.213	0.2595	-0.82	0.4156	1
ago2	h	1	gfp	h	1	0.05955	0.2595	0.23	0.8195	1
ago2	h	1	gfp	h	3	-0.2041	0.2595	-0.79	0.4354	1
ago2	h	1	gfp	h	6	-0.7792	0.2595	-3	0.0042	0.3174
ago2	h	1	gfp	v	1	-0.04639	0.2595	-0.18	0.8588	1
ago2	h	1	gfp	v	3	-0.2528	0.2595	-0.97	0.3347	1
ago2	h	1	gfp	v	6	-0.408	0.2595	-1.57	0.1224	0.9934
ago2	h	1	w	h	3	-0.0672	0.2595	-0.26	0.7968	1
ago2	h	1	w	h	6	-0.5056	0.2595	-1.95	0.0571	0.9376
ago2	h	1	w	v	1	0.2153	0.2901	0.74	0.4615	1
ago2	h	1	w	v	3	0.08996	0.2595	0.35	0.7303	1
ago2	h	1	w	v	6	-0.5306	0.2595	-2.04	0.0463	0.9061
ago2	h	3	ago2	h	6	-0.2497	0.2595	-0.96	0.3406	1
ago2	h	3	ago2	v	1	0.3851	0.2321	1.66	0.1035	0.9877
ago2	h	3	ago2	v	3	-0.08927	0.2595	-0.34	0.7323	1

ago2	h	3	ago2	v	6	-0.2414	0.2595	-0.93	0.3569	1
ago2	h	3	dcr2	h	1	-0.9542	0.2595	-3.68	0.0006	0.0732
ago2	h	3	dcr2	h	3	-0.1944	0.2595	-0.75	0.4575	1
ago2	h	3	dcr2	h	6	-0.2141	0.2595	-0.83	0.4133	1
ago2	h	3	dcr2	v	1	-0.3541	0.2321	-1.53	0.1335	0.9954
ago2	h	3	dcr2	v	3	0.00357	0.2595	0.01	0.9891	1
ago2	h	3	dcr2	v	6	-0.2481	0.2595	-0.96	0.3438	1
ago2	h	3	gfp	h	1	0.02453	0.2595	0.09	0.9251	1
ago2	h	3	gfp	h	3	-0.2391	0.2595	-0.92	0.3613	1
ago2	h	3	gfp	h	6	-0.8142	0.2595	-3.14	0.0029	0.2466
ago2	h	3	gfp	v	1	-0.08141	0.2595	-0.31	0.7551	1
ago2	h	3	gfp	v	3	-0.2879	0.2595	-1.11	0.2727	1
ago2	h	3	gfp	v	6	-0.443	0.2595	-1.71	0.0941	0.9831
ago2	h	3	w	h	3	-0.1022	0.2595	-0.39	0.6954	1
ago2	h	3	w	h	6	-0.5406	0.2595	-2.08	0.0425	0.8911
ago2	h	3	w	v	1	0.1803	0.2901	0.62	0.5371	1
ago2	h	3	w	v	3	0.05494	0.2595	0.21	0.8332	1
ago2	h	3	w	v	6	-0.5656	0.2595	-2.18	0.0341	0.8475
ago2	h	6	ago2	v	1	0.6348	0.2321	2.73	0.0087	0.4874
ago2	h	6	ago2	v	3	0.1605	0.2595	0.62	0.5392	1
ago2	h	6	ago2	v	6	0.008364	0.2595	0.03	0.9744	1
ago2	h	6	dcr2	h	1	-0.7045	0.2595	-2.71	0.0091	0.5015
ago2	h	6	dcr2	h	3	0.05536	0.2595	0.21	0.8319	1
ago2	h	6	dcr2	h	6	0.03561	0.2595	0.14	0.8914	1
ago2	h	6	dcr2	v	1	-0.1044	0.2321	-0.45	0.6548	1
ago2	h	6	dcr2	v	3	0.2533	0.2595	0.98	0.3338	1
ago2	h	6	dcr2	v	6	0.001667	0.2595	0.01	0.9949	1
ago2	h	6	gfp	h	1	0.2743	0.2595	1.06	0.2958	1
ago2	h	6	gfp	h	3	0.01061	0.2595	0.04	0.9676	1
ago2	h	6	gfp	h	6	-0.5644	0.2595	-2.18	0.0345	0.8498
ago2	h	6	gfp	v	1	0.1683	0.2595	0.65	0.5196	1
ago2	h	6	gfp	v	3	-0.03813	0.2595	-0.15	0.8838	1
ago2	h	6	gfp	v	6	-0.1933	0.2595	-0.74	0.46	1
ago2	h	6	w	h	3	0.1475	0.2595	0.57	0.5723	1
ago2	h	6	w	h	6	-0.2909	0.2595	-1.12	0.2678	0.9999
ago2	h	6	w	v	1	0.4301	0.2901	1.48	0.1447	0.9968
ago2	h	6	w	v	3	0.3047	0.2595	1.17	0.2461	0.9999
ago2	h	6	w	v	6	-0.3159	0.2595	-1.22	0.2294	0.9998
ago2	v	1	ago2	v	3	-0.4743	0.2321	-2.04	0.0464	0.9065
ago2	v	1	ago2	v	6	-0.6264	0.2321	-2.7	0.0095	0.5124
ago2	v	1	dcr2	h	1	-1.3393	0.2321	-5.77	<.0001	0.0001
ago2	v	1	dcr2	h	3	-0.5794	0.2321	-2.5	0.016	0.6545
ago2	v	1	dcr2	h	6	-0.5992	0.2321	-2.58	0.0129	0.595

ago2	v	1	dcr2	v	1	-0.7392	0.201	-3.68	0.0006	0.0731
ago2	v	1	dcr2	v	3	-0.3815	0.2321	-1.64	0.1067	0.9889
ago2	v	1	dcr2	v	6	-0.6331	0.2321	-2.73	0.0088	0.4924
ago2	v	1	gfp	h	1	-0.3605	0.2321	-1.55	0.1268	0.9943
ago2	v	1	gfp	h	3	-0.6242	0.2321	-2.69	0.0098	0.5192
ago2	v	1	gfp	h	6	-1.1992	0.2321	-5.17	<.0001	0.0009
ago2	v	1	gfp	v	1	-0.4665	0.2321	-2.01	0.05	0.9185
ago2	v	1	gfp	v	3	-0.6729	0.2321	-2.9	0.0056	0.379
ago2	v	1	gfp	v	6	-0.8281	0.2321	-3.57	0.0008	0.0959
ago2	v	1	w	h	3	-0.4873	0.2321	-2.1	0.041	0.8844
ago2	v	1	w	h	6	-0.9257	0.2321	-3.99	0.0002	0.0322
ago2	v	1	w	v	1	-0.2047	0.2659	-0.77	0.445	1
ago2	v	1	w	v	3	-0.3301	0.2321	-1.42	0.1613	0.9982
ago2	v	1	w	v	6	-0.9507	0.2321	-4.1	0.0002	0.0239
ago2	v	3	ago2	v	6	-0.1521	0.2595	-0.59	0.5605	1
ago2	v	3	dcr2	h	1	-0.8649	0.2595	-3.33	0.0016	0.1645
ago2	v	3	dcr2	h	3	-0.1051	0.2595	-0.4	0.6872	1
ago2	v	3	dcr2	h	6	-0.1249	0.2595	-0.48	0.6326	1
ago2	v	3	dcr2	v	1	-0.2649	0.2321	-1.14	0.2594	0.9999
ago2	v	3	dcr2	v	3	0.09284	0.2595	0.36	0.7221	1
ago2	v	3	dcr2	v	6	-0.1588	0.2595	-0.61	0.5434	1
ago2	v	3	gfp	h	1	0.1138	0.2595	0.44	0.6629	1
ago2	v	3	gfp	h	3	-0.1499	0.2595	-0.58	0.5663	1
ago2	v	3	gfp	h	6	-0.7249	0.2595	-2.79	0.0074	0.4476
ago2	v	3	gfp	v	1	0.007853	0.2595	0.03	0.976	1
ago2	v	3	gfp	v	3	-0.1986	0.2595	-0.77	0.4478	1
ago2	v	3	gfp	v	6	-0.3537	0.2595	-1.36	0.1791	0.999
ago2	v	3	w	h	3	-0.01295	0.2595	-0.05	0.9604	1
ago2	v	3	w	h	6	-0.4513	0.2595	-1.74	0.0883	0.9793
ago2	v	3	w	v	1	0.2696	0.2901	0.93	0.3573	1
ago2	v	3	w	v	3	0.1442	0.2595	0.56	0.581	1
ago2	v	3	w	v	6	-0.4763	0.2595	-1.84	0.0725	0.9642
ago2	v	6	dcr2	h	1	-0.7128	0.2595	-2.75	0.0084	0.4792
ago2	v	6	dcr2	h	3	0.047	0.2595	0.18	0.857	1
ago2	v	6	dcr2	h	6	0.02724	0.2595	0.1	0.9168	1
ago2	v	6	dcr2	v	1	-0.1128	0.2321	-0.49	0.6292	1
ago2	v	6	dcr2	v	3	0.2449	0.2595	0.94	0.3499	1
ago2	v	6	dcr2	v	6	-0.0067	0.2595	-0.03	0.9795	1
ago2	v	6	gfp	h	1	0.2659	0.2595	1.02	0.3106	1
ago2	v	6	gfp	h	3	0.002242	0.2595	0.01	0.9931	1
ago2	v	6	gfp	h	6	-0.5728	0.2595	-2.21	0.032	0.8335
ago2	v	6	gfp	v	1	0.16	0.2595	0.62	0.5405	1
ago2	v	6	gfp	v	3	-0.04649	0.2595	-0.18	0.8585	1

ago2	v	6	gfp	v	6	-0.2016	0.2595	-0.78	0.4409	1
ago2	v	6	w	h	3	0.1391	0.2595	0.54	0.5943	1
ago2	v	6	w	h	6	-0.2992	0.2595	-1.15	0.2545	0.9999
ago2	v	6	w	v	1	0.4217	0.2901	1.45	0.1525	0.9975
ago2	v	6	w	v	3	0.2963	0.2595	1.14	0.2591	0.9999
ago2	v	6	w	v	6	-0.3242	0.2595	-1.25	0.2174	0.9997
dcr2	h	1	dcr2	h	3	0.7598	0.2595	2.93	0.0052	0.3612
dcr2	h	1	dcr2	h	6	0.7401	0.2595	2.85	0.0063	0.4091
dcr2	h	1	dcr2	v	1	0.6001	0.2321	2.59	0.0128	0.5924
dcr2	h	1	dcr2	v	3	0.9578	0.2595	3.69	0.0006	0.0707
dcr2	h	1	dcr2	v	6	0.7061	0.2595	2.72	0.009	0.497
dcr2	h	1	gfp	h	1	0.9787	0.2595	3.77	0.0004	0.0575
dcr2	h	1	gfp	h	3	0.7151	0.2595	2.76	0.0082	0.4733
dcr2	h	1	gfp	h	6	0.14	0.2595	0.54	0.5919	1
dcr2	h	1	gfp	v	1	0.8728	0.2595	3.36	0.0015	0.1539
dcr2	h	1	gfp	v	3	0.6663	0.2595	2.57	0.0133	0.6047
dcr2	h	1	gfp	v	6	0.5112	0.2595	1.97	0.0545	0.9313
dcr2	h	1	w	h	3	0.852	0.2595	3.28	0.0019	0.1831
dcr2	h	1	w	h	6	0.4136	0.2595	1.59	0.1174	0.9922
dcr2	h	1	w	v	1	1.1345	0.2901	3.91	0.0003	0.0398
dcr2	h	1	w	v	3	1.0091	0.2595	3.89	0.0003	0.0422
dcr2	h	1	w	v	6	0.3886	0.2595	1.5	0.1407	0.9964
dcr2	h	3	dcr2	h	6	-0.01976	0.2595	-0.08	0.9396	1
dcr2	h	3	dcr2	v	1	-0.1598	0.2321	-0.69	0.4945	1
dcr2	h	3	dcr2	v	3	0.1979	0.2595	0.76	0.4493	1
dcr2	h	3	dcr2	v	6	-0.0537	0.2595	-0.21	0.8369	1
dcr2	h	3	gfp	h	1	0.2189	0.2595	0.84	0.403	1
dcr2	h	3	gfp	h	3	-0.04476	0.2595	-0.17	0.8638	1
dcr2	h	3	gfp	h	6	-0.6198	0.2595	-2.39	0.0208	0.7269
dcr2	h	3	gfp	v	1	0.113	0.2595	0.44	0.6653	1
dcr2	h	3	gfp	v	3	-0.09349	0.2595	-0.36	0.7202	1
dcr2	h	3	gfp	v	6	-0.2486	0.2595	-0.96	0.3427	1
dcr2	h	3	w	h	3	0.09215	0.2595	0.36	0.7241	1
dcr2	h	3	w	h	6	-0.3462	0.2595	-1.33	0.1883	0.9992
dcr2	h	3	w	v	1	0.3747	0.2901	1.29	0.2026	0.9995
dcr2	h	3	w	v	3	0.2493	0.2595	0.96	0.3414	1
dcr2	h	3	w	v	6	-0.3712	0.2595	-1.43	0.1589	0.998
dcr2	h	6	dcr2	v	1	-0.14	0.2321	-0.6	0.5491	1
dcr2	h	6	dcr2	v	3	0.2177	0.2595	0.84	0.4056	1
dcr2	h	6	dcr2	v	6	-0.03394	0.2595	-0.13	0.8965	1
dcr2	h	6	gfp	h	1	0.2387	0.2595	0.92	0.3623	1
dcr2	h	6	gfp	h	3	-0.025	0.2595	-0.1	0.9236	1
dcr2	h	6	gfp	h	6	-0.6	0.2595	-2.31	0.025	0.7745

dcr2	h	6	gfp	v	1	0.1327	0.2595	0.51	0.6114	1
dcr2	h	6	gfp	v	3	-0.07374	0.2595	-0.28	0.7775	1
dcr2	h	6	gfp	v	6	-0.2289	0.2595	-0.88	0.3821	1
dcr2	h	6	w	h	3	0.1119	0.2595	0.43	0.6682	1
dcr2	h	6	w	h	6	-0.3265	0.2595	-1.26	0.2143	0.9997
dcr2	h	6	w	v	1	0.3945	0.2901	1.36	0.1802	0.999
dcr2	h	6	w	v	3	0.2691	0.2595	1.04	0.3049	1
dcr2	h	6	w	v	6	-0.3515	0.2595	-1.35	0.1818	0.9991
dcr2	v	1	dcr2	v	3	0.3577	0.2321	1.54	0.1297	0.9948
dcr2	v	1	dcr2	v	6	0.1061	0.2321	0.46	0.6497	1
dcr2	v	1	gfp	h	1	0.3787	0.2321	1.63	0.1092	0.9898
dcr2	v	1	gfp	h	3	0.115	0.2321	0.5	0.6225	1
dcr2	v	1	gfp	h	6	-0.46	0.2321	-1.98	0.0531	0.9276
dcr2	v	1	gfp	v	1	0.2727	0.2321	1.17	0.2457	0.9999
dcr2	v	1	gfp	v	3	0.06627	0.2321	0.29	0.7764	1
dcr2	v	1	gfp	v	6	-0.08887	0.2321	-0.38	0.7035	1
dcr2	v	1	w	h	3	0.2519	0.2321	1.09	0.2831	1
dcr2	v	1	w	h	6	-0.1865	0.2321	-0.8	0.4257	1
dcr2	v	1	w	v	1	0.5345	0.2659	2.01	0.05	0.9185
dcr2	v	1	w	v	3	0.4091	0.2321	1.76	0.0842	0.9762
dcr2	v	1	w	v	6	-0.2115	0.2321	-0.91	0.3667	1
dcr2	v	3	dcr2	v	6	-0.2516	0.2595	-0.97	0.337	1
dcr2	v	3	gfp	h	1	0.02096	0.2595	0.08	0.9359	1
dcr2	v	3	gfp	h	3	-0.2427	0.2595	-0.94	0.3543	1
dcr2	v	3	gfp	h	6	-0.8177	0.2595	-3.15	0.0028	0.24
dcr2	v	3	gfp	v	1	-0.08498	0.2595	-0.33	0.7447	1
dcr2	v	3	gfp	v	3	-0.2914	0.2595	-1.12	0.2669	0.9999
dcr2	v	3	gfp	v	6	-0.4466	0.2595	-1.72	0.0916	0.9815
dcr2	v	3	w	h	3	-0.1058	0.2595	-0.41	0.6853	1
dcr2	v	3	w	h	6	-0.5442	0.2595	-2.1	0.0412	0.8854
dcr2	v	3	w	v	1	0.1768	0.2901	0.61	0.5452	1
dcr2	v	3	w	v	3	0.05137	0.2595	0.2	0.8439	1
dcr2	v	3	w	v	6	-0.5692	0.2595	-2.19	0.0331	0.8406
dcr2	v	6	gfp	h	1	0.2726	0.2595	1.05	0.2987	1
dcr2	v	6	gfp	h	3	0.008939	0.2595	0.03	0.9727	1
dcr2	v	6	gfp	h	6	-0.5661	0.2595	-2.18	0.034	0.8466
dcr2	v	6	gfp	v	1	0.1666	0.2595	0.64	0.5238	1
dcr2	v	6	gfp	v	3	-0.0398	0.2595	-0.15	0.8787	1
dcr2	v	6	gfp	v	6	-0.1949	0.2595	-0.75	0.4561	1
dcr2	v	6	w	h	3	0.1458	0.2595	0.56	0.5767	1
dcr2	v	6	w	h	6	-0.2925	0.2595	-1.13	0.2651	0.9999
dcr2	v	6	w	v	1	0.4284	0.2901	1.48	0.1462	0.997
dcr2	v	6	w	v	3	0.303	0.2595	1.17	0.2486	0.9999

dcr2	v	6	w	v	6	-0.3175	0.2595	-1.22	0.2269	0.9998
gfp	h	1	gfp	h	3	-0.2637	0.2595	-1.02	0.3146	1
gfp	h	1	gfp	h	6	-0.8387	0.2595	-3.23	0.0022	0.2039
gfp	h	1	gfp	v	1	-0.1059	0.2595	-0.41	0.6849	1
gfp	h	1	gfp	v	3	-0.3124	0.2595	-1.2	0.2345	0.9998
gfp	h	1	gfp	v	6	-0.4675	0.2595	-1.8	0.0778	0.9702
gfp	h	1	w	h	3	-0.1268	0.2595	-0.49	0.6274	1
gfp	h	1	w	h	6	-0.5651	0.2595	-2.18	0.0343	0.8484
gfp	h	1	w	v	1	0.1558	0.2901	0.54	0.5937	1
gfp	h	1	w	v	3	0.03041	0.2595	0.12	0.9072	1
gfp	h	1	w	v	6	-0.5901	0.2595	-2.27	0.0274	0.7969
gfp	h	3	gfp	h	6	-0.575	0.2595	-2.22	0.0314	0.8289
gfp	h	3	gfp	v	1	0.1577	0.2595	0.61	0.5462	1
gfp	h	3	gfp	v	3	-0.04874	0.2595	-0.19	0.8518	1
gfp	h	3	gfp	v	6	-0.2039	0.2595	-0.79	0.4359	1
gfp	h	3	w	h	3	0.1369	0.2595	0.53	0.6002	1
gfp	h	3	w	h	6	-0.3015	0.2595	-1.16	0.251	0.9999
gfp	h	3	w	v	1	0.4195	0.2901	1.45	0.1546	0.9977
gfp	h	3	w	v	3	0.2941	0.2595	1.13	0.2627	0.9999
gfp	h	3	w	v	6	-0.3265	0.2595	-1.26	0.2143	0.9997
gfp	h	6	gfp	v	1	0.7328	0.2595	2.82	0.0068	0.4275
gfp	h	6	gfp	v	3	0.5263	0.2595	2.03	0.048	0.9121
gfp	h	6	gfp	v	6	0.3712	0.2595	1.43	0.159	0.998
gfp	h	6	w	h	3	0.712	0.2595	2.74	0.0085	0.4815
gfp	h	6	w	h	6	0.2736	0.2595	1.05	0.297	1
gfp	h	6	w	v	1	0.9945	0.2901	3.43	0.0012	0.1332
gfp	h	6	w	v	3	0.8691	0.2595	3.35	0.0016	0.1588
gfp	h	6	w	v	6	0.2486	0.2595	0.96	0.3428	1
gfp	v	1	gfp	v	3	-0.2064	0.2595	-0.8	0.4301	1
gfp	v	1	gfp	v	6	-0.3616	0.2595	-1.39	0.1698	0.9986
gfp	v	1	w	h	3	-0.02081	0.2595	-0.08	0.9364	1
gfp	v	1	w	h	6	-0.4592	0.2595	-1.77	0.083	0.9752
gfp	v	1	w	v	1	0.2617	0.2901	0.9	0.3714	1
gfp	v	1	w	v	3	0.1364	0.2595	0.53	0.6017	1
gfp	v	1	w	v	6	-0.4842	0.2595	-1.87	0.0681	0.9581
gfp	v	3	gfp	v	6	-0.1551	0.2595	-0.6	0.5527	1
gfp	v	3	w	h	3	0.1856	0.2595	0.72	0.4778	1
gfp	v	3	w	h	6	-0.2527	0.2595	-0.97	0.3349	1
gfp	v	3	w	v	1	0.4682	0.2901	1.61	0.113	0.991
gfp	v	3	w	v	3	0.3428	0.2595	1.32	0.1927	0.9993
gfp	v	3	w	v	6	-0.2777	0.2595	-1.07	0.2897	1
gfp	v	6	w	h	3	0.3408	0.2595	1.31	0.1952	0.9994
gfp	v	6	w	h	6	-0.0976	0.2595	-0.38	0.7085	1

gfp	v	6	w	v	1	0.6233	0.2901	2.15	0.0367	0.8625
gfp	v	6	w	v	3	0.4979	0.2595	1.92	0.0608	0.9456
gfp	v	6	w	v	6	-0.1226	0.2595	-0.47	0.6387	1
w	h	3	w	h	6	-0.4384	0.2595	-1.69	0.0975	0.9849
w	h	3	w	v	1	0.2825	0.2901	0.97	0.3349	1
w	h	3	w	v	3	0.1572	0.2595	0.61	0.5476	1
w	h	3	w	v	6	-0.4634	0.2595	-1.79	0.0803	0.9728
w	h	6	w	v	1	0.7209	0.2901	2.48	0.0164	0.6625
w	h	6	w	v	3	0.5955	0.2595	2.29	0.0261	0.7848
w	h	6	w	v	6	-0.02501	0.2595	-0.1	0.9236	1
w	v	1	w	v	3	-0.1254	0.2901	-0.43	0.6675	1
w	v	1	w	v	6	-0.7459	0.2901	-2.57	0.0132	0.6024
w	v	3	w	v	6	-0.6205	0.2595	-2.39	0.0207	0.7251

Table C.3 Statistical test of percent survival with highlighted numbers indicating significant differences from GFP dsRNA control.

Treatment	Condition	Day 2	Day 3	Day 4	Day 5	Day6
DCR2	Healthy	0.0002	0.017	0.036	0.099	0.22
DCR2	Virus	0.0188	0.0171	0.0361	0.0391	0.0995
AGO2	Healthy	0.017	0.035	0.37	0.43	0.68
AGO2	Virus	0.142	0.0171	0.193	0.46	0.41

Table C.4 Statistical test of percent survival with highlighted numbers indicating significant differences from GFP dsRNA control.

Type III Tests of Fixed Effects

Effect	Num DF	Den DF	F Value	Pr > F
Treatment	3	55	38.87	<0.0001
Condition	1	55	0.95	0.3347
Treatment*Condition	3	55	0.11	0.9537

Treatment	Estimate	Error	DF	t Value	Pr > |t|	Alpha	Lower	Upper	Mean
AGO2	2.2446	0.08115	55	27.66	<.0001	0.05	2.0819	2.4072	9.4363
DCR2	2.0823	0.08795	55	23.68	<.0001	0.05	1.9061	2.2586	8.0232
GFP	2.7333	0.06359	55	42.99	<.0001	0.05	2.6059	2.8607	15.3837
Water	3.0295	0.05491	55	55.17	<.0001	0.05	2.9194	3.1395	20.686

Appendix D - RNAi Microinjections: Targeted transcript sequences for Dicer-2 and Argonaute-2

Key:

qRT-PCR Primer Region

dsRNA Synthesis Primer Region

dsRNA Synthesized (- Primers)

>Dicer2_ABE93B89423916ED9E1583E55C46E266(sequence:mRNA)4734residues[Scaffold27:1859731-1868407+strand][cds]

ATGGATGATTTTGTGGAGCGTCAGTACCAATCTGTATTAGCTGAGCAAGCTATGCAA
CAAAACAGTATACTTTTCCTCCCCACGGGCAGTGGAAAGACATTTATTTCAATTATG
GTTTTAAAGAAAATATTTCATTTGTTGGAACCGGACTATTTTTCCGGTGGTAAGAGA
GCAATGTTTTTGGTAAATACTGTTGCACTTGTTGACCAACAAGCTAAAGTTTTAGAG
AGGCATTTGTTACTGGATAAAGTTGGCCGATATTCTGGGGACATGAATTTAGATATG
TGGAATATGAGTATATGGAACGAGGAATTTTGTAAATTTCAGGTCATGGTCATGACT
GCTGAGATTTTGAATCAACTCCTATTAAAGAAATATATAAGTTTGGCTAATATTGCA
TTAATTATTCTTGATGAATGTCATCATGCTGTAGAGGACCATCCGATGAGACAAATA
ATGAAGCTATTTGAAGACTGTCCTTTAGCAGATCAGCCAAAGGTTATTGGATTAACA
GCAACTCTGTTGAACGCCACACCAAAAAGTCTTGCAAGGGTGCCGGAGGATGTGAA
AAAATTGGAAGTTACCTTGCATAGCACTGTTGCGACAGTAAACTCATGGGAACTAGT
AAAGCAATTTTCCACAAGTCCTCAAGAGATGTTTAAACCATTTCAGACACATTCAGA
CCTCGTTTTGACAAATTTTATAGATGATAAAGTCAATGAAGTTCATGAAATTTGTAA
GAACTTTCAATTTGTGACCCAAGATACTGGTCCTCCAAAACAACTGGCGGGATTTGT
CCCATTCTTTACGAAAAAGGGCAATGATATACCAAATCTTTGGAGACAAATTTCAAA
ACAACTTGGCTGGCTTGGGCCATACGGATGTTCTAAAACCCTCCAAGCTATTTATGT
CACACTAAGACTACAACAACAAAAAATGGAAGACAAAGACAGCATCATTATGATCA
ACTCAATTATTTGCTGTCTGATTTCTCTTAGTCGCTTTTTGGAATCTCACATGGAGAA
CTATGATCACCCTGAAAATGTGAAAGCTTATCAGTTCTCCTCTCCGAAAGTTAAGGC
CCTTGTTGAGGTGCTTGAGAGACAGTACGAAAAGTGCAAGAATGGGCCAGAACAGA
TGCAAGCACTAGTTTTTGTTGAAGAAAAAATGACAGCAAAAGTATTGTGCAGTGTAC
TAAAGAATATTGCAGAAAAAAGTGCAAGATATTCCTTTATAAAAGCAGGTTTCATA

GTTGGAGGAACTTACAATCCTTTCACCGAAACTTGGGAAGGTGCATTCAATAAGCAC
ATCAATGATAAAATTGTAGATCGCTTTCGGGAGCATGAGATAAACATTTTAGTGTGT
ACTGATGTTCTAGAAGAGGGCATTGATATACCAGCTTGCAACTTAGTTGTGAGATTT
GACTTAGCTAAACACTTCCGATCCTATGTTCAAAGTAAAGGCAGAGCCAGACATGA
CTCAAGCCTGTTCTGCCTCATGTCGAGCATTGAAGAGTTGAGTCGATACAGTGGAAA
AATTAATAGCTTTAAAGAGATATACTCTCGCCTTGAAGAACTACTAGTAGGACACAC
AGATACCAGAGCAGCTCCATCTGAAAGAGAGTTGGATGATTTGTATGAATCTGAGA
TTGAGCCTTATTATACACCTTTGGGTTCAAAAGTAACAATGACTTCTTCAATTTCTCT
TGTGACCAATTACTGCTCATCCTTTGCTCATGATCGTTTCTGCCGAATACCACCTTAC
TGGCATAAGAAAAAAATTGGTTCTAAAATCCAGGTTGCCCTTCAATTACCTAAATTT
TCTCCAATGCAAGATGTTGTGAAGGGTTTACCAATGGCCAATCTGAAAGTTGCAAAA
AGAGCTGCTGCTCTAGAAATGTGTAAAACTTTGCATCAAGTTGGGGAATTGAATGAT
AATTTGCTACCCAACACAAAATATTTGGAAGAGAGTGACATGAACGATTTGCTTCCG
CTCTGGGAATCAGAAGAACAGGGATCAGAGGCCAAGTCTGGTACCAATAAAAGAAC
TCGGCCTTACCAATTGAAGACACCAGCCTCCTTTGAAGATTGTAAACCATGTGAAAA
TGGAAAAGTTTATGTGCATCACATAGAAATTTATCCTGCTTTTGATGCACCTACATC
GGATAACAGAAAACTAGCAATTTATTTGACACTGAAAGAACAGAGAAATTTTGCAA
TAATATCATCAAAACCTATGAATCAGGTTTGCCAGTTTCCGGTATTTTCTAAATTTGG
AGCTATGAATGTGAGGTTGAAGAGTGCAGTAAAGTGCATCAATCTTGATAAAAGAC
AATTATTCATCATTGCCAATTATCATTTTAATCTGTTTACTTCCATGATTCCATTGGC
AAAAAGTTACCTAGGTTTTGCAAAAGATTCTTTTCTGATTGCACCAACCAAAATTGA
CAATAGGGGACTTGTGTGTTTGGATTGGGATGCAATGCAGATCGCAATGGAAACTA
AAGATACATTGGGAAATATGGAAAAGTGCATTGTCACACCTGTCCACCGTGGAGTA
TCAGTTCTCCATGAGGTATACTTTGTGACCCGTGTTTGCCGTGAACTTACAAGTGTTA
GTAAATTTCCTAGCCCCTTATATTCAACATACGAAGAGTACTTTAAAAAGAAGCATA
ATTTCAAAGTATGTCAACCCACCCTACCCCTACTTGAGGTTCAACCATTGAAACTAA
TTTCTAATGACCTCATTCCCAGGTATGGGAAAGCTGAAAGTGATTCAAGTGATGCAA
TTCATTTCCCCATAGAGACCTGTGAGATAAAGATTTCTGATGGATCATTGTTTCTAAA
AGCTGTTTTACTGCCATCAATTCTCCACCGGCTAGAACGCTTGTTGGTAGCTGATGA
GCTGCGGGAAATTATACCTGTTGCCCTTACAATTGGGGAGGATTCTAACTGTGGTAA
CAGCTGCATGTTGTGGAAAACAGCACACATTTTAAATTTGCCAAATGAAGATGTTAA

AAGGGTTACAAATGACATTTCACATGTACTAAGAGTGACTACTTCTCCTGTAAAGAA
AAGAAAAATTTCTGTAAAGCCTTGGGGTGATGACGAGCCTGTGGATATTGAACACA
ATTTTGATACAGTCACTTTTAAAGACATTGAAAAATATGGTGAATTTTCTAAAAGAA
AAACTTCTTCAACCAATTCTCCGTTTATAACAAGAAATCAACGGCCACTGATGACCC
TGCCTACACTGCATTCTGGAGAGGGTGTAATAACATTACTTTGTGAAAGGAAAAATA
GTCCTCATGCTTGCACCATATTAGAAGCAATAACAGCAGCTTCAGCGGATGACTTCT
GGAATCTGGAAAGGCTAGAAACTTTGGGAGATTCATTTTTAAAGTTTGCTGTTTCAT
TTATGTTGTTTTGCCGATTCCCTAATTTGTCAGAGGGAAAATTGACTACAGTAAAAG
GCCAAATCCTTGGGAATCGCAATTTGTTTTACTGTGCTAGAGCAAAGGACCTTGCAC
AATATCTGAAGGTTGACAAAATGGTTCCTTCTGAAGGATGGATTCCACCCTCATTTG
CTGTTCCTGAAATAATTCTTCAAGAGAACCTTACTGCTCATGCAAAACATCTTCTGCT
GTCAAGAGATGAGCAGTATAACAATGTTGTGAAAGATTCTACTTTGAGTGAACTCAA
AAGAAAAGTTTCGTCAAGTGTAATTGCAGTTTCCACTTCAGACCAGACTCCAAATAA
GAAAATGTCAAAAATTTCTGATAAAACTGTAGCAGACTCTGTTGAGTCATTATTAGG
AGCATTCTTGGAGACAACTGGACCCATAGCTGCTATGTCGTTTTTGGAGTGGATGAG
AGTGCTGCCTCATGGTACTGGAGCCCTACTAAAAATACAGACTCATGATATTTCCTC
ACATCCTCAAATGCATTTTAGCATTAATGATGTAGCCCAAAAGATGCATCAACGCTT
GGGCTATAAATTCAAAGACATCAATCTTCTTAATGAAGCAATAACACATGCTTCCAG
CACCTCACCATTTCGAACATATGAGCGGTTGGAATTTGTAGGTGACGCAGTTTTAGA
TTTTCTTATCACTGCATTCATTTATGAAAACTGTGGAAGACTTACTCCTGGTGAACTA
ACTGATTTGCGGTCAGCTCTAGTTAACAATATAACATTTGCTTGTTTATCCGTCCGTT
ATGGATTTTACAAATTTCTTAATGCTGGTTCTATAGCACTCATGAGTGCCATTGATAG
ATTTGTCAGTTTTCAAGAAGATCGAGAACATGTCATTGATGAGGAGGTGCTTATTTT
ACTAGAGGAGCATGAGACCAGATTGGCAGAAACTGTTAATGTCCCTAAAGCCTTAG
GTGATGTGTTTGAGGCTCTAATTGGAGCAGTATTTCTTGATTGTGGCCGTAACCTTTC
TGTAGTTTGGAAGGTCATTTATAGACTTATGAAAAATGAAATCAGTGCCTTTAGCAA
GGAAGTTCCCAAGCAGGTGGTCAGACAGCTGTATGAACGTGTTGGAGAGCAATATA
TGATTTTTAGAGTCTCAGAATCAACAAAGGAGATGCAAATGGAGCAGGTGCATGTA
GTTTTAACTGTAAGGTCGACTGAAGGAGATCTGCATTTTGATGGATTTGGGGTCAAT
AAGACGCAGGCCAAGAAGTCAGCAGCAAAACTGGCTTTAAGGCGATTAAAATTTGG
TATTTAG

>AGO2_2137A7E630181CB12ADF26469F60A92A(sequence:mRNA)3285residues[Scaffold53:1085697-1090686-strand][cds]

ATGGGGAAAAAAGGAAAAGGTAAAGGAGGAGGAGCAGGAGGAAATGCTGCCTCTG
GCTCTCAGGGAGGCGCTCAGCAAACTTCAGCTCAATCAGGAAACGCTCAGCGTCAA
GGGCAGAACCCAGGTCAAGCACAAAATCAAGGACAGGGGCAAGCTCAAAATCCTG
GTCAAGCACAAGGCCGAAACCCAGGACAGGGACAAGGTCAAAACCCAGGACAGGC
ACGAGTCCAAAACCCTGGTCAAGCGCAAAGCCAAAATCCAGCCTTGGGACAAAGTC
AAAACCCTGGTCAAGCTCAGGGACAGAACCCTCGGCAAGCTCAGGGACAAAACCCT
ACAGCCTGGGGACCAGGACAAAATCCTGGTCAGAATCCAGGTCAGGGAAGAGGCC
GTGGCCAGAACCCCGGTCAGGGTCAAGGAAGGGGACGTGGCCAGAACCCCAGTCA
GGGTCAAGGAAGGGGACGTGGTGCCCCAAATCCAGGTTTTCAACCTCCTATCCAGC
ACCAGGGGCCAGCCCAAGTTTTGCCTCCAGGGCAAGCCCAAGGCTATGCTTCAGGG
CCTAGGCAGCCACCCTGGGGCCAACCAAGCCCTAATCCAACACAACAAGGACACCC
CCCAGGATTTGCTTCAGGGTCTAGGGCGCCACAGCCTTCATCATGGGGCCAACCAAG
CCCTAATCCAACACAACAAGGACAACCCCCGGGATCTGCTCCAGGGCCTAGGCCGC
TACAGCCTTCATCATGGGGCCAACCGAGTCCACCTCCAGCACAAGGAGTTCCTCCAC
AAGTTGTTCATGGGGACACTGTACAAAAGTCTTCTGCGCAGTCCGAGTCCTCTAAAG
GACCACAACAGGCACCTTCTTCATCGGGTGATGCACGAGTGACTCCTGCTGGTGGCC
AAGTTAGCAGGGCTCAACCAGGAAAGTCCTTTGCCTTACCCCAGCGGGCCAATTGTC
CTCCGGACCCCAAAGTAGGAAGACCAATCCAGCTAGAAGTAAACCATTTACTTCTTC
AAATTAGAGATCCAACCGTTAAGATTTATCATTATGACGTGGCGATTGATCCAGATA
AGCCAAAGCGTTTTATGAGACTTGTAATGGAGGAAATGCAAAAAAAGTTTTATCCA
AGGAACTTCCCTGGTTTTGATGGGAAAAAAAATTTATATAGCAAAGGCCCTCTGCCC
TTTAACACAGAGATATCTGAAGAGGTGAATGTCAGAGATGACGAACGCCAAGATAA
TAAACCCAAAACTTTCAAAGTAACCATCAAACTTGCTAGAAACAACATATCGTTGCA
AGAACTCTTTGCATACCAAAAGAGTGGAAGGTCAACTTCTACTCCTCAAGATGTGAT
TCAGGCACTTGATGTGATCCTACGATTTGTACAGGTTGGTCGATCATTCTTCTGTCCT
CCCGTATCGCCCATGGATTTGGGTAATGGAATGGAGCTGTGGTATGGATATTTCCAG
TCGTTCATAATGGGAAATAAGCCGTATTTAAATATTGATGTGGCACACAAAGGTTTT
CCAACATCTCAGTCGCTTCTCAAGCTGCTGAAAGCATTTGATTCAAGGTCAGCAACC
CCCGAGGAAGCCATGAAATACAATCAACATGAACTGGAAAGGTTTATTAAGGGCTT
GAAAGTTGAGTATCAAGTGCCAAATATTGAAACAAGCAAGAGGACATATCGAGTGA

ATGGCCTGAGAAGGAATGCATTTGAAGAAAGATTTCAGATGGGTGATGATGGCAAA
ACTATTACTATTGGAGAATATTTTGCCAAACACAAAGGTTATCAATTACGTTTTCCA
AATCTTCCTTGTGTGCATGTGGGACACAGAGAAAAGGACGTATTGGTTCCCTTTGAA
CTTTGTGTTCTGCTGCCTGGTCAAGCTACCCAGAAGAAACTTGATGAAGGCCAAACT
GCAAAAATGGTTAAAGTTGCTGCCACTAATGTACAAGACCGTAAAAACAAAATAAA
AGAAGCTATGCAAAGGGCAAATGTTAATGCTAGTCCTCAAGTAAAGGAGTTGGGAC
TGTCAGTAGCAACTGAATTTGCAAAAATCAATGGTCGTATTCTACCAGCTCCCAAGC
TGGCCTACTATCAGAATAGGACTGTTCAGCCTATGAAAGGAGTATGGCGTGGCGGG
CAATTCCGGGAGACACGCGCGCTGAAAAAGTGGATTTGTCTTCAAATCTGCAATATT
CCCAGAGAAGCACTCAGTTCATTTGCTGAAAATCTGAGGAGTGAAGCGGGCAAAGT
AAACATGTTCATGGAAAAACCTGACCCCCCAATAATTATGGATGGCAGGGGAAACC
CGCAAAAGATTTTAAAAGATCTTAGAGAGAGACTTGGGGAGCTGAGCAAACAGGGA
TACCAATTAGTTTTGGTTGTTATAAGTGGTTATAACAAACAAATATATGGCCAAGTA
AAGCAAGTTGCGGAACTACAAGTTGGAGTACTGACTCAGTGTGTCAAAGATCTCACT
GTTACCAGGCGTAACAACCAAGCAACAGTGCATAATATCATGCTGAAAATCAATGC
AAAGTTTAATGGAATTAACCAAGTTATTGACGATAGTTCAAAAGTGAAATGCTTCAA
CAACAAGGTGTTAGTATTTGGTGCTGATGTTACTCATCCTTCACCAGATGCAAAAGA
TATTCCCTCCGTAGCAGCTGTTACAGCATCACATGATGTAAAGGGCTTCAAGTATAA
CATGAGAATCCGCTTACAAGCCCCAAGGCAAGAAATGATTGAAGATTTGGAAGCTA
TTGTCTACGAACAAGTAGGCATTTACAGTAAAGAGACTGGTGGTCTTCCTCAGCATG
TTGTGTTCTACAGAGATGGTGTCAGTGAAGGACAATTTCAGCAGGTCCTTGGGATTG
AATTAACTGCTATTTTTAAAGCATGTGCGAGACACAGCTTTAAACCAAAAGTAACCT
TTTTGGTGGTCCAGAAACGTCACCATACAAGGTTTTTCCCAATGAACCCACGTGATT
CCGATGATAGAAATGGTAATGTTCCGGCTGGAACAATTGTTGATATGGAAATAACTC
ACCCCAATGAAATTGATTTTTATCTGGTTAGCCATGCCAGTATTCAAGGTGTTGCTCG
TCCTACCAAGTATCATGTGCTATGGGATGATGCGAACATGTCAGAAAATGACATACA
ACTAATGACGTACAATCTATGTCATCTTTTCACGCGATGTGATCGTGCTGTGTCATAT
CCTGCGCCTACATATTATGCTCACCTTGCTGCTTCACGTGGTCGAGTTTATTTGGAGG
GGTAA